Antigen recognition by MR1-restricted T cells

Inauguraldissertation

zur

Erlangung der Würde eines Doktors der Philosophie

vorgelegt der

Philosophisch-Naturwissenschaftlichen Fakultät

der Universität Basel

von

QINMEI YANG

Basel, 2021

Genehmigt von der Philosophisch-Naturwissenschaftlichen Fakultät

auf Antrag von

Prof. Dr. Gennaro De Libero, Prof. Dr. Jean Pieters und Prof. Paolo Dellabona

Basel, 21.09.2021

Prof. Dr. Marcel Mayor

The Dean of Faculty

Acknowledgements

Firstly, I would like to show my gratitude to my supervisor Prof. Dr. Gennaro De Libero for giving me the opportunity to work under his guidance on this very interesting project. The conversations and discussion with him over my project were very educational and he has reinforced my interest in immunology. Additionally, I would like to thank Dr. Lucia Mori, for mentoring, and all the discussions on experiments and my future careers. Thanks to Alessandro, Andrew, and Julian for their help, support and guidance and all the wise advices on the experiments. Thank you to Dr. Paula Cullen Baumann for all the great help in my thesis writing. To Aisha, Pedro, Jan, thank you for being PhD students with me in our lab, thanks for their invaluable friendship and all the inspiration and encouragement. I would like to thank to Giuliano, Daniel, Marco, and Gennaro for all the scientific discussions and supports and for maintaining a pleasant working atmosphere. Thanks to Verena and Corinne for their great assistances during my PhD and efficient team work. I am so lucky to be involved in this great and supportive team. I also want to thank all past and present members of De Libero's lab for their support and encouragement.

I would like to acknowledge all members of my PhD committee, Prof. Dr. Gennaro De Libero, Prof. Dr. Jean Pieters and Prof. Paolo Dellabona for their invaluable advice regarding my projects. I also want to acknowledge FACS group in DBM for their excellent work. I would like to thanks to a fruitful collaborators, Prof. Silvia Balbo and Dr. Peter Villalta from University of Minnesota, Daniel Joss, Prof. Dr. Daniel Häussinger and Prof. Dr. Olivier Potterat from University of Basel, Dr. Mirko Wagner from University of Munich, Dr. Alexander Flohr, Dr. Luca Arista, and many other members of Matterhorn Biosciences AG. Thanks for providing us many compounds for biological tests, sharing great scientific work and advices.

I would like to thank my Chinese friends, Ya Peng, Haijie Zhao, Shuaishuai Cao, Zhihui Chen, Ruize Gao, Renxuan Dong, Kai Zheng, Juan Liang, Liang Zhou who make this unforgettable Ph.D. journey full of joy.

Last but not the least, I would like to thank my parents, Hongfang Yang and Xiaojuan Ma, for supporting me spiritually throughout my life. I would like to thank my brother, Qinhan Yang. Thank you for his kind and generous support and for always believing in me. I would like to thank my boyfriend, Jiaqi Wu for his support and love. I am deeply grateful to have him in my life.

This thesis contains the following materials that were obtained in collaboration with other members of our laboratory, or that were provided by other collaborators:

- Figure 3-1, 3-2, 3-4, 3-5, Figure 4-1 and 4-2 were obtained in collaboration with Dr. Alessandro Vacchini

- Figure 3-3 is provided by Dr. Alessandro Vacchini

- Figure 3-22 was obtained in collaboration with Dr. Julian Spagnuolo

- Figure 1-4 was used from paper [1] with minor modifications

- Figure 2-1, Figure 4-3, 4-4, and 4-5 are provided by group of Prof. Silvia Balbo and Dr. Peter Villalta at Division of Environmental Health Sciences, Masonic Cancer Center, University of Minnesota

- Figure 3-15, 3-17, 3-18 and 3-19 are provided by Dr. Daniel Joss from group of Prof. Dr. Daniel Häussinger, Department of Chemistry, University of Basel

- Figure 3-26 is provided by group of Prof. Dr. Olivier Potterat at group Pharmaceutical Biology, Pharmacenter, University of Basel

- Some compounds in Table 2-1 are provided by Dr. Mirko Wagner at Group of Prof. Carell, Department of Chemistry, University of Munich

- Compounds in Table 4-2 are provided by Matterhorn Biosciences AG

Abstract

T cells recognize antigens when associated with dedicated antigen-presenting molecules. Conventional T cells recognize peptides presented by polymorphic MHC molecules, whereas unconventional T cells recognize non-peptide antigens bound to non-polymorphic antigen-presenting molecules. These latter ones include cluster differentiation 1 (CD1), butyrophilin 3A1 (BTN3A1) and MHC class-I related molecule (MR1). Due to their unique structural properties, CD1 molecules bind and present an array of self-, bacteria-, and plant-derived lipid antigens recognized by TCR αβ and γδ T cells. A major population of TCR γδ cells react to phosphoantigens interacting with BTN3A1, whereas other rare TCR γδ cells react to CD1-presented lipids or to MR1-self-antigen complexes. Finally, small metabolites generated during riboflavin synthesis in microbes, are presented by MR1 and stimulate mucosal-associated invariant-T cells (MAITs). Recently our laboratory isolated a novel population of MR1-restricted T (MR1T) cells from healthy donors [1]. MR1T cells are distinct from MAIT cells as they do not recognize riboflavin-related metabolites, exhibit polyclonal TCRs and are adaptive-like T cells. Strikingly, they demonstrate preferential recognition of tumour cells and not of healthy cells. Their role in health and disease remains poorly characterized.

The aim of my PhD project was to study the physiology of MR1T cells, and mostly, to characterize the antigens that stimulate MR1T cells. I participated in the characterization and identification of the tumour-derived antigens which stimulate MR1T cells. These antigens belong to a new class of T cell-stimulatory antigens and are represented by nucleobases adducts, generated during different stress conditions and accumulating in tumour cells. I also established methods to synthesize and purify nucleobase adducts which I used to investigate their T cell-stimulatory activities. In my studies I then investigated how large is the repertoire of stimulatory nucleobase adducts, including molecules derived from both DNA and RNA.

In summary, this dissertation describes a novel class of T cell-stimulatory antigens made of nucleobases adducts. The nucleobase adducts accumulate upon combined alterations in the metabolism of nucleobases, carbonyls and reactive oxygen species. These molecules bind and form stable complexes with MR1 and stimulate MR1T cells. The metabolic changes generating nucleobase adducts preferentially occur in tumour cells, explaining MR1T cell recognition of many different cancer types. This novel type of antigen specificity suggests that MR1T cells survey cells for metabolic alterations, laying the groundwork for novel genetically-unrestricted T cell-based immunotherapies targeting the altered metabolome.

List of manuscript and patents

This thesis contains materials that have been submitted in the peer-reviewed journal: (The manuscript is currently under the second round of reviewing)

Vacchini A.*, Chancellor A.*, **Yang Q**.*, Spagnuolo J.*, Joss D., Øyås O., Beshirova A., De Gregorio C., Pfeffer M., Zippelius A., Stelling J., Häussinger D., Lepore M., Mori M., De Libero G. (2022). T cell activation by nucleobase adduct-containing metabolites. * Co-first author

This thesis contains materials that have been included for patents:

1. De Libero G., Mori M., Vacchini A., Chancellor A., **Yang Q**., Spagnuolo J, MR1 Ligands and Pharmaceutical Compositions for Immunomodulation, Patent No. WO/2021/144475, filed on 18. Jan. 2021, issued on 22. July. 2021

2. De Libero G., Mori M., **Yang Q**., Vacchini A., MR1 Ligands and Pharmaceutical Compositions for Immunomodulation, U.S. Patent Application No. 64/224,054, filed on 21. July. 2021, Patent Pending

Abbreviations

5-A-RU	5-amino-6-D-ribitylaminouracil
5-OP-RU	5-(2-oxopropylidineamino)-6-D-ribitylaminouracil
6-FP	6-formyl pterin
Ac-6-FP	acetyl-6-FP
ADA	adenosine deaminase
ADP	adenosine diphosphate
AMP	adenosine monophosphate
ANOVA	analysis of variance
APC	antigen-presenting cells
ATP	adenosine triphosphate
BBG	S-Bromobenzylglutathione
BCR	B cell receptor
BTN	transmembrane butyrophilin
BTNL	butyrophilin-like
CCR	C-C chemokine receptor
CD	cluster of differentiation
DAPI	4',6-diamidino-2-phenylindole dihydrochloride
DC	dendritic cell
DHAP	dihydroxyacetone phosphate
DMSO	dimethyl sulfoxide
DN	double-negative
DP	double-positive
EC50	half maximal effective concentration
EHNA	erythro-9-(2-Hydroxy-3-nonyl) adenine hydrochloride
ER	endoplasmic reticulum
FACS	fluorescence activated cell sorting
FCS	fetal calf serum
G3P	glyceraldehyde 3-phosphate
GDP	guanosine diphosphate
GLO	glyoxalase I
GM-CSF	granulocyte Macrophage Colony Stimulating Factor
GMP	guanosine monophosphate
GPX	Glutathione peroxidase
GSH	glutathione
GST	glutathione S-transferase
GTP	guanosine triphosphate
HLA	histocompatibility Leukocyte Antigen
HMB-PP	(E)-4-hydroxy-3-methyl-but-2-enyl pyrophosphate

HNE	4-hydroxy-2-nonenal
IFN	interferon
IL	interleukin
iNKT	invariant natural killer T
IPP	isopentenyl pyrophosphate
mAb	monoclonal antibody
MAIT	mucosal Associated Invariant T cell
MDA	malondialdehyde
MFI	median fluorescence intensity
MG	methylglyoxal
MHC	major histocompatibility complex
MPA	mycophenolic acid
MR1	MHC-related protein-1
MSA	mercaptosuccinic acid
NAC	N-acetylcysteine
NK	natural Killer
ONE	4-oxo-2-nonenal
PAMP	pathogen-associated molecular pattern
PBMC	peripheral blood mononuclear cell
PBS	phosphate buffered saline
PRR	pattern recognition receptor
RAG	recombination activating gene
RNA	ribonucleic acid
ROS	reactive oxygen species
ROS	reactive oxygen species
SD	standard deviation
SEM	standard Error of the Mean
TCR	T cell receptor
Th	T helper
TLR	toll-like Receptor
TNF	tumour Necrosis Factor
Vα / Vβ	variable α / variable β
WT	wildtype
αGalCer	α-galactosylceramide
β2m	β2 microglobulin

Table of contents

List of Figures

List of Tables

Chapter 1 Introduction

1.1 Immune system

The immune system is made of a complex network of biological processes that protect the host from infection. It is composed of many different types of cells, and of various tissues and organs. The immune system has evolved to respond to a wide range of invaders. These invaders can be common pathogens, like bacteria, viruses and parasites worms. In addition, the immune system can also respond to our own aberrant cells in tumour immunity and our own molecules in autoimmunity. The immune system of many species is divided into two major mechanisms: the innate (non-specific) immunity and adaptive (specific) immunity [2]. To fight against infections, these two immune systems are interdependent and operate jointly.

1.1.1 Innate immunity

The innate immune system is our first line of defence against invading organisms. Most pathogens are detected and destroyed rapidly within minutes or hours by the innate immune system [2]. It contains of several elements including anatomical barriers, secretory molecules and cellular components [3].

Some well-known mechanical anatomical barriers are skin, epithelial layers prevent bacteria and other infectious agents; mucus located on mucosal epithelia traps infectious agents; the flushing action of tears and urine also expels pathogens [3]. In addition, chemical components also contribute to protection against infection. Fatty acids in sweat inhibit the growth of bacteria; lysozyme and phospholipase from tears, saliva and nasal secretions can digest the cell wall of bacteria and destabilize bacterial membranes. Finally, the skin and gut flora serve as biological barriers and prevent the colonization of pathogenic bacteria by secreting toxic substances.

The anatomical barriers can efficiently reduce the amount of infection. However, once the pathogens overcome these barriers via damaged tissue, acute inflammation is immediately triggered [2]. During this early stage of infection, many innate immune cells come into play, including phagocytic cells, eosinophils, basophils, natural killer (NK) cells and mast cells. Phagocytic cells are macrophages, neutrophils and dendritic cells. They express pattern recognition receptors (PRRs), which recognize the conserved structural motifs shared by many pathogens, so-called pathogen-associated molecular patterns (PAMPs) [4]. Upon infection, phagocytes engulf microbes via PPRs and kill microbes with broad sets of antimicrobial proteins and toxic molecules [5]. Therefore, the innate immunity is pathogen non-specific. In

order for cells to work effectively, innate immune cells also secrete chemokines, which attract other immune cells to the site of infection [6, 7]. Inflammation may also be triggered by the activation of complement system [8]. Activated complement components consist of a number of plasma proteins that can directly destroy invading pathogens and also enhance the ability of phagocytic cells to destroy microbes.

The innate immune cells are immediately available to recognize a broad range of pathogens in a non-specific manner. Innate immune cells are also essential for triggering the activation of adaptive immunity.

1.1.2 Adaptive immunity

When innate immunity does not eliminate infectious agents, adaptive immunity is activated. In contrast to the innate (non-specific) immunity, adaptive immunity confers a high level of antigen specificity carried out by the formation of antigen-specific receptors on T and B cells (TCRs and BCRs), respectively [9]. Additionally, Somatic recombination and rearrangement of BCR and TCR genes allow joining of variable (V), joining (J) and in some cases diversity (D) gene segments in a random fashion [10, 11]. Furthermore, genetic mutations may occur in mature B cells, thus facilitating the generation of antibodies with high affinity for selecting antigens. Each T and B cell carries a unique antigen specificity, which is the consequence of unique gene rearrangement processes and also of the addition of N nucleotides at the sites of gene junctions. Collectively, over 10^8 TCRs and 10^{10} antibody specificities can be produced by human T and B cells [9].

Unlike the innate immunity, the adaptive immunity takes a few days to develop [2] and allows an immune response, which is antigen specific and characterized by generation of receptors with discrete to high affinities. Initially, naive B and T cells emerged from the thymus and bone marrow where they undergo gene rearrangement during maturation. To maximize the antigen encounter, secondary lymphoid organs such as lymph nodes, and spleen provide the microenvironment for antigen display and recognition [12]. The induction of an adaptive immune response begins when antigen presenting cells (APCs), particularly dendritic cells, ingest pathogens and present the processed microbial antigens to naïve T cells [13]. This leads naïve T cells to undergo clonal expansion and further differentiate into effector T cells [14, 15]. Activated T cells leave lymphoid tissues and upon attraction via chemokines move to the site where microbes are located or inflammation started. In parallel, B cells are stimulated by direct

binding to antigens via their BCR, which in some instances are displayed by follicular dendritic cells [16]. Activated B cells undergo clonal expansion and differentiate into plasma cells [17]. Plasma cells are the sole producers of soluble antibodies, which can be made by five different isotypes: IgM, IgD, IgG, IgA and IgE according to their heavy chains, which provide each isotype with distinct characteristics and roles [18].

Another feature of adaptive immune cells is their persistence that provides long-lasting protection from the recognized pathogen [9]. After the primary immune response, surviving T and B cells can differentiate into antigen-specific long-lived memory cells that rapidly respond to subsequent infection with the same pathogen. This immediate response that may also occur many years after the first exposure, represents the immunological memory [19]. Immunological memory provides the fundamental principle of vaccination, which has highly eliminated many infectious diseases and consequently changed social and economic history of humanity [20].

1.2 Conventional T cells

T cells play an essential role in adaptive immunity. Originally, T cells are born from hematopoietic stem cells in the bone marrow [21]. Developing T cells migrate via the blood to thymus where they undergo positive and negative selection and become mature T cells. This complex mechanism of selection ensure the mature T cells that leave the thymus are tolerant to self-antigens, but also have an intrinsic capacity to recognize foreign peptides presented by self-MHC molecules [22]. Mature T cells circulate in the blood and seed lymphoid organs where they are ready for antigen recognition and priming [23].

A vital step of T cell maturation in the thymus is making a functional TCR. Each mature T cell expresses a unique TCR derived from random TCR gene rearrangement. The majority of T cells express paired TCR α and β chains, while a minority express the TCR γ and δ chains [24]. In contrast to BCR that directly interacts with the antigen, the TCR detects short antigen fragments associated with antigen presenting molecules [25]. Conventional T cells are stimulated by peptides presented by the major histocompatibility complex (MHC) molecules, Class I and Class II [26, 27]. MHC I molecules are found on all nucleated cells and also in platelets, and present intracellular protein-derived peptides to TCRs of CD8+ T cells [28, 29]. Conversely, MHC II molecules are mainly expressed by "professional" APCs, such as dendritic cells, B cells, and macrophages. These cells capture proteins by endocytosis, partially digest them in the endo-lysosomal compartments, where the generated short peptides my bind MHC II molecules which are then recycled to plasma membrane and stimulate CD4+ T cells [28].

In order to trigger an effective immune response, T cells not only require the interaction of their TCR with the antigen-MHC complex, but also need co-stimulatory signals provided by molecules expressed on both APCs and T cells [30]. T cell co-stimulation is compulsory for T cell proliferation, differentiation and survival. T cells without co-stimulation may fail to respond and undergo to a state of unresponsiveness called T cell anergy [31].

Based on their function, activated T cells are grouped into cytotoxic T cells, mostly CD8+, and T helper cells, mostly CD4+ [1]. Cytotoxic T cells kill infected cells and tumour cells by binding death receptors on the cell surface and by releasing pore-forming proteins [32], enzymes as well as cytokines IL-2 and IFN-γ that induce apoptosis of the target cell [33]. In parallel, activated T helper cells divide rapidly and secrete cytokines to regulate and assist various immune response. Several subsets of T helper cells have been identified based on their

functional diversity, such as T helper (Th) 1, Th2, and Th 17 cells [34, 35]. For example, Th1 cells mainly effect the immunity of macrophages and CD8 T cells [36]. They secrete cytokines like IFN-γ, TNF-β, IL-2, and IL-10. While, Th2 cells mainly promotes activation of B cells. They release cytokines like IL-4, IL-5, IL-6, IL-10, IL-13 and so on. In addition, regulatory T cells is the third population of T cells that also express CD4 protein on the cell surface. They are known as suppressor T cells for preventing self-reactivity, like autoimmune disease. Several mechanisms are involved in regulating T cell immunity, including direct interaction with APCs, releasing inhibitory cytokines and induction of immune cell apoptosis [37-39].

1.3 Non-conventional T cells

Most studies of T cells have focused on the MHC-restricted T cells, which are also called "conventional T cells". However, a large group of T cells are not restricted to MHC molecules. These are the so called "non-conventional T cells", which recognize non-peptide antigens bound to diverse non-polymorphic MHC molecules. They include CD1-restricted T cells, TCR γδ T cells and mucosal associated invariant T (MAIT) cells.

1.3.1 CD1-restricted T cells

CD1 (cluster of differentiation 1) is a family of glycoproteins involved in the presentation of lipid antigens to T cells. In humans, CD1 isoforms are encoded by five genes. Based on their unique primary structure, cellular and tissue distribution, they are classified into three groups [40], Group I (with CD1a, CD1b, and CD1c), Group II (with CD1d) and Group III (CD1e).

Group I molecules are mainly expressed on professional APCs [41]. Each isoform of Group I molecule can be uniquely expressed. CD1a is expressed by Langerhans cells in the skin, CD1b is expressed by activated monocytes and dendritic cells, and CD1c is expressed on some B cells. Group I molecules present exogenous lipid antigens derived from the cell wall of several bacteria, for example *Mycobacterium tuberculosis*, the cause of Tuberculosis [42]. Mycolic acids were the first lipid antigens found to stimulate human CD1b-restricted T cells [43]. This lipid is made by a very long fatty acid and is an essential component of the cell wall of several mycobacteria.

CD1d is expressed on a wider variety of cells, mostly on hematopoietic cells, but also on gut epithelial cells, adipocytes, and some keratinocytes [40]. The most frequent population of CD1d-restricted T cells is represented by the invariant Natural killer T (iNKT) cells. iNKT cells recognize lipid and glycolipid antigens presented by the CD1d molecule [44], and share features of both T cells and natural killer (NK) cells, as they express the TCR αβ as well as the NK cell-associated molecular marker NK 1.1 (CD161). iNKT cells are the best-characterized CD1d-restricted T cells. They express highly conserved TCR in both Human (Vα24-Jα18 chain paired with Vβ11 chain) and in mice (Vα14-Jα18 chain paired with a few Vβ chains) [45]. iNKT cells are abundant in mice, they represent approximately 0.5% in blood and 20-30% in liver, while in humans the proportion is much less [46, 47]. In 1997, α-galactosylceramide (αGalCer) was extracted from the marine sponge *Agelas mauritianus*, and was identified as the

first antigen stimulating iNKT cells [48]. iNKT cells play important roles in immune response. They recognize both exogenous and endogenous lipid antigens during various microbial infections [49]. The deficiency of iNKT cells may induce autoimmune diseases and facilitate cancer development [50].

CD1e is a unique CD1 molecule as it not expressed on the cell surface but remains intracellularly [40]. CD1e is mostly expressed by dendritic cells and after egression from the ER it stacks in the Golgi compartment before moving to late endosomes [51]. CD1e does not present lipids to T cells, while instead it facilitates antigen processing and presentation by other CD1 molecules [52, 53].

1.3.2 Antigen presentation to CD1-restricted T cells

The CD1 proteins are structurally similar to the MHC I molecule, as they are heterodimers composed of a heavy chain with three domains, the α1 and α2 antigen-binding domains and an α3 domain. They are noncovalently associated with β2-microglobulin (β2m) [54]. When compared with the MHC I molecule, CD1 molecules have a deeper antigen binding site with a larger volume [55]. All of the CD1 molecules contain at least two hydrophobic pockets (A′ and F′ pockets) for antigen binding. Each CD1 isoform has distinct structural features, like different size, shape or more pockets. These differences allow binding and presentation of a large variety of self and foreign antigens [56]. In the past 20 years, CD1-restriceted antigen presentation has become much clearer. Various lipid-transfer-proteins (LTPs) [57, 58] and surface receptors [59] have been found to be involved in the uptake and transport of lipid antigens to endosomal compartments. Additionally, LTPs are also known for their important function of editing and degradation of lipid antigens [52, 60]. Multiple modes of TCR-antigen-CD1 complex interaction have been identified. Activation of iNKT cells is mainly based on the interaction between the TCR Vα chain and the CD1d–α-GalCer complexes [61], while some of the non-iNKT cells establish interactions with the CDR3 loops of TCR [62, 63]. Some TCR also establish antigen-independent interaction with the A' pocket of CD1a molecules [64], which is sufficient for T cell activation. The stimulation of CD1-restricted T cells does not involve the costimulatory molecules CD4 and CD8 [56].

1.3.3 TCR γδ T cells

The main characteristic of γδ T cells is the expression of a distinctive TCR on their surface, which is composed of the TCR γ chain paired with the TCR δ chain. Like αβ T cells, γδ T cells

develop in the thymus and undergo TCR rearrangement of the VDJ gene segments. In human genome are encoded only six Vγ genes and a limited number of Vδ genes [65, 66]. As Vδ genes are located within the Vα locus some Vα genes are also used as Vδ upon their rearrangement with Jδ gene segments. Unique VγVδ TCR combinations are expressed and their distribution is not random [67]. Indeed, certain Vγ chains exclusively pair with unique Vδ chain, for example the major population of human TCR γδ cells in the blood, tonsils and spleen express the Vγ9-Vδ2 heterodimer. TCR γδ cells account for 0.5-16% of all CD3$^+$ cells in peripheral blood and lymphoid organs, but number is much larger in mucosal tissues, and represent 20-30% of the total intestinal intraepithelial T cells [68].

Several ligands of γδ T cells have been identified. A group of Vδ1 T cells recognize CD1a and CD1d-presented lipids [69, 70], as well as stress-induced MHC class I-related chain A and B (MICA and MICB) molecules [71, 72]. A unique T cell population in human, the Vγ9Vδ2 T cells are the most well-studied γδ T cells. They are activated by microbial and endogenous phosphoantigens (pAg), which are represented by the microbial isoprenoid precursor (*E*)-4-hydroxy-3-methyl-but-2-enyl pyrophosphate (HMB-PP) [73], and by the endogenous isopentenyl pyrophosphate (IPP), which is generated in the mevalonate pathway [74, 75]. Both pAgs are stimulatory upon binding to the butyrophilin 3A1 protein (BTN3A1) [76, 77]. Stimulation also requires the presence of the butyrophilin 2A1 molecule, which directly interacts with the TCR Vγ9 chain [78]. Like CD1-restricted T cells, γδ T cells show diverse functions typical of both innate and adaptive immunity [79]. They mount rapid responses to highly conserved antigens, and are able to trigger phagocytosis of innate immunity cells [80]. On the other hand, they are part of adaptive immunity as they have a memory phenotype and express diverse TCR which are generated by TCR gene rearrangement. They show cytotoxic activities against infected cells [72] and also secret many different types of cytokines [81] and chemokines. TCR γδ cells may facilitate the activation of other immune cells, may trigger proliferation of other cells and kill target cells [82]. As of these properties, they are being tested in several clinical trials, mostly in cellular anti-tumour immunotherapy [83-87].

1.3.4 Antigen recognition by TCR γδ T cells

Butyrophilins (BTN) and butyrophilin-like (BTNL) molecules are structurally related to B7 proteins, which are found on activated APCs and behave as costimulatory or coinhibitory molecules for T cell regulation [88]. Like B7 molecules, most of BTN and BTNL proteins have two extracellular immunoglobulin-like domains, namely a IgV-like and a IgC-like domain [89].

Additionally, most of the BTN and BTNL proteins contain an intracellular B30.2 domain (also termed SPRY domain), which interacts with cytoplasmic molecules and participate in various activities [90]. BTN and BTNL molecules have multiple roles in innate and adaptive immunity. Importantly it was found that a member of BTN proteins, BTN3A1 is absolutely required for the activation of Vγ9Vδ2 T cells by pAgs [76, 77] Both the extracellular V-like domain and the intracellular B30.2 domains [77, 91] of BTN3A in antigen presentation. BTNL proteins share on average 40% identity with the BTN proteins [88] and are expressed on the surface of different cells. BTNL3 and BTNL8 promote the activation of γδ T cells expressing the TCR Vγ4 chain [92-95].

1.3.5 Mucosal Associated Invariant T (MAIT) cells

The first detection of an invariant TCR rearrangement involving the Vα7.2-Jα33 segments was reported by Porcelli and colleagues in 1993 [96]. this study showed the abundance of this rearrangement in the $CD4^-CD8^-$ double negative (DN) T cell population of healthy individuals. Subsequently, researchers found that more than five different phenotypic subsets of MAIT cells exist in humans, predominantly either $CD8\alpha\alpha^+$ or $CD8\alpha\beta^+$ (which represent approximately 80% of total MAIT cells), 10-20% DN and less than 1% $CD4^+CD8^-$ or $CD4^+CD8^+$ cells [97, 98]. As these cells are highly abundant in human gut mucosal and murine lamina propria, they named as mucosal associated invariant T (MAIT) cells [99]. In humans, MAIT cells comprise roughly 5% of the peripheral T cells [100] and up to 45% of T cells in the liver [101]. Like all the other T cell subsets, MAIT cells develop in the thymus and undergo TCR gene rearrangement. MAIT cells express semi-invariant TCRs, composed of a Vα7.2-Jα33 (TRAV1-2-TRAJ33) chain paired to a limited number of β chains [96, 97, 99, 102]. In humans, MAIT cells express high levels of CD161, the peptidase CD26, IL-7, IL-12, IL-18, and IL-23 receptors; as well as the chemokine receptors CCR5, CXCR6 and CCR6 [103-106].

MAIT cells are restricted to MHC class I-like molecule MR1 [99]. They recognize vitamin B2-related metabolites derived from bacteria which form complexes with MR1, suggesting they participate in immune response during infections [107, 108]. In addition to microbial infection, a number of studies have shown that MAIT cells could have a role also in non-infectious diseases, such as auto-immune rheumatoid arthritis [109], chronic inflammation [110-113] and cancer [114-117].

MAIT cells can be activated in either a MR1-dependent or a MR1-independent manner. During MR1-dependent activation, MAIT cell's TCR interacts with the MR1-antigen complex. The MR1-independent activation is induced by several cytokines, including IL-12 and IL-18 and IL-23 [118]. The blockade of IL-12 and IL-18 abolished IFN-γ production by MAIT cells [118-120], patients with IL-23R mutation showed reduced MAIT cell numbers and altered functions [121]. Moreover, MAIT cells can be activated during viral infections in a MR1 independent manner [120, 122].

Once activated, MAIT cells can secrete Th1 and Th17 cytokines, including IFN-γ, TNF-α, and IL-17 [100, 109]. IFN-γ, and TNF-α are important in controlling invasive infections, they activate macrophages, assists in the maturation of dendritic cells and promote the expression of MHC class II molecules [123-125]. IL-17 is involved in inducing and mediating proinflammatory response [126, 127]. Moreover, human MAIT cells isolated from the small intestine showed IL-22 secretion after *E.coli* stimulation. This cytokine was not released by MAIT cells isolated from lung and liver, suggesting that MAIT cells populating different tissues are endowed with different functions, probably as result of facing different environments [128]. Collectively, MAIT cells display effector-like response allowing them to immediately react to various infections. In addition to cytokine production, they also produce cytotoxic molecules, allowing them to lyse infected cells [129-131]. IL-7 was found to assist the cytotoxic potential of MAIT cells [132]. Resting MAIT cells showed low expression of granzyme B and perforin, which instead were greatly increased after bacterial infection [130] and before the onset of diabetes [133]. In general, MAIT cells bear both innate-like and adaptive-like features, giving them heterogeneous functional profiles in eliminating bacteria and participating in various diseases.

1.3.6 MR1 and MAIT cell agonists and antagonists

MR1 is a protein encoded by one non-polymorphic gene. In humans, it is located on chromosome 1, close to the CD1 gene locus[78, 134, 135]. Like other MHC class I molecules, MR1 is composed of α1, α2, and α3 domains which are non-covalently associated with β2m [136]. MR1 is highly conserved across species, with humans and mice sharing more than 90% protein sequence in the MR1 antigen-binding site that is formed by residues within the α1and α2 domains [136]. These findings suggested that the MR1-ligands are also highly conserved [107].

Although the MR1 transcript is ubiquitously expressed in multiple tissues and species, the MR1 expression on the cell surface is almost undetectable under physiological conditions [137, 138]. For a long time, the intracellular trafficking of MR1 has remained controversial. Some studies suggested that MR1 is almost entirely localized in the endoplasmic reticulum (ER) in a ligand-receptive and unfolded form without β2m association [139]. Inside the ER, MR1 refolding with ligands is facilitated by the chaperone proteins tapasin and TAP-binding protein related (TAPBPR) [140]. The binding of ligand triggers a conformational change which also stabilizes MR1 [139]. When MR1 is loaded with ligand, a Schiff base is formed between the amine group of MR1 lysine-43 (K43) and the ligand, which facilitates MR1-β2m association and promotes MR1 surface expression [139-141]. In some instances, the stimulatory MR1-antigen complexes are formed in late endosomes and lysosomes, where they associated with β2m [138, 142]. In addition, using fixed APCs, other studies showed that some ligands can bind to surface MR1 and stimulate MAIT cells without entering cells [139, 143]. These findings directly showed that in the presence of adequate amounts of antigen, MR1 can also present extracellular ligands.

A first group of antigens that stimulate MAIT cells was identified in 2012 [107]. They were the pterin-like ribityl lumazine compounds generated in the riboflavin (vitamin B2) biosynthesis pathway. These compounds were the reduced 6-hydroxymethyl-8-D-ribityllumazine (rRL-6-CH2OH), 7-hydroxy-6-methyl-8-D-ribityllumazine (RL-6-Me-7-OH), and 6,7-dimethyl-8-D-ribityllumazine (RL-6,7-diMe). Subsequently, other groups of antigens were identified as highly potent but very unstable MAIT agonists, they are 5-(2-oxoethylideneamino)-6-D-ribitylaminouracil (5-OE-RU) and 5-(2-oxopropylideneamino)-6-D-ribitylaminouracil (5-OP-RU) [108]. These compounds are pyrimidines derived by nonenzymatic condensation between the riboflavin precursor 5-amino-6-D-ribitylaminouracil (5-A-RU) and either methylglyoxal or glyoxal. These stimulatory metabolites are commonly produced by various microbes [143, 144], suggesting that MAIT cells can be activated in an MR1-dependent manner by various riboflavin producing microorganisms. A third group of compounds behave as MAIT cell antagonists [107]. They are derived from the photodegradation of folic acid (vitamin B9), and include 6-formyl pterin (6-FP), its acetylated form, acetyl-6-FP (Ac-6-FP) and two other variants. They all bind and stabilize MR1, upregulate MR1 surface expression, and prevent MAIT cell activation by competing with MAIT antigens for MR1 binding [107, 145-147]. MR1 tetramers were generated after identifying the last MR1 ligands [108, 146, 148] and were used to track MAIT cells by flow cytometry and tissue- and cell-imaging [149, 150]. By using 5-OP-RU tetramers, MAIT cells

can be specifically detected. More recently, a range of small organic molecules, drugs, drug-like molecules and drug metabolites have been identified as novel MR1 ligands [151]. Overall, MR1 can bind a broad range of small compounds. Notably, none of the identified ligands are accumulated endogenously.

1.3.7 MAIT cell TCR recognition of MR1-ligand complexes

Mutagenesis studies showed that the MAIT TCR α chain is very important in MR1 antigen recognition [152], whereas the TCR β chain establishes contacts mostly with MR1 protein residues [153]. Comparing the structure of ribityl lumazines, pyrimidines and folic acid derived pterins, the stimulatory antigens contain an extra ribityl moiety. Crystallography studies showed that the ribityl moiety of MAIT antigens forms a hydrogen bond with tyrosine at position 95 (Y95) in the CDR3α loop of the MAIT TCR [108, 152]. As folic acid derived pterins lack this structure, they do not interact with the TCR CDR3α loop, and therefore do not activate MAIT cells [146, 154].

MAIT agonists 5-OE-RU, 5-OP-RU and the antagonists 6-FP and Ac-6-FP form a Schiff base with MR1 at amino group K43, which is located in the antigen-binding pocket [107, 108, 146]. The Schiff base stabilizes antigen binding to MR1 and contributes to MR1 cell surface upregulation [139]. In contrast, although the ribityl lumazine RL-6-Me-7-OH establishes multiple interactions with MR1, without forming a Schiff base [108, 145]. An important consequence is that this ligand is much less potent in MR1 stabilization and surface upregulation [151]. The MR1 binding groove consists of two distinct compartments, an A′ pocket and an F′ pocket. So far, all of the known ligands sit in the A′ pocket and leave the F′ pocket empty [141], suggesting that bigger MR1-binding ligands may exist and may be recognized not only by MAIT cells but also by additional T cell populations.

1.4 MR1-restricted T (MR1T) cells

MAIT cells are known as a group of classical MR1-restricted T cells and several groups of novel non-MAIT T cells restricted by MR1 have been more recently identified [1, 155-157]. In particular, in 2017 Lepore et al. reported an atypical MR1-restricted T cell population (called MR1T) that does not respond to microbial antigens and folate-derivatives but exhibits anti-tumour responses [1]. A few years later, Crowther et al. found that a single MR1T cell clone can induce cell death in many different cancer types via MR1 [157]. These findings indicated that a population of MR1-restricted T cells recognize endogenous antigens accumulating in tumour cells.

1.4.1 MAIT versus MR1T cells

The MR1T cells were initially isolated after stimulation of T cells from healthy donors with a melanoma cell line expressing large amounts of MR1 molecules (A375-MR1) in the absence of any exogenous antigens [1]. The activated and proliferating T cells were isolated, cloned and characterized. As they were MR1-restricted but did not recognize the microbial ligands that stimulate MAIT cells, they were named MR1T cells. In contrast to MAIT cells, MR1T cells showed many diverse features (Figure 1-1 and Table 1-1). MR1T cells may express both the TCRαβ or TCRγδ, which are polyclonal and do express unique V-J rearrangements. In the blood of healthy individuals, MR1T cells are found at a frequency ranging between 1:2500 (0.04%) and 1:5000 (0.02%) of circulating total T cells, which is much less than MAIT cells [1]. MAIT cells are enriched in various tissues and organs, while whether MR1T cells preferentially localize in some tissues is not clear yet. MAIT cells express various surface markers, which are distinct from MR1T cells. In our laboratory, more than 200 MR1T cell clones were isolated and found mainly double negative, CD8$^+$, and CD4$^+$ (our unpublished results). Only a few of them express CD161 [1]. Functional studies also showed that MAIT and MR1T cells can be diverse. After stimulation with tumour cells, MR1T cell clones display diverse profiles of Th1, Th2 and Th17 cells, and can release other soluble factors (MIP-1β, soluble CD40L, PDGF-AA and VEGF) [1]. In contrast, under the same conditions MAIT cells showed mainly Th1-biased responses. Additionally, MR1T cell clones showed lower expression of chemokine receptors CCR4 and CCR6 than MAIT clones. Altogether, these findings suggested that MR1T cells are phenotypically and functionally heterogeneous.
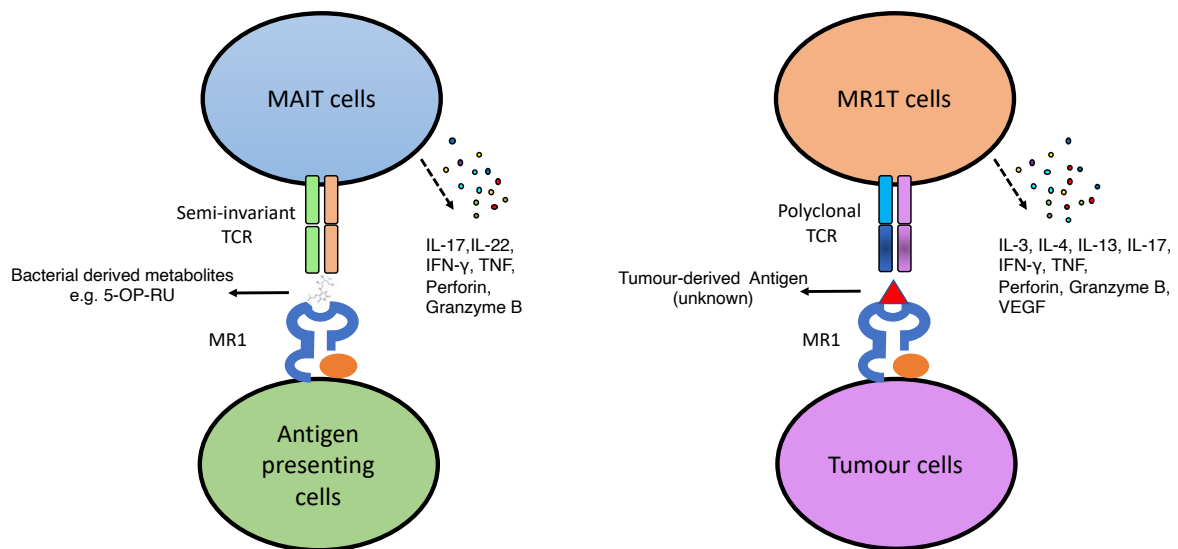
Figure 1-1. Overview of MAIT cell and MR1T cell antigen recognition and function.

(Left) Schematic image of a MAIT cell recognizing bacteria-derived antigens (5-OP-RU) presented by MR1. Once MAIT cells get activated, they produce proinflammatory cytokines and cytolytic proteins. (Right) Schematic image of a MR1T cell recognizing a tumour-derived antigen with unknown structure presented by MR1. The recognition of the tumour-derived antigen is mediated by its polyclonal TCR. Once MR1T cells become activated, they produce more diverse cytokines, cytolytic proteins and induce direct tumour cell killing.

Table 1-1. Main characteristics of human MAIT cells and MR1T cells.

Name	TCR	Frequency in blood T cells	Presence in organs	Cell Surface Phenotype	Antigen Recognition	Effector Function	Ref.
MAIT	Semi-invariant	1-10%	Liver, gastrointestinal tract, lung, thymus, lymph nodes, spleen, kidney, skin	DN or DP or CD8 or CD4, CD161, CD26	Microbes, Vitamin B2, B9 related metabolites	Th1, Th2 and Th17 cytokines	[151, 158-160]
MR1T	Polyclonal, TCRαβ or TCRγδ	0.02% - 0.04%	Unknown	DN or CD8 or CD4	Tumour-derived antigens	Th1, Th2 and Th17 cytokines growth factors	[1, 157]

1.4.2 Antigens stimulating MAIT and MR1T cells

MR1T cells are activated by antigens accumulating in tumour cells from different tissues in a MR1 dependent manner [1]. T cells transfected with one MR1T TCR could recognize a tumour cell line [157], suggesting that at least in that case the activation was TCR mediated. Currently, the antigens of MR1T cells remain unknown. Initial characterization of MR1T-stimulatory

antigens showed that individual MR1T cell clones recognize multiple cancer cell lines, illustrating that cancer cells share common antigens with MR1T cells [1, 157]. However, different MR1T TCRs may recognize different tumour antigens. Indeed, the stimulatory molecules were isolated from a freshly explanted mouse breast tumour expanded *in vivo* or from lysates of human leukemia cells expanded *in vitro* and purified they stimulated in a specific manner different MR1T cell clones [1]. The MR1 binding of the stimulatory molecules was displaced by the microbial MR1 ligands 5-OP-RU [108] and also by Ac-6-FP [107], illustrating that they occupy the same binding pocket as the other MR1 ligands [1, 157]. In addition, antigens derived from tumour lysates formed stable complex with the plastic-bound MR1 K43A mutant and activated specific MR1T cell clones without the need of antigen processing within living APCs [1]. These findings also clearly showed that they do not need the formation of a Schiff base with K43, like some of the microbial MAIT antigens [107]. In our collection of MR1T cell clones we also found some clones which did not react to the MR1 K43 mutant, like the single TCR of the published study [157]. Whether K43 is required to form a Schiff base or instead to provide the correct conformation to MR1 for TCR recognition, remains to be investigated. Collectively, the antigens recognized by MR1T cells are different from those stimulating MAIT cells, and are self-antigens expressed by tumour cells grown *in vitro* or *in vivo*.

1.4.3 Perspectives on use of MR1T cells in cancer immunotherapy

MR1T cells offer the opportunity to novel approaches of cancer cell therapy. This possibility is justified by the following considerations. First, MR1 is ubiquitously expressed on all types of human cells [137, 138], and it is highly conserved in mammals [136]. Furthermore, it is encoded by a non-polymorphic gene, thus the same MR1 protein is present in the human population. This peculiar characteristic avoids selection of tumour-specific T cells which must be MHC compatible with the MHC of the cancer patient to be treated. Secondly, many MR1T cells recognize different tumours but not normal cells, thus they represent *bona fide* tumour - specific T cells [1, 157]. Thirdly, MR1T cells recognize metabolites which are important in tumour cell proliferation (see Results section). Thus, it is difficult to envisage ready selection of tumour cells which escape recognition by avoiding antigen generation. Fourth, MR1T cells use a polyclonal TCR repertoire and recognize multiple antigens. This feature increases the chance of finding tumours, which are stimulatory and thus can be recognized and killed by

killer cells engineered to express MR1T TCR. Taken together, these features attribute novel and unique features that will need to be exploited in the clinic in the near future.

As my results also showed that a class of MR1T-stimulating molecules are represented by nucleoside adducts generated by condensation of carbonyls with different nucleosides and some of these contain ribose, in the following paragraphs I briefly describe the features of carbonyls and RNA adducts biology, which are most relevant to my studies.

1.5 Reactive carbonyl species

Reactive oxygen species (ROS) are continuously produced as a natural by-product of normal aerobic metabolism of oxygen [161, 162]. Examples of ROS include hydroxyl radical, singlet oxygen, peroxides, and superoxide [163]. In normal cells, the concentration of ROS is maintained in a steady range, while accumulation of ROS can occur within the cells and potentially lead to the progression of various diseases and disorders, including diabetes [164], hypertension [165], neurodegenerative disorders induced Alzheimer's disease [166] and different types of cancers [167].

More than 20 reactive carbonyl species have been identified in biological samples [168], such as acrolein, acetaldehyde, glyoxal, methylglyoxal (MG), 4-hydroxynonenal, 4-oxo-2-nonenal and malondialdehyde (MDA). Their structures are shown in Figure 1-2. Reactive carbonyl species are implicated in the development of cancer and other diseases, due to their damaging effects on proteins, nucleic acids, and lipids [169-171]. They can enter cell from the exogenous environment, such as pollutants of chemical industry, cigarette smoke, and food additives [172-175], and are also produced endogenously as the main products of ROS [176]. The intercellular production of reactive carbonyl species is generated endogenously during enzymatic reaction, such as glycolysis, or the nonenzymatic processes, such as lipid peroxidation, amino acid oxidation, and glycation [177-179]. In this thesis, we are mainly introducing two major mechanisms of endogenous reactive carbonyl species production, glycoxidation and lipid peroxidation[167].
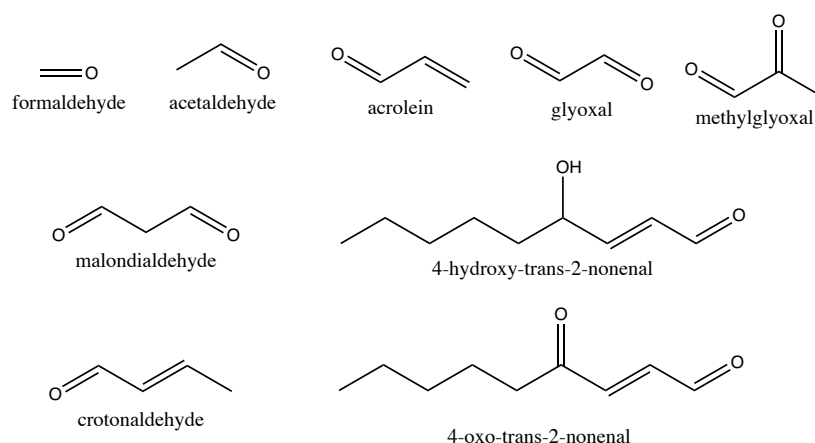
Figure 1-2. The structures of some common biological reactive carbonyl species.

1.5.1 Carbonyls produced *via* glycoxidation

Glycation is a nonenzymatic process which occurs mainly in the bloodstream, where carbonyl products of the metabolism of sugars such as glucose and fructose bind to protein or lipid through various chemical reactions[180]. Methylglyoxal (MG) and glyoxal are reactive carbonyl species primarily generated as side products of glycolysis [181, 182]. They are also known to be involved in the formation of advanced glycation end products (AGEs) [183]. When a cell has an excess of glucose and free oxidants, glycoxidation occurs and consequently increases the endogenous AGE formation. AGEs affect almost all type of cells and molecules and have been implicated in vascular complications of diabetes related diseases [183-185]. In addition, high levels of MG and AGE have also been detected in Alzheimer's disease patients as well as in breast and colon cancer tissues [176, 183].

1.5.2 Carbonyls produced *via* lipid peroxidation

Oxidative degradation of lipids, so called lipid peroxidation, arises as the consequence of increased intracellular oxidant levels [186, 187]. More than 30 different aldehydes were identified as products of lipid peroxidation. Malondialdehyde (MDA), acrolein, crotonaldehyde, 4-hydroxy-2-nonenal (HNE), and 4-oxo-2-nonenal (ONE) are major end products [188] (Figure 1-2). MDA is the most abundant by-product of lipid peroxidation, comprising approximately 70% of the total produced by lipid peroxidation [187]. Many lipid peroxidation products are highly reactive and potentially carcinogenesis. They form adducts with DNA and RNA and induce cellular damage [188]. Pyrimido[1,2-α]purine-10(3H)-one-2'-deoxyribose (M1dG), the major adduct of malondialdehyde with DNA was detected in human larynx cancer and breast cancer tissues [189,

190]. 4-oxo-2-nonenal and DNA formed adducts were detected in a colorectal cancer mouse model[191], and in samples of gastric mucosa from gastric cancer biopsies [192]. Acrolein-DNA adducts were found in human bladder cancer [193] and in lung cancer [194]. In addition, researchers found that knockout Glutathione peroxidase 4 (GPX4) induces embryonic death in mice [195, 196]. GPX4 is a phospholipid hydroperoxidase for reduction of membrane lipid peroxidation, suggesting that elimination of lipid peroxidation is essential for mammals [197].

1.5.3 Carbonyl metabolizing enzymes and their roles

Many enzymatic systems are involved in metabolism of reactive carbonyl species (Figure 1-3). Important for cell survival is the presence of an efficient system to degrade toxic carbonyl compounds [169, 171, 198]. Oxidation of several reactive carbonyl species is mostly performed by the enzymes aldehyde dehydrogenases (ALDH) and cytochrome P450 (CYP). ALDH enzymes are present mainly in liver, and at lower levels in many tissues [199]. They convert aldehydes to carboxylic acids [200, 201]. The ALDH family is constituted by 19 different enzymes in humans [202]. Each ALDH enzyme is involved in the oxidation of different reactive carbonyl species generated in different metabolic processes. The most abundant carbonyls are those generated during lipid peroxidation and they are substrates of several members of ALDH family enzymes [203]. Similar to ALDH, CYP are a large family of enzymes involved in detoxification of exogenous drugs [204] and products of endogenous metabolism, including reactive carbonyl species. In humans, CYP are mainly located in the inner membrane of mitochondria or in the endoplasmic reticulum [205]. This localization facilitates the immediate degradation of carbonyls generated in different cellular compartments.

Three additional families of enzymes participate in reduction of reactive carbonyl species, and they include Alcohol dehydrogenases (ADH), short chain dehydrogenase reductases (SDR) and Aldo-keto reductases (AKR) [206]. ADH enzymes are present in many organisms. They catalyse the conversion of toxic aldehydes and ketones to useful alcohols by the reduction of the coenzyme nicotinamide adenine dinucleotide (NAD^+) to NADH. In humans, five classes of ADH isozymes have been identified (ADH I-V) [207]. They function as homodimers that have different expression levels. Around 95% percent of ADH I, II and III are located in the liver [208], while, other ADH enzymes are ubiquitously present in other tissues, like stomach, brain and gastrointestinal tract for local detoxification [207, 209]. The SDR superfamily catalyses the NADPH-dependent reduction of many reactive carbonyl species [210]. Some of the SDR enzymes metabolize lipid peroxidation products, for example 4-oxo-2-nonenal [211,

212]. SDRs are ubiquitously expressed in human tissue [213-215] and they are mainly located in cytosol, but are also found in the endoplasmic reticulum and mitochondria [171]. AKR family is also composed of many enzymes that are involved in the detoxification of aldehydes into alcohols in a NADPH-dependent manner [216]. AKR enzymes reduce a broad range of carbonyl compounds, including those related to glucose [217], to lipid peroxidation [218, 219], to steroid metabolism [220], and also chemical and metabolic carcinogens [221-224]. This family is composed of more than 100 members and is ubiquitously expressed in different tissues, such as liver, brain, lung, and kidney [216, 225].

Conjugation with glutathione (GSH) by glutathione S-transferases (GST) is the major detoxication pathway for several reactive carbonyl species [226], such as glyoxal, methylglyoxal, acrolein and HNE. With the help of GST, GSH conjugation is catalysed up to 600 times faster than in GST absence [171]. Several classes of GST have been identified in cytosol, mitochondria, and microsomes [227]. In addition, higher levels of GST are detected in tissues with susceptible oxidative damage, like aorta, heart, and brain [228]. Glyoxalase (GLO) system is also known to detoxify some reactive carbonyl species in a GSH-dependent manner [171]. This detoxification process is catalysed by the sequential action of two enzymes, GLO I and GLO II. Unlike other enzymes that degrade reactive carbonyl species , GLO enzymes are mainly involved in reducing the intracellular quantities of methylglyoxal [176].
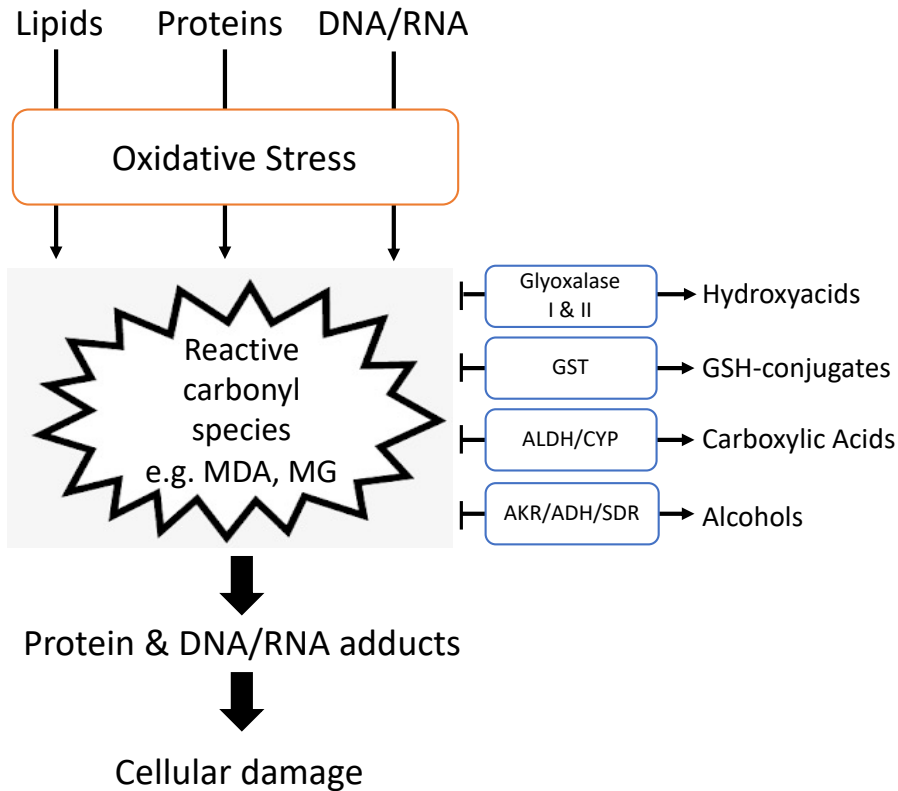
Figure 1-3. Simplified representation of reactive carbonyl species production and detoxification pathways.

Lipids, proteins, DNA and RNA are modified by reactive carbonyl species as consequence of oxidative stress. Reactive carbonyl species such as MDA and MG may accumulate inside stressed cells and form adducts with protein and nucleosides, thus inducing cell damage. Several enzymatic systems are involved in detoxifying reactive carbonyl species. They include glyoxalase I/II that generate hydroxy acids of MG and glyoxal, ALDH and CYP that generate respective carboxylic acids, ADH, AKR or SDR that generate alcohols, GSH by GST that form carbonyl GSH conjugates.

1.6 Naturally occurring RNA modifications

RNA consists of four ribonucleosides, adenosine (A), guanosine (G), cytidine (C), and uridine (U). They are essential in various biological processes [229]. Messenger RNA is essential for transcription of genetic sequences and their translation into protein. In addition to mRNA, other types of RNA exist that not directly involved in protein translation. They include transfer RNA (tRNA), ribosomal RNA (rRNA), small RNA (sRNA), and microRNA (miRNA). Their biological functions are not been fully characterized [229]. The relevance of non-protein-coding RNAs has been assesses also to have some roles in epigenetic modifications of the genome [230, 231]. More than 100 RNA modifications have been found mainly within RNAs and most of them are non-protein-coding RNAs [232-235]. Their chemical structures and their links to human diseases are shown in Figure 1-4 [229, 235]. Some modifications are generated by nonenzymatic processes, such as glycation, or oxidative damage as described in Chapter 1.5. Enzymes may add chemical moieties and their effects result in nucleoside modifications, such as methylations, hydroxylation, thiolations, ring closures, glycosylation, and addition of multiple ribose or amino acids [229].

Increasing evidence suggests that RNA epigenetic processes are also closely involved in various human diseases. Dysregulation of approximately half of the known RNA modification enzymes is associated with pathogenesis of human diseases, ranging from cancer [236-238] neurological disorders [239-242] metabolic illnesses [243, 244], and genetic defects [245-247]. Dysregulated RNA modifications may cause imbalanced control of cellular metabolism and protein synthesis. As a whole, better understanding of RNA modifications would clarify their biological functions as well as their potential roles as therapeutic targets. In my thesis, I focus on RNA modifications, as they accumulate in some cancers and have a known connection to cancer pathogenesis. They can stimulate some MR1T cells and upon accumulation in cancer cells they can be novel types of tumour-associated antigens.
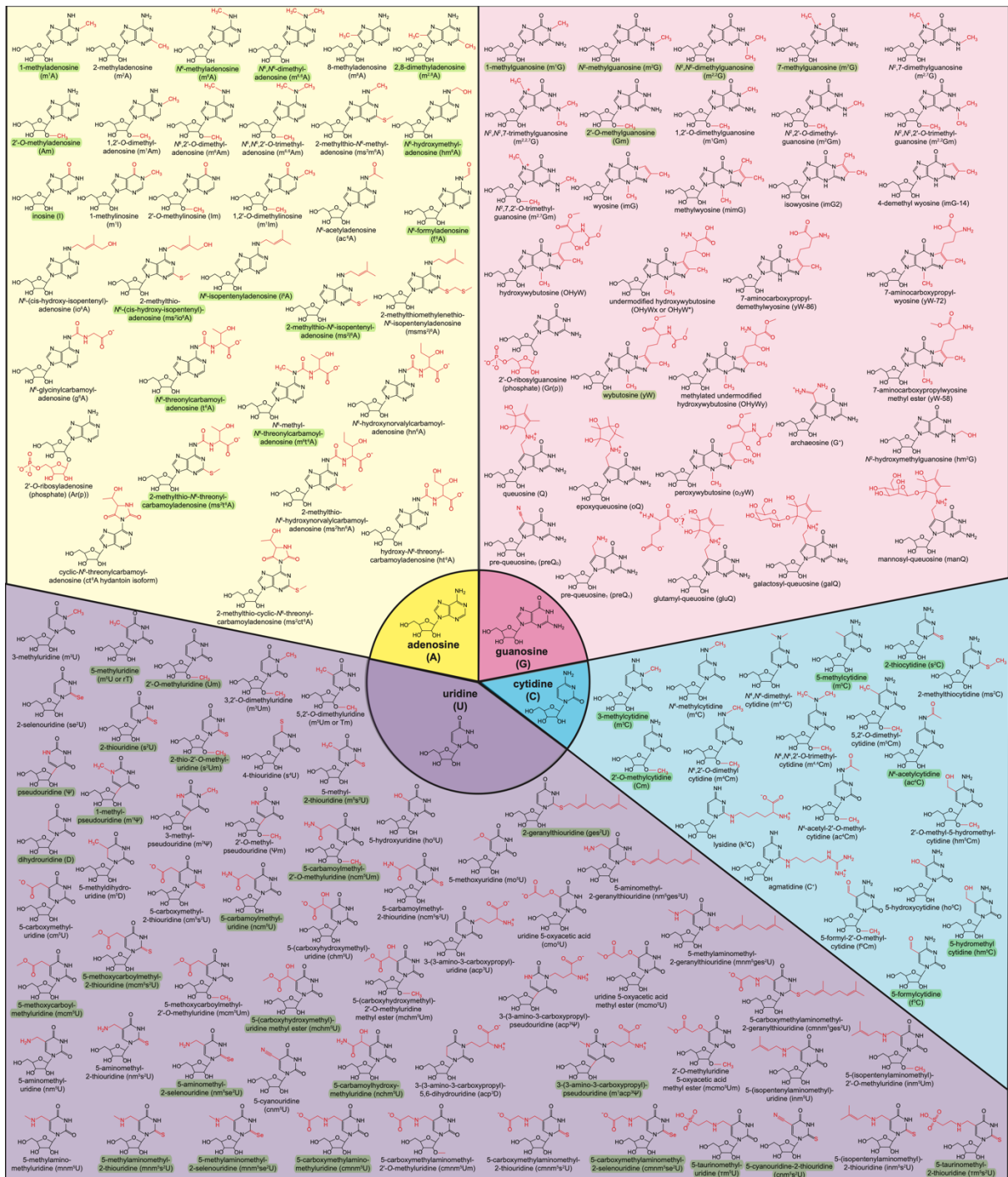
Figure 1-4. Chemical structures of all currently known RNA modifications and their links to human disease.

Figure was modified from [229, 235]. Adenosine-derived (yellow), guanosine-derived (pink), uridine-derived (purple), and cytidine-derived (cyan) modifications are classified based on the reference nucleotide. Red moieties indicate the site of modification. The ones have been associated with human diseases are highlighted in green.

1.7 Aims

In recent years, our laboratory isolated a novel population of MR1-restricted T cells that we called MR1T cells. MR1T cells are distinct from MAIT cells as they do not recognize riboflavin-related metabolites and exhibit polyclonal TCRs. Strikingly, they demonstrate preferential recognition of tumour cells and not of healthy cells, indicating that the stimulatory antigens accumulate in tumour cells.

The aim of my PhD project was to identify and characterize the tumour antigens that stimulate MR1T cells. The specific goals of the project were:

1) to identify and characterize nucleobase-aldehyde adducts that stimulate MR1T cells (described in Chapter 3).

2) to purify and characterize MR1T antigens from tumour cells (described in Chapter 4).

3) to explore the capacity of naturally modified RNA and DNA nucleobases to stimulate MR1T cells (described in Chapter 5).

Chapter 2 Materials and methods

2.1 Human blood samples

Blood samples from healthy donors used for T-cell cloning, FACS analysis and antigen-presentation assays were obtained from the University Hospital Basel. The study was approved by the local ethical review board (EKNZ, Ethics Committee North-West & Central Switzerland, EKNZ 2017-01888 and EK128/13), and all healthy donors consented in writing to the analysis of their samples. The representative MAIT clone (MRC25) used in this study was generated from blood of a healthy donor and maintained in culture as previously described [102]. MR1T cells were isolated from the peripheral blood of healthy individuals following a previously described protocol from our lab [1]. T-cell clones were periodically re-stimulated following the same protocol [102].

2.2 Cell culture

Tumour cell lines A375 and THP-1 were cultured in RPMI-1640 supplemented with 10% Fetal Calf Serum (FCS), 2 mM L-glutamine, 1 mM sodium pyruvate, 1x MEM NEAA and 50 μg/ml kanamycin (all from Bioconcept). Cells were free from Mycoplasma as evaluated by PCR analysis on DNA samples. When possible, cells were authenticated by staining with mAb for specific cell surface markers. Lentiviral transductions were carried out as previously described [1]. Transduced cells were selected by FACS based on the expression of EGFP or mCherry reporters, or by 2 μg/mL puromycin (Calbiochem, Cat#540411) resistance.

CHO-K1 cells stably expressing MR1 K43A mutant as soluble recombinant β2m-MR1-IgG-Fc fusion protein obtained as described before [1] are maintained in RPMI-1640 supplemented with 1 mM sodium Pyruvate, 2 mM stable Glutamine (Ala-Gln), 1% NEAA and 50 μg/mL Kanamycin (complete medium) and with 3% heat-inactivated FCS.

All human T-cell clones were cultured in RPMI-1640 supplemented with 5% AB-positive human serum (Blutspendezentrum SRK beider Basel, Basel, Switzerland), 2 mM L-glutamine, 1 mM sodium pyruvate, 1x MEM NEAA and 50 μg/ml kanamycin (all from Bioconcept) and 100 U/ml recombinant human IL-2 (Peprotech).

2.3 Preparation and purification of synthetic antigens

2.3.1 Synthesis of 8-(9H-purin-6-yl)-2-oxa-8-azabicyclo[3.3.1]nona-3,6-diene-4,6-dicarbaldehyde (M₃ADE)

M₃ADE was synthesized as previously described [248] with some modifications. 1,1,3,3-Tetraethoxypropane (1.1 g, 5 mmol, 4.0 equivalent (eq.), Sigma-Aldrich, Cat#T9889) in aqueous (aq.) HCl (25 mL, 1 M) was stirred at 40°C for 1 h. Subsequently, a solution of adenine (168.9 mg, 1.25 mmol, 1.0 eq., Sigma-Aldrich, Cat#A8626) in water (25 mL) was added. The mixture was adjusted to pH 4.0 with aq. NaOH (1 M) and stirred for 5 days at 37 °C. M₃ADE was purified by solid phase extraction over Sep-Pak C18 2 g cartridges (Waters Corp., Milford, MA, Cat#WAT036915). Cartridges were preconditioned with 10 mL water and 10 mL acetonitrile. Raw M₃ADE was washed with 20 mL water, 20 mL 10% acetonitrile, then eluted with 20 mL 20% acetonitrile.

M₃ADE HPLC purification was performed on a JASCO RHPLC system equipped with an MD-4010 Photo Diode Array detector. General adduct assessment was performed using an analytical 100 mm x 4 mm 5 µM NUCLEODUR C18 Pyramid HPLC column (Macherey-Nagel, Cat# 760204.40) at a temperature of 23°C where the mobile phases A and B were water and 95% methanol in water, respectively. Elution was performed with a flow rate of 1 mL/min with a linear gradient of 0% B for 2 min, 0-50% B from 2 to 17 min, 50-100% B from 17 to 18 min, 100% B from 18 to 20 min, 100-0% B from 20 to 21 min and 0% B until 25 min. Semi-preparative HPLC purification was performed using a semipreparative 250 x 10 mm 5 µM NUCLEODUR C18 Pyramid HPLC column (Macherey-Nagel, Cat# 762272.100) with same mobile phases and column temperature. Separation was performed with a flow rate of 6 mL/min with a linear gradient of 0-50% B from 0 to 15 min, 50-100% B from 15 to 38 min, 100% B from 38 to 43 min, 100-0% B from 43 to 44 min and 0% B until 50 min. M₃ADE yield was 12.5 mg. Biologically active HPLC peaks were collected for mass spectrometric and NMR analyses.

[1]**H-NMR** (600 MHz, D_2O, δ/ppm): 9.24 (s, 1H, H_{21}), 9.11 (s, 1H, H_{19}), 9.09 (s, 1H, H_{15}), 8.61 (s, 1H, H_2), 8.38 (s, 1H, H_8), 7.64 (s, 1H, H_{17}), 7.33 – 7.29 (m, 1H, H_{11}), 4.09 – 4.07 (m, 1H, H_{13}), 2.21 (ddd, $^2J_{H12a-H12b}$ = 13.7 Hz, $^3J_{H12a-H11}$ = 2.8 Hz, $^3J_{H12a-H13}$ = 2.8 Hz, 1H, H_{12a}), 2.03 (ddd, $^2J_{H12b-H12a}$ = 13.7 Hz, $^3J_{H12b-H11}$ = 2.2 Hz, $^3J_{H12b-H13}$ = 2.2 Hz, 1H, H_{12b}).

13C-NMR (151 MHz, D_2O, extracted from HSQC and HMBC, δ/ppm): 193.2 (C_{19}), 192.2 (C_{21}), 166.5 (C_{17}), 154.3 (C_4), 152.7 (C_2), 150.3 (C_6), 149.3 (C_{15}), 144.8 (C_8), 126.2 (C_{14}), 125.7 (C_{16}), 121.8 (C_5), 79.9 (C_{11}), 25.0 (C_{12}), 17.4 (C_{13}).

HR-ESI-MS: calcd. for $[M+Na]^+$ $C_{14}H_{11}N_5NaO_3$ m/z = 320.0754, found 320.0758.

2.3.2 Synthesis of pyrimido[1,2-α]purin-10(3H)-one (M_1G, CAS 103408-45-3)

M_1G was synthesized as previously described [249] with some modifications. 1,1,3,3-Tetraethoxypropane (1.4 g, 6.25 mmol, 5.0 eq.) in aq. HCl (25 mL, 1 M) was stirred at 40°C for 1 h. Subsequently, a solution of guanine (188.9 mg, 1.25 mmol, 1.0 eq., Sigma-Aldrich, Cat#G11950) in aq. HCl (25 mL, 1 M) was slowly added. The mixture was stirred at 40 °C for 1 h and then kept at 4 °C for 16 h. The precipitate was washed three times with absolute ethanol at 2000 x *g* for 10 min. The raw M_1G was extracted three times from the precipitate with 65°C water. The combined extracts were filtered with 0.22 µm filter. The mixture was adjusted to pH 7.0 with aq. NaOH (1 M).

M_1G HPLC purification was performed as for M_3ADE purification using the same type of HPLC column and mobile phases. General adduct assessment was performed using an analytical HPLC column with a flow rate of 1 mL/min with a linear gradient of 10% B for 2 min, 10-17% B from 2 to 8 min, 17-100% B from 8 to 8.5 min, 100% B from 8.5 to 11.5 min, 100-0% B from 11.5 to 12 min and 0% B until 16 min. Adducts separation was performed using a semipreparative HPLC column with a flow rate of 6 mL/min and a linear gradient of 0-20% B from 0 to 40 min, 20-100% B from 40 to 41 min, 100% B from 41 to 46 min, 100-0% B from 46 to 47 min and 0% B until 55 min. M_1G yield was 12.5 mg. Biologically active HPLC peaks were collected for mass spectrometric and NMR analyses.

1H-NMR (600 MHz, D_2O, δ/ppm): 9.31 (d, $^3J_{H13\text{-}H12}$ = 7.2 Hz, 1H, **H13**), 8.97 (dd, $^3J_{H11\text{-}H12}$ = 4.1 Hz, $^4J_{H11\text{-}H13}$ = 2.0 Hz, 1H, **H11**), 8.22 (s, 1H, **H8**), 7.30 (dd, $^3J_{H12\text{-}H13}$ = 7.2 Hz, $^3J_{H12\text{-}H11}$ = 4.2 Hz, 1H, **H12**).

13C-NMR (151 MHz, D_2O, extracted from HSQC and HMBC, δ/ppm): 162.9 (C_{11}), 154.4 (C_4), 154.1 (C_6), 149.9 (C_2), 146.0 (C_8), 138.4 (C_{13}), 116.7 (C_5), 112.0 (C_{12}).

HR-ESI-MS: calcd. for $[M+H]^+$ $C_8H_6N_5O$ m/z = 188.0567, found 188.0571.

2.3.3 Synthesis of N^6-(3-Oxo-1-propenyl)-2'-deoxyadenosine (OPdA, CAS 178427-43-5)

OPdA was synthesized as previously described [250] with some modifications. 2'-deoxyadenosine monohydrate (219 mg, 0.813 mmol, 1 eq., Sigma-Aldrich, Cat#D7400) was dissolved in 2 mL anhydrous dimethyl sulfoxide under argon atmosphere. Propargyl aldehyde (12 µl, 11.0 mg, 0.203 mmol, 0.25 eq., Toronto Research Chemicals, Cat#TRCP838440) was added to the stirred solution and additional propargyl aldehyde (1.25 eq.) was added over a 72h period. The reaction mixture was filtered and purified by preparative HPLC on a Shimadzu LC system (LC-20AT prominence liquid chromatograph, with an SPD-20A prominence UV/VIS detector (λ = 254 and 280 nm). Preparative HPLC purification was performed using a Reprosil-Pur 120 ODS 3,5 µM, 150 x 20 mm column (Maisch GmbH, Cat#r15.93.s1520), where the mobile phases A and B were water and 90% acetonitrile in water, respectively. Separation was performed with a flow rate of 9 mL/min with a linear gradient of 1-30% B from 5 to 15 min, 30-100% B from 15 to 17 min, 100% B from 17 to 21 min, 100-0% B from 21 to 22 min and 1% B until 25 min. Analytical HPLC was performed with a LC-20AD prominence liquid chromatograph combined with a Shimadzu LCMS-2020 liquid chromatograph mass spectrometer. Biologically active HPLC peaks were collected for mass spectrometric and NMR analyses. The OPdA yield was 13.5 mg.

General adduct assessment of OPdA was performed as for M_3ADE purification using the same type of HPLC column and mobile phases. Elution was performed using an analytical HPLC column with a flow rate of 1 mL/min with a linear gradient of 0% B for 2 min, 0-50% B from 2 to 17 min, 50-100% B from 17 to 18 min, 100% B from 18 to 20 min, 100-0% B from 20 to 21 min and 0% B until 25 min.

^{1}H-NMR (500 MHz, D$_2$O, δ/ppm): 9.21 (d, $^3J_{H13-H12}$ = 8.7 Hz, 1H, **H$_{13}$**), 8.49 (d, $^3J_{H11-H12}$ = 13.5 Hz, 1H, **H$_{11}$**), 8.43 (s, 1H, **H$_8$**), 8.38 (s, 1H, **H$_2$**), 6.45 (dd, $^3J_{H1'-H2'a}$ = 6.8 Hz, $^3J_{H1'-H2'b}$ = 6.8 Hz, 1H, **H$_{1'}$**), 5.89 (dd, $^3J_{H12-H11}$ = 13.5, $^3J_{H12-H13}$ = 8.7 Hz, 1H, **H$_{12}$**), 4.65 (ddd, $^3J_{H3'-H2'a}$ = 6.1 Hz, $^3J_{H3'-H2'b}$ = 3.5 Hz, $^3J_{H3'-H4'}$ = 3.5 Hz, 1H, **H$_{3'}$**), 4.19 (ddd, $^3J_{H4'-H5'b}$ = 3.8 Hz, $^3J_{H4'-H5'a}$ = 3.5 Hz, $^3J_{H4'-H3'}$ = 3.5 Hz, 1H, **H$_{4'}$**), 3.86 (dd, $^2J_{H5'a-H5'b}$ = 12.5 Hz, $^3J_{H5'a-H4'}$ = 3.4 Hz, 1H, **H$_{5'a}$**), 3.80 (dd, $^2J_{H5'b-H5'a}$ = 12.6 Hz, $^3J_{H5'b-H4'}$ = 4.3 Hz, 1H, **H$_{5'b}$**), 2.80 (ddd, $^2J_{H2'a-H2'b}$ = 13.7 Hz, $^3J_{H2'a-H1'}$ = 7.1 Hz, $^3J_{H2'a-H3'}$ = 6.4 Hz, 1H, **H$_{2'a}$**), 2.58 (ddd, $^2J_{H2'b-H2'a}$ = 14.0 Hz, $^3J_{H2'b-H1'}$ = 6.3 Hz, $^3J_{H2'b-H3'}$ = 3.5 Hz, 1H, **H$_{2'b}$**).

13C-NMR (126 MHz, D$_2$O, extracted from HSQC and HMBC, δ/ppm): 195.7 (**C$_{13}$**), 151.9 (**C$_2$**), 151.1 (**C$_{11}$**), 150.6 (**C$_4$**), 148.9 (**C$_6$**), 142.6 (**C$_8$**), 120.8 (**C$_5$**), 111.1 (**C$_{12}$**), 87.5 (**C$_{4'}$**), 84.7 (**C$_{1'}$**), 71.1 (**C$_{3'}$**), 61.6 (**C$_{5'}$**), 39.1 (**C$_{2'}$**).

HR-ESI-MS: calcd. for [M+Na]$^+$ C$_{13}$H$_{15}$N$_5$NaO$_4$ m/z = 328.1016, found 328.1020.

2.3.4 Synthesis of N^4-(3-Oxo-1-propenyl)-2'-deoxycytidine (OPdC, CAS 129124-79-4)

OPdC was synthesized as previously described [250] with some modifications. 2′-deoxycytidine (185 mg, 0.813 mmol, 1 eq., Sigma-Aldrich, Cat#D3897) was dissolved in 2 mL anhydrous dimethyl sulfoxide under argon atmosphere. Propargyl aldehyde (12.0 µL, 11.0 mg, 0.203 mmol, 0.25 eq.) was added to the stirred solution and additional propargyl aldehyde (1.25 eq.) was added over a 72-h period.

HPLC purification was performed as described for OPdA. The OPdC yield was 7 mg. Biologically active HPLC peaks were collected for mass spectrometric and NMR analyses.

1H-NMR (500 MHz, D$_2$O, δ/ppm): 9.31 (d, $^3J_{H10\text{-}H9}$ = 8.6 Hz, 1H, **H$_{10}$**), 8.29 (d, $^3J_{H8\text{-}H9}$ = 13.7 Hz, 1H, **H$_8$**), 8.19 (d, $^3J_{H6\text{-}H5}$ = 7.4 Hz, 1H, **H$_6$**), 6.28 (d, $^3J_{H5\text{-}H6}$ = 7.4 Hz, 1H, **H$_5$**), 6.24 (dd, $^3J_{H1'\text{-}H2'a}$ = 6.1 Hz, $^3J_{H1'\text{-}H2'b}$ = 6.1 Hz, 1H, **H$_{1'}$**), 5.91 (dd, $^3J_{H9\text{-}H8}$ = 13.7 Hz, $^3J_{H9\text{-}H10}$ = 8.6 Hz, 1H, **H$_9$**), 4.43 (ddd, $^3J_{H3'\text{-}H2'a}$ = 6.4 Hz, $^3J_{H3'\text{-}H2'b}$ = 4.3 Hz, $^3J_{H3'\text{-}H4'}$ = 4.3 Hz, 1H, **H$_{3'}$**), 4.12 (ddd, $^3J_{H4'\text{-}H5'b}$ = 4.8 Hz, $^3J_{H4'\text{-}H5'a}$ = 4.1 Hz, $^3J_{H4'\text{-}H3'}$ = 4.1 Hz, 1H, **H$_{4'}$**), 3.87 (dd, $^2J_{H5'a\text{-}H5'b}$ = 12.5 Hz, $^3J_{H5'a\text{-}H4'}$ = 3.5 Hz, 1H, **H$_{5'a}$**), 3.77 (dd, $^2J_{H5'b\text{-}H5'a}$ = 12.5 Hz, $^3J_{H5'b\text{-}H4'}$ = 5.3 Hz, 1H, **H$_{5'b}$**), 2.55 (ddd, $^2J_{H2'b\text{-}H2'a}$ = 14.1 Hz, $^3J_{H2'b\text{-}H1'}$ = 6.3 Hz, $^3J_{H2'b\text{-}H3'}$ = 4.3 Hz, 1H, **H$_{2'b}$**), 2.32 (ddd, $^2J_{H2'a\text{-}H2'b}$ = 14.2 Hz, $^3J_{H2'a\text{-}H1'}$ = 6.5 Hz, $^3J_{H2'a\text{-}H3'}$ = 6.5 Hz, 1H, **H$_{2'a}$**).

13C-NMR (126 MHz, D$_2$O, extracted from HSQC and HMBC, δ/ppm): 196.2 (**C$_{10}$**), 161.5 (**C$_4$**), 156.8 (**C$_2$**), 149.6 (**C$_8$**), 144.3 (**C$_6$**), 112.1 (**C$_9$**), 96.8 (**C$_5$**), 87.1 (**C$_{1'}$**), 87.1 (**C$_{4'}$**), 70.3 (**C$_{3'}$**), 61.1 (**C$_{5'}$**), 39.8 (**C$_{2'}$**).

HR-ESI-MS: calcd. for [M+Na]$^+$ C$_{12}$H$_{15}$N$_3$NaO$_5$ m/z = 304.0904, found 304.0902.

2.3.5 MS and NMR analysis of M$_3$ADE, M$_1$G, OPdA and OPdC

MS and NMR analysis of M$_3$ADE, M$_1$G, OPdA and OPdC was performed at Department of Chemistry, University of Basel. Unless otherwise stated, chemicals were used as received without further purification. NMR analysis of all of the antigens was performed at 298 K on a

Bruker Avance III NMR spectrometer operating at 500 MHz proton frequency equipped with a BBFO probehead or on a Bruker Avance III HD NMR spectrometer operating at 600 MHz proton frequency equipped with a cryogenic QCI-F probe. Standard pulse sequences were used for cosy, tocsy, noesy, hsqc, hmqc and hmbc 2D-NMR experiments and the spectra were processed using the topspin 4.0 software package. All compounds were fully characterized by means of 2D-NMR and HR-ESI-MS. For all compounds ^{1}H- and ^{1}H-^{13}C-HSQC or ^{1}H-^{13}C-HMQC spectra, as well as experimental and calculated HR-ESI-MS spectra are shown in Figure 3-15, 3-17-19.

HR-ESI-MS spectra were measured on a Bruker MaXis 4G high resolution ESI Mass Spectrometer in direct injection mode using methanol containing 0.1% v/v formic acid.

2.3.6 Synthesis of MGG

The protocol was based on [251] with some modifications. MGG was produced by mixing 100mM guanosine (Sigma, Cat#G6752) with 200mM methylglyoxal solution (Sigma, Cat#M0252) in DMSO (33.3%, v/v in water, Sigma Cat#D4540). The mixture was incubated for 5 hours at 70°C under 400 rpm shaking.

HPLC purification of MGG was performed on a JASCO RHPLC system as for M$_3$ADE purification using the same type of HPLC column and mobile phases. General adduct assessment was performed using an analytical HPLC column with a flow rate of 1 mL/min with a linear gradient of 3% B for 1 min, 3-13% B from 1 to 11 min, 13-100% B from 11 to 12 min, 100% B from 12 to 14 min, 100-0% B from 14 to 15 min and 3% B until 20 min. Adducts separation was performed using a semipreparative HPLC column with a flow rate of 6 mL/min. The initial mobile phase was 97% Solvent A, 3% Solvent B for 2.5min following a linear gradient of 3-13% B from 2.5 to 27.5 min, 13%-100% B from 27.5 to 30 min, 100% B from 30 to 35 min, 100-0% B from 35 to 37 min and 0% B until min 50. Biologically active HPLC peaks were collected for mass spectrometric and NMR analyses.

2.3.7 MS and NMR analysis of MGG

NMR analysis of MGG was performed by collaborators at the Pharmaceutical Biology group, Pharmacenter, University of Basel. ^{1}H-NMR results are shown in Figure 3-26.

2.3.8 Synthesis of Methylglyoxal-deoxyadenosine adducts (MGdA)

MGdA was synthesized using Methylglyoxal solution (909.1 μL, 100 mmol, 4.0 eq., Sigma-Aldrich, Cat#M0252) with 2′-deoxyadenosine monohydrate (336.6 mg, 25 mmol, 1 eq., Sigma-Aldrich, Cat#D7400) in water (50 mL) was added. The mixture was adjusted to pH 4 with Acetic acid (10 M) and stirred for 5 days at 37 °C. MGdA was purified by solid phase extraction over Sep-Pak C18 2 g cartridges (Waters Corp., Milford, MA, Cat#WAT036915). Cartridges were preconditioned with 10 mL methanol and 10 mL water. Raw MGdA was washed with 20 mL water, 20 mL 30% methanol, then eluted with 20 mL 100% methanol.

Sample eluted with C18 cartridge was further purified with SEP-PAK VAC QMA 12CC 2G cartridge (Waters Corp., Milford, MA, Cat#WAT054640). Cartridges were preconditioned with 10 mL methanol and 10 mL water. Raw MGdA was washed with 20 mL water, then eluted with 10ml 2% formic acid in H_2O, pH 2.0. The pH of eluted fraction after QMA cartridge was justified to pH 7 with aq. NaOH (1 M) and further purified with DSC-Ph 500mg cartridge (Sigma-Aldrich, Cat#52728). Cartridges were preconditioned with 5 mL methanol and 5 mL water. Raw MGdA was washed with 5 mL water and 5 mL 30% methanol, then eluted with 6 mL 60% methanol.

MGdA HPLC purification was performed as for M_3ADE purification using the same type of HPLC column and mobile phases. Separation was performed with a flow rate of 6 mL/min. The initial mobile phase was 3% Solvent B for 1 min following a linear gradient of 2-50% B from 1 to 41 min, 100% B from 41 to 44 min, 100-0% B from 44 to 45 min and 0% B until min 54.

2.3.9 Information of other synthetic compounds.

In Chapters 4 and 5, 37 synthetic compounds were tested for different biological assays. They were provided by different collaborators and from different companies (Table 2-1).

Table 2-1. List of other synthetic compounds used in this thesis.

Short name	MW (g/mol)	CAS Number	Company/Collaborator	Cat. No.
m6,6A	295.29	2620-62-4	Biosynth carbosynth	ND04708
i6A	335.36	7724-76-7	Toronto Research Chemicals	I821840
M1A	321.29	90107-94-1	Martterhorn Biosciences	MC-0000012
Etheno-A	291.27	2072145-55-0	Martterhorn Biosciences	MC-0000120
Crot-G 1	353.34	NA	Martterhorn Biosciences	MC-0000147
Crot-G 2	353.34	496909-40-1	Martterhorn Biosciences	MC-0000148
ONEC	379.40	190439-08-8	Martterhorn Biosciences	MC-0000119
m1A	281.27	15763-06-1	Cayman Chemical	CAY-16937-25
m2A	281.27	16526-56-0	University of Munich	--
Am	281.27	2140-79-6	Cayman Chemical	CAY-16936-5
t6A	412.35	24719-82-2	Toronto Research Chemicals	T405560
io6A	351.36	6025-53-2 or 15896-46-5	University of Munich	--
ms2io6A	397.45	52049-48-6	University of Munich	--
ms2i6A	381.45	20859-00-1	University of Munich	--
m6t6A	426.38	39667-81-7	University of Munich	--
Ar(p)	479.34	28050-13-7	University of Munich	--
me1G	297.27	2140-65-0	Toronto Research Chemicals	B426593
m2G	297.27	2140-77-4	University of Munich	--
m7G	297.27	20244-86-4	Sigma-Aldrich	M0627
Gm	297.27	2140-71-8	Cayman Chemical	CAY-21039-250
m2,2G	311.30	2140-67-2	University of Munich	--
Gr	415.13	NA	University of Munich	--
m6dA	265.27	2002-35-9	Sigma-Aldrich	M2389
i6Ade	203.20	2365-40-4	Cayman Chemical	CAY-17906-100
6DMAP	163.18	938-55-6	Sigma-Aldrich	D2629
MTA	297.33	2457-80-9	Sigma-Aldrich	D5011
Cm	257.25	2140-72-9	University of Munich	--
m3U	258.23	2140-69-4	University of Munich	--
m5U	258.23	1463-10-1	Sigma-Aldrich	535893
m3Um	272.26	NA	University of Munich	--
Q	409.39	57072-36-3	University of Munich	--
yW	508.49	55196-46-8	University of Munich	--
OHyW	524.49	NA	University of Munich	--
Psi	244.20	1445-07-4	Toronto Research Chemicals	P839605
N2MedG	281.27	19916-77-9	Toronto Research Chemicals	M293035
m6A	281.27	1867-73-8	Toronto Research Chemicals	M275895
MeP	134.14	2004-03-7	Sigma-Aldrich	M6502

NA: Not avaliable

2.4 Compound elution from soluble recombinant human MR1 produced by mammalian tumour cells

2.4.1 Cell adaptation and expansion for protein production

For soluble K43A MR1-IgG production, CHO-K1 cells were grown in serum-free medium (MAM-PF2 from Bioconcept 10-02F25-I, supplemented with 1 mM sodium Pyruvate, 2 mM stable Glutamine (Ala-Gln), 1% NEAA and 50 µg/mL Kanamycin). Medium containing soluble MR1-IgG was collected every 48h and replaced each time with new pre-warmed serum-free medium for two additional production batches from the same cells. Collected supernatants were centrifuged 5 min at 600xg, sterile-filtered through a 0.22 µM filter and stored at 4°C until further steps. As a control, supernatant from parental non-transduced CHO-K1 cells was collected and treated the same way in the following steps.

2.4.2 Soluble MR1 quantification and purification

Supernatant from cells was concentrated with Vivaspin 20 centrifugal concentrator with molecular cut-off at 100 kDa (MR1-IgG is ~160 kDa) (Sigma Aldrich Z614661). Tubes were repeatedly centrifuged at 3000xg for 15-20 min until the supernatant volume reached a final concentration of 20-30 times the initial volume. Concentrated protein was sterilized through a 0.22 µM syringe-filter.

Protein was quantified by ELISA using capture antibodies against β2m (clone HB28) and a detection antibody against MR1 (clone 26.5). As a standard, soluble MR1 monomers made in house were used. In addition, protein was also quantified by SDS-PAGE on 7.5% acrylamide gel in non-reducing conditions in parallel with known amounts of purified IgG antibodies. MR1-IgG concentration was calculated based on gel staining with SimplyBlue Safestain (ThermoFisher scientific, cat# LC6060) and band densitometry interpolation of IgG standards.

MR1-IgG was purified with Protein A MagBeads (Genscript L00273), according to manufacturer's instruction (for purification of 1 mg of MR1-IgG, 400 µL of 25% beads slurry is used). Beads were mixed with the supernatant and incubated overnight at 4°C under constant mixing. Beads were then extensively washed with PBS to remove contaminants and were transferred to a silanized glass tube (Thermo Fisher scientific CTS-1275).

2.4.3 Elution of MR1-bound compounds and HPLC fractionation

To elute compounds from MR1, beads were incubated sequentially twice in ddH_2O for 5 min, and then twice in 30% methanol (diluted in ddH_2O) for 5 min, with collection of the supernatant after each step. All the eluted material was pooled in silanized glass vials (Thermo Fisher Scientific SAA-SV2-2) and volume was reduced under N_2 stream. The material is dried or used directly for HPLC separation.

The HPLC purification of compounds were performed on a JASCO RHPLC system as for M_3ADE purification. The mobile phases A and B were water and 100% acetonitrile, respectively. Initially, elution was performed for biological assay (Figure 4-1). HPLC purification followed a flow rate of 1 mL/min with a linear gradient of 5 % B for 10 min, 5-50% B from 10 to 25 min, 50-100% B from 25 to 27 min, 100% B from 27 to 37 min, 100-5% B from 37 to 38 min and 5% B until 50 min. For MS analysis, a longer purification was performed using the same HPLC system (Figure 4-2). HPLC purification followed a flow rate of 1 mL/min with a linear gradient of 5 % B for 15 min, 5-35% B from 15 to 25 min, 35-100% B from 25 to 35 min, 100% B from 35 to 50 min, 100-5% B from 50 to 51 min and 5% B until 61 min. Fractions were collected each minute in silanized glass tubes, transferred to silanized glass vials and stored at -80°C until biological assays and Mass Spectrometry.

2.5 MS data acquisition and analysis of compounds from sMR1 CHO cells

The detection and identification of compounds from CHO sMR1 cells were made by Division of Environmental Health Sciences, Masonic Cancer Centre, University of Minnesota. The approach utilized a high resolution/accurate mass data dependent-constant neutral loss-MS^3 methodology developed for DNA adductomics [252]. The accurate mass measurements of the observed DNA or RNA adducts allows determination of their molecular formulas and the triggered MS^3 fragmentation spectrum provides structural information, as shown in Figure 2-1.
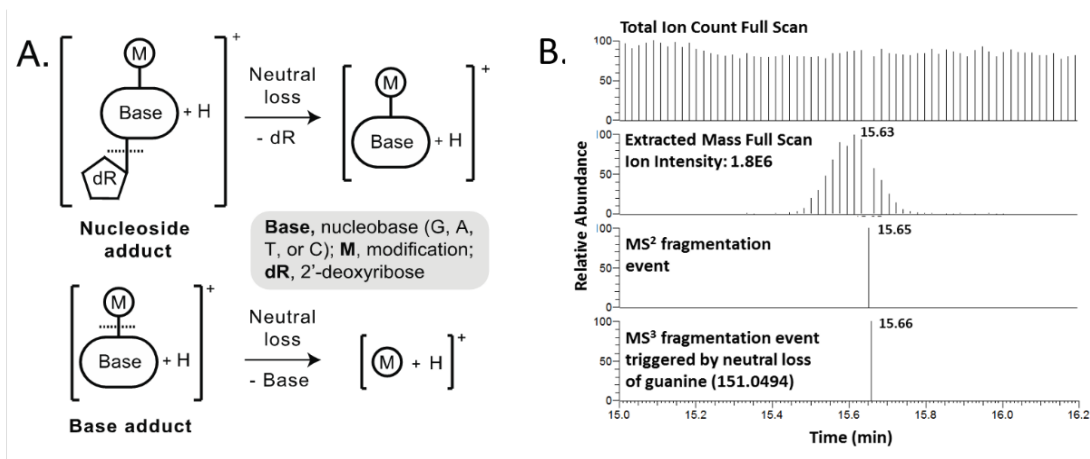
Figure 2-1.Overview of the untargeted DNA adductomics approach which was modified to include detection of modified RNA nucleosides.

Figure was modified from [252, 253]. (A) Typical fragmentation used for the identification of DNA adducts. (B) Example of a chromatogram illustrating the signal resulting from the detection of the neutral loss in the MS^2 fragmentation indicating the presence of an adduct whose peak can then be identified and extracted in the full scan.

2.5.1 Untargeted adductomics technical details

LC-MS experiments were performed on an Orbitrap Lumos mass spectrometer (Thermo Scientific, Waltham, MA) coupled to a Dionex RSLCnano UPLC (Thermo Scientific, Sunnyvale, CA). Reverse phase chromatography was performed with a hand-packed Luna C18 column (5 μm, 120 Å, 200 mm x 75 μm ID, Phenomenex, Torrance, CA) at room temperature and flow rate of 0.3 μL/min using 0.05% formic acid as mobile phase A and acetonitrile as mobile phase B. The LC gradient started at 2% B for the first 5.5 min with a flow rate of 1.0 μL/min, followed by switching of the injection valve to remove the 5 μL loop from the flow path, and reducing the flow rate to 0.3 μL/min over 0.5 minute. A linear gradient from 2% to 50% B over 39 min was used, then ramped to 95% B over 1 minute. The mobile phase composition was allowed to stay at 95% B for 2 min. Finally, re-equilibration was performed by changing the mobile phase composition from 95% to 2% B over 2 minute and increasing the flow rate to 1.0 μL/min over 1 minute, then held at 2% B for 2 min. The total run time was 52 min.

CNL-MS^n DDA was performed with the instrument operating in positive ionization mode, by repeated full scan detection followed by MS^2 acquisition and constant neutral loss triggering of MS^3 fragmentation over a cycle time of 3s. Full scan (range 100-1000 Da) detection was performed by setting the Orbitrap detector at 120,000 resolutions, using EASY-IC internal

37

mass calibration, normalized automatic gain control (AGC) target settings of 1E6, and maximum ion injection time set at 50 ms. The MS^2 fragmentation parameters were as follows: quadrupole isolation window of 1.5 amu, HCD collision energy of 25%, Orbitrap detection at a resolution of 15,000, AGC of 2E5, and maximum injection time of 50 ms. Data-dependent conditions were as follows: triggering intensity threshold of 2E4, repeat count of 1, and exclusion duration of 15 s. The MS^3 fragmentation parameters were as follows: 2 amu isolation window, HCD collision energy of 30%, Orbitrap detection at a resolution of 15,000, AGC of 2.0E5, and maximum injection time of 200 ms. Fragmentation was triggered upon the observation of neutral loss of deoxyribose (-116.0474), ribose (-132.0423), adenine (-135.0545), guanine (-151.0494), cytosine (-111.0433), thymine (-126.0429), uracil (-111.0433), adenine + water (-152.0651) and guanine + water (-169.0600) between the parent ion from the full scan and one of the product ions. The "AcquireX" feature was used with a blank injection used to generate timed ion exclusion lists of approximately 4500 ions with mass tolerances of 5 ppm. The identified MS^2 were compared with reference standards, with the RNA modifications database [232] and with the mzCloud compound database (https://www.mzcloud.org) in the untargeted method.

2.5.2 Targeted adductomics method

Targeted MS/MS was also performed using the same LC conditions as for the untargeted analysis and performed on a list of suspected modified nucleosides [254], with the following parameters: Orbitrap detection at a resolution of 30,000, HCD collision energy of 25%, quadrupole isolation window of 1.6 amu, AGC of 5.0E4, and a maximum injection time of 100 ms. Product ion detection was based on extracted ion chromatograms using mass accuracy tolerances of 5 ppm for all masses.

2.5.3 Adductomics data analysis

For modified nucleoside screening data analysis, FreeStyle 1.7 (Thermo Scientific, Waltham, MA) software was used to manually interrogate all MS^3-triggering analytes (not observed in negative controls) to identify all unknown modified nucleosides. Extracted ion chromatograms for all putative modified nucleosides were generated at 5 ppm mass tolerance. MS^2 and MS^3 spectra of each putative adduct was subsequently evaluated for structural information and the peak area of the precursor mass was determined using the known DNA adducts list [254] as reference.

2.6 Evaluation of compound biological activity

2.6.1 Cell surface MR1 upregulation

THP-1 or THP-1 MR1 cells (10^5 cells/well) were tested for MR1 surface expression after incubation with or without synthetic compounds for 6 h at 37°C with the following concentrations: M_3ADE (1 μM), OPdA (100 μM), M_1G (13μM) and OPdC (100 μM), i6A (25 μM), m6,6A (100 μM), M1A (50 μM), Etheno-A (50 μM), Croto-G1(50 μM), Croto-G2 (50 μM) and ONEC (50 μM). In addition, the other synthetic compounds were incubated with various concentrations as indicated in the figure axis. Ac-6-FP (100 μM) (Schircks Laboratories, Cat# 11.418) was used as positive control for MR1 surface upregulation. After blocking unspecific binding with 50% human AB serum in FACS Buffer (PBS with 0.1% BSA with 0.02% NaN$_3$, both from Sigma-Aldrich) for 15 min at 4°C, cells were stained with an anti-human-MR1-APC mAb (1μg/mL, clone 26.5, Biolegend Cat# 361108) or with APC-labelled mouse IgG2a, k isotype control (1μg/mL, clone MOPC-173, Biolegend Cat# 400220) antibodies for 20 min at 4°C. Cells were then washed with FACS buffer, centrifuged 5min at 600xg, resuspended in FACS buffer with 0.5 μg/ml DAPI (4′,6-diamidino-2-phenylindole, Sigma-Aldrich) and analysed by flow cytometry. For each condition, anti-MR1 median fluorescence intensity (MFI) was compared.

2.6.2 Activation assay with living and fixed antigen presenting cells (APCs)

MR1T cells ($5×10^4$/well unless otherwise indicated) were co-cultured with the indicated APCs (10^5 cells per well unless otherwise indicated) for 18 h in 120 μL volume in duplicate or triplicate. In some experiments, 30 μg/mL anti-MR1 mAbs (Ultra-LEAF™ Purified clone 26.5, Biolegend, Cat#361110) were added and incubated for 30 min at 37°C prior to the addition of T cells.

When nucleobases, nucleosides or nucleotides (Figure 3-1, all 250 μM, all from Sigma-Aldrich) and synthetic compounds were used to stimulate T cells, the THP-1 cells (10^5/well) were cultured 2 h with the indicated molecules or medium only, prior to T-cell addition. In Figure 3-22, and 3-23 100 μM OPdA, 100 μM OPdC and 13 μM M_1G were used for all clones, while 100 μM M_3ADE was used for all clones except DGB129, AC1A4, AC1B76 and AVA46 for which 1 μM was used. In Chapter 4, i6A (50 or 100 μM), m6,6A (33 μM), M1A (50 μM), Etheno-A (50 μM), Croto-G1(50 μM), Croto-G2 (50 μM), ONEC (50 μM) were used as the

highest concentration and the other synthetic compounds were incubated with various concentrations as indicated in the figure axis. In some experiments, MAIT cells were stimulated by APCs pulsed 2 h with freshly-prepared 5-OP-RU with indicated concentrations.

In experiments with Mycophenolic acid (10 µM, Sigma-Aldrich, Cat#M3536), EHNA (25 µM, Sigma-Aldrich, Cat#E114), S-p-bromobenzylglutathione cyclopentyl diester (BBG, 20 µM, Sigma-Aldrich, Cat#SML1306), THP-1 cells (10^6/mL) were treated with the indicated concentrations of drugs in complete medium at 37°C for 18 h before being washed twice with PBS, counted and used for T-cell activation. In experiments where THP-1 cells (10^6/mL) were treated with Doxorubicin (75 nM, Selleck Chemical, Cat#S1208) and Paclitaxel (5 µM, Sigma-Aldrich, Cat#T7191), the cells were incubated at 37°C for 18 h before being washed twice with PBS, counted, and incubated for 2 h with vehicle or 150 µM dAdo and 150 µM Guanosine (Sigma-Aldrich, Cat#D7400 and G6752, respectively) prior to T-cell addition.

In experiments where fixed A375-MR1 cells were used to activate MR1T cells, APCs ($4x10^5$/mL) were treated with Apocynin (APO, 100 µM, Sigma-Aldrich, Cat#W508454), L-Glutathione reduced (GSH, 4 mM, Sigma-Aldrich Cat#G6013), N-acetyl cysteine (NAC, 4 mM, Sigma-Aldrich, Cat#A9165), L-Buthionine-sulfoximine (BSO, 400 µM, Sigma-Aldrich, Cat#B2515) Mercaptosuccinic acid (MSA, 3.3 µM, Sigma-Aldrich, Cat#M6182), ML-210 (6 µM, Sigma-Aldrich Cat#SML0521) or 1S,3R-RSL3 (RSL3, 1 µM, Sigma-Aldrich, Cat#SML2234), Oleanolic acid (50 µM, Sigma-Aldrich, Cat#O5504) for 18 h at 37°C before being washed twice with PBS, fixed with 0.05% Glutaraldehyde (Sigma-Aldrich, Cat#G5882), counted and used for MR1T cell stimulation.

2.6.3 Activation assay with plate-bound soluble MR1

Recombinant human β2m-MR1-Fc was produced in CHO-K1 cells as previously described [1] and 4 µg/mL were coated onto 96 wells plates (Nunc, Cat#439454) for 18 h at 4°C. Plate-bound MR1 was then washed twice with wash buffer (150 mM NaCl, 20 mM Tris and 2% Glycerol, pH 5.6) to remove bound antigens. Then, the synthetic antigens (M_3ADE, OPdA, M_1G and OPdC) were added at the indicated concentrations and incubated for 6 h at room temperature. Unbound antigens were washed twice with PBS before the addition of excess PBS. In some experiments, bacteria-produced and refolded MR1-M_3ADE protein was serially diluted in PBS and added to a high protein binding plate (Nunc) for 2 h at 37°C then washed

twice and used in the stimulation assay. Indicated MR1T cell clones (10^5/100 µl/well) were added and supernatants were collected after 18 h. Released cytokines were detected by ELISA.

2.6.4 Competition assay

Competition assays were performed by incubating APCs (10^5 cells/well) with compounds for 3 hours at 37°C, then adding the antigen for each clone of interest at optimal concentration ($\geq$ EC50) and incubating for 2 additional hours before the addition of T cells (10^5 cells/well). As positive control for competition with antigens, Ac-6-FP was used (100 µM). Supernatants were collected after 18 h for cytokine analysis.

2.6.5 Cytokine Analysis

The following human cytokines were assessed by ELISA as previously described [1]: human IFN-γ (capture MD-1 mAb; revealing biotinylated 4S.B3 mAb, Biolegend Cat#507502 and 502504, respectively), human IL-13 (capture JES10-5A2 mAb; revealing biotinylated SB126d mAb, SouthernBiotech Cat#10125-01 and 15930-08, respectively).

2.6.6 ROS production measurement

CM-H2DCFDA (Thermo Fisher Scientific Cat#C6827) was used to assess ROS production in cell upon cell treatment with Doxorubicin and Paclitaxel (Figure 3-5 A). THP-1 cells (10^7/mL) were labelled with 10 µM CM-H2DCFDA for 30 min at 37 °C in the dark, then washed with PBS and resuspended in complete medium. 10^5 cells were seeded per well and treated with 75 nM Doxorubicin, 5µM Paclitaxel or vehicle for 18 h at 37 °C. Phorbol 12-myristate 13-acetate (PMA, 50 ng/mL, Sigma-Aldrich Cat#P8139) was used as positive control.

2.7 Data Analysis and Statistical Analysis

Data analysis, statistical tests and visualization were conducted in GraphPad Prism (v8.1.0, GraphPad Software, Inc.). Analysis was performed using multiple t-test, One- or Two-way ANOVA as indicated for each assay in figure legends. A p value < 0.05 was considered statistically significant. *$p < 0.05$, **$p \leq 0.01$, ***$p \leq 0.005$.

Chapter 3 MR1T cell activation by nucleobase-aldehyde adducts

3.1 Introduction

Previous studies conducted in our laboratory showed the presence of a novel population of human T cells, which efficiently recognize and kill various tumour cell types [1, 157]. These cells were called MR1T cells. They are restricted to MR1 and are distinct from MAIT cells as they do not recognize riboflavin-related metabolites. MR1T cells exhibit polyclonal TCRs and are adaptive-like T cells [42]. In particular. MR1T cell clones react to different compounds isolated from different tumour cells which can be purified and characterized, suggesting the presence of multiple stimulatory compounds and that different MR1T cells may recognize different antigens [1]. So far, the nature of the MR1T-stimulatory compounds as well as the role of MR1T cells in health and diseases remained unknown.

A common feature of tumour cells is their ability to reprogram their metabolic pathways to meet their abnormal demands of migration, malignant proliferation, and survival [255, 256], including a higher rate of glycolysis, of glutamine decomposition, upregulation of nucleotide and protein synthesis and important changes in lipid metabolism [257]. In order to get a close overview of the changes in tumour cell metabolism relevant to MR1T cell stimulation, a genome-wide CRISPR/Cas9-mediated gene disruption approach was performed as described [258]. It was expected that disruption of genes involved in antigen biosynthesis would affect formation of stimulatory compounds, thereby modifying MR1T cells recognition of tumour cells. For this purpose, A375 melanoma tumour cells were transduced with an MR1-β2m and Lenti Cas9-Blast construct (A375-MR1-Cas9 cells) containing a library of single guide RNAs (sgRNAs) covering the total human genome. These transduced cells were selected and then used as targets for the cytotoxic MR1T cell clone TC5A87. After three rounds of T-cell killing, each followed by a recovery phase, surviving A375-MR1 cells were analysed by amplicon-sequencing. The enriched or depleted sgRNAs in surviving cells were compared to the same cells not subjected to killing. Using binomial enrichment analysis of gene-ontology terms [259, 260] annotated to significant hits, several enriched and depleted (n=127 and 650, respectively) gene targets were revealed. Many of these genes were associated with metabolic processes. Multiple genes appeared coordinated in A375-MR1 cells and appeared to promote MR1T cell recognition. In parallel, a genome scale *in silico* model of human metabolism was performed [261] to explore the potential roles of the identified genes.

In summary, the CRISPR/Cas9 screen provided the first evidence that several metabolic pathways are related to A375 tumour cell recognition by MR1T cells. These genes were part

of nucleobase and nucleic acid metabolic processes, glycolytic pathway, methylglyoxal degradation, oxidative phosphorylation and purine metabolism. A manuscript with all these data has been submitted.

To validate the relevance of these genes and to address whether they contribute to accumulation of MR1T cell-stimulatory compounds, single gene KO A375-MR1 cells were generated and in parallel various drugs were tested to investigate their stimulatory or inhibitory behaviour. I contributed to these studies in the following experiments. I synthetized several candidate antigens, which I purified and tested for their capacity to stimulate various MR1T cell clones. To confirm and evaluate the biological role of these synthetic MR1T antigens, various assays were established, including activation of T cell clones, antigen presentation, and MR1 protein upregulation assays. In addition, the purification of synthetic compounds was established using solid-phase extraction (SPE) and HPLC procedures. Several tumour cell lines with different levels of MR1 expression were selected as APCs. In some experiments, THP-1 cells were used as APC because they constitutively express low surface levels of MR1 and induce a very low spontaneous MR1T cell stimulation. THP-1 and A375 cells transduced with the MR1 gene (THP-1-MR1 and A375-MR1 cells) expressing high surface levels of MR1. They were also utilized to check the surface upregulation of MR1 molecule and to stimulate MR1T cells for cytokine production assays. MR1T cell clones isolated from PBMCs of healthy donors were used to check their antigen specificity. As control, a MAIT-cell clone was included (Table 3-1).

Table 3-1. Phenotype, TCR gene usage of selected MR1T and MAIT cell clones

Clone	CD8α	CD8β	CD161	TCRα	TCRβ	React to tumour cells	React to riboflavin-related antigens
AC1A4	+	+	-	TRAV8-2	TRBV5-6	+	-
AVA34	+	+	-	TRAV19	TRBV12-4	+	-
AVA46	+	+	-	TRAV14/DV4	TRBV6-5	+	-
AC1B76	+	+	-	TRAV29/DV5	TRBV28	+	-
DGB129	+	+	-	TRAV29/DV5	TRBV12-4	+	-
LMC1D1	+	+	-	TRAV3	TRBV24-1	+	-
MCA2B1	+	+	-	TRAV10	TRBV4-3	+	-
MCA2E7	+	+	-	TRAV29/DV5	TRBV28	+	-
MCA3C3	+	+	-	TRAV12-1	TRBV24-1	+	-
QY1A16	+	+	+	TRAV9-2	TRBV6-5	+	-
QY1B42	+	+	-	TRAV25	TRBV20-1	+	-
QY1C3	+	+	-	TRAV27	TRBV29-1	+	-
TC5A87	+	-	-	TRAV13-1	TRBV25-1	+	-
TRA44	+	+	-	TRAV12-1	TRBV29-1	+	-
MRC25 (MAIT)	+	-	+	TRAV1-2	TRBV6-1	-	+

3.2 Purine metabolism is involved in MR1T antigen accumulation

Based on the results of our CRISPR/Cas9 screening, we first focused on the purine metabolism. To investigate the possible role of purines in MR1T cell stimulation, T cell activation assays were performed measuring IFN-γ release by ELISA. Initially, fifteen synthetic nucleotides, nucleosides or nucleobases (Adenine, Adenosine, Deoxyadenosine, AMP, ADP, ATP, Guanine, Guanosine, Deoxyguanosine, GMP, GDP, GTP, Inosine, Uridine, Xanthosine) were incubated with THP-1 cells as APCs, a human acute monocytic leukaemia cell line, and then the reactivity of different MR1T cells was investigated. MAIT cell clones were used as negative controls, as they do not react to A375-MR1 cells in the absence of microbial antigens (Table 3-1). As we expected, all tested MR1T cell clones reacted to A375-MR1 cells (in agreement with the fact that this reactivity was the selection criteria of MR1T cells), such responsiveness was used as positive control of MR1T cells capacity to become activated and release cytokines. A second positive control was represented by stimulation of MAIT cells with the MAIT antigen 5-OP-RU [108].

Three MR1T cell clones reacted differently to tested compounds: TC5A87 did not react to any of the tested compounds (Figure 3-1A); DGB129 was activated by adenine, adenosine, deoxyadenosine (dAdo) and inosine (Figure 3-1B); and MCA3C3 reacted to ADP, guanine,

guanosine, deoxyguanosine and xanthosine (Figure 3-1C). THP-1 cells incubated with the synthetic compounds did not stimulate MAIT cells (Figure 3-1D). Notably, despite high doses of the compounds being used, their release of cytokine was minimal compared to MR1T stimulation with A375-MR1, suggesting that these molecules might be intermediate precursors of antigens. In general, these findings suggested that human MR1T cell clones cross-react with antigens containing nucleobase/nucleoside cores and presented by MR1 molecules displayed on cancer cells.
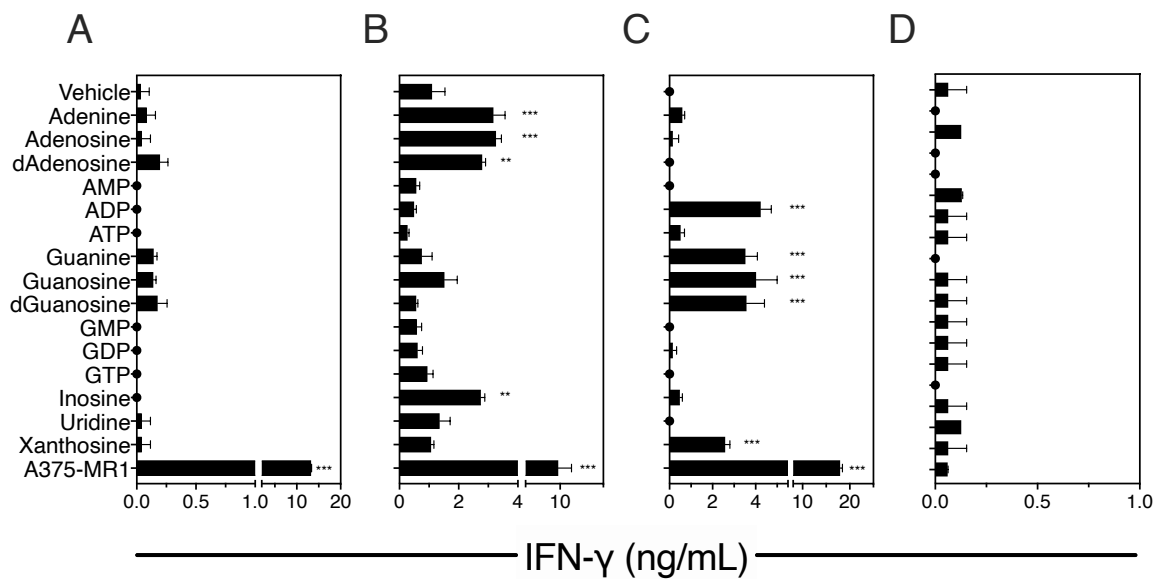
Figure 3-1. Purine metabolism is involved in MR1T antigen accumulation.

Activation of MR1T clones TC5A87 (A), DGB129 (B), MCA3C3 (C) and MRC25 (D) by THP-1 cells pre-incubated with 250 μM of the indicated molecules or A375-MR1 or vehicle. IFN-γ released is the mean ± SD of triplicate cultures or duplicate cultures (MRC25). One representative experiment of at least three independent replicates is shown in each panel. *p<0.05, **p≤0.01 and ***p≤0.001 compared to vehicle, One-way ANOVA with Dunnett's multiple comparison.

3.3 Methylglyoxal and purine metabolism cooperate in MR1T cell stimulation

To understand which metabolic pathways might be involved in recognizing nucleobase/nucleoside antigens on tumour cells by MR1T cells, the significantly depleted sgRNAs from our CRISPR/Cas9 screening caught our attention. Several glycolysis related genes were depleted including *TPI1* and *GLO1*. *TPI1* encodes the enzyme triosephosphate isomerase, which is responsible for converting dihydroxyacetone phosphate (DHAP) into

glyceraldehyde 3-phosphate (G3P) with the generation of methylglyoxal (MG) in the glycolytic pathway [181, 182]. Glyoxalase 1 (GLO1) is a ubiquitous expressed enzyme in the glyoxalase system for detoxification of a glycolysis by-product, MG [262-265]. MG is a highly reactive carbonyl. It is known to form advanced glycation end-products (AGEs) by inducing protein and nucleotides modification [266, 267]. To investigate the possible role of glycolysis in MR1T antigen formation, GLO1-deficient and GLO1-overexpressing A375-MR1 cell lines were generated and the reactivity tested with the MR1T cell clones TC5A87 and DGB129 (Figure 3-2). These knock-out and transduced A375-MR1 cells showed increased and reduced stimulatory capacity, respectively (Figure 3-2 A, B). Next, we also investigated whether additional MG could influence endogenous antigen formation, thus having an impact on MR1T cell activation. The IFN-γ release was measured using the MR1T cell clone DGB129 stimulated with THP-1 GLO1-dificient and GLO1-overexpressing cells in the presence of various doses of MG (Figure 3-2 C, D). We found that GLO1-deficient and wild type THP-1 cells both had significant increase of IFN-γ release in a MG dose dependent manner (Figure 3-2 C). Furthermore, GLO1-deficient cells had much higher effects than wildtype cells. Conversely, GLO1-overexpressing cells had no response even when treated with high doses of MG (Figure 3-2 D). The GLO1 transduction or inactivation did not impact on MR1 cell surface levels or 5-OP-RU presentation to MR1-restricted MAIT cells (Figure 3-3), thus excluding that MR1 protein modulation was responsible for the observed effects. Taken together, both positive results showed that the stimulation of tested MR1T cells can be ascribed to the presence of nucleobases and of MG.
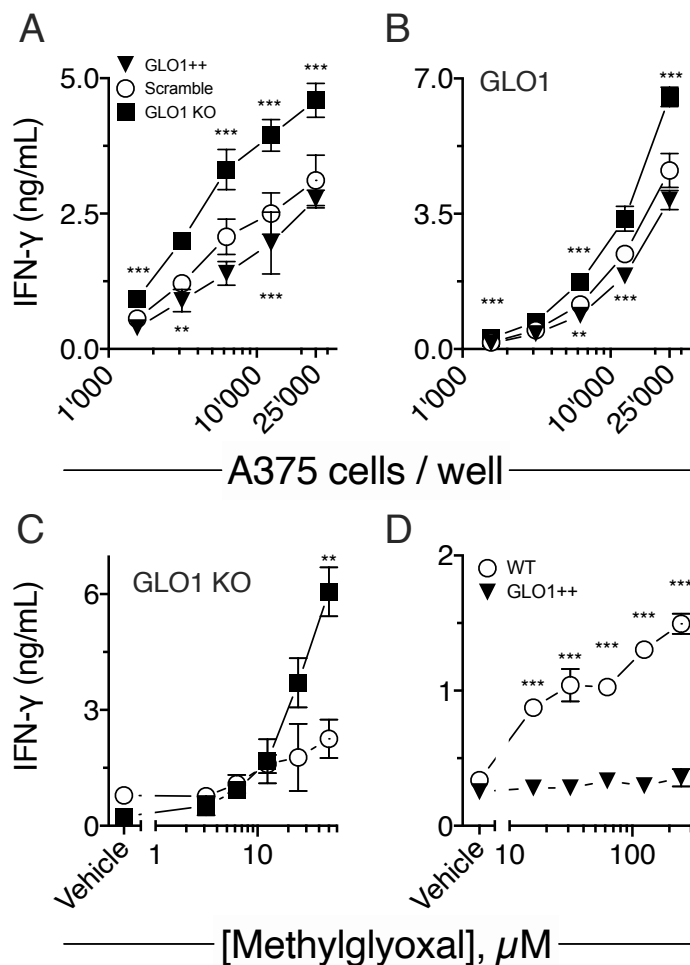
Figure 3-2. Glycolysis and methylglyoxal lead to MR1T antigen accumulation

(A and B) Stimulation of MR1T cell clone TC5A87 (A) and DGB129 (B) with A375-MR1 cells transduced with sgRNAs against GLO1 (■), scrambled sgRNAs control (○) or a vector to overexpress GLO1 (GLO1++ ▼). (C and D) MR1T clone DGB129 activation in response to THP-1 cells (○), GLO1++ (▼) and GLO1 knockout (■) THP-1 cells, in the presence of Methylglyoxal. IFN-γ released is the mean ± SD of triplicate cultures. The data shown are representative of at least three independent experiments. *$p < 0.05$ **$p \leq 0.01$ and ***$p \leq 0.001$. (A and B) two-way ANOVA with Dunnett's multiple comparison. (C and D) Multiple t-test.
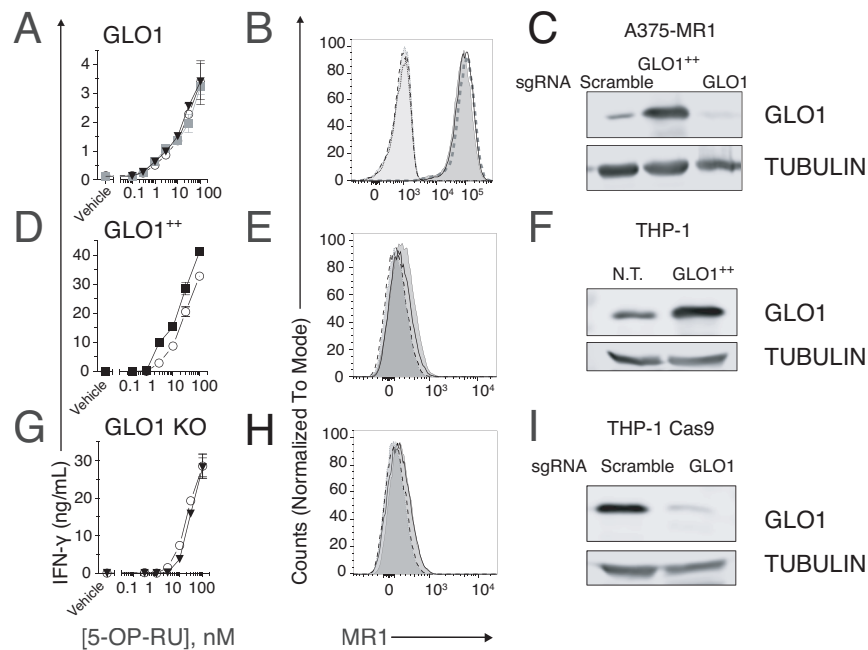
Figure 3-3. Characterization of genetically-engineered cell lines.

(A, D, G) Activation assay of MAIT clone MRC25 in response to A375-MR1 (A) and THP-1 (D and G) cells pulsed with 5-OP-RU. Cells are either wild type (O), knockout (▼) or overexpressing (A ▪, D ■) of *GLO* gene. IFN-γ is expressed as mean ± SD of triplicate cultures. (B, E, H) Surface MR1 expression of the genetic engineered cell lines. MR1 staining of wild type cells (dark grey shadow), knockout lines (black line) and GLO1-overexpressing A375-MR1 (B, grey thick dashed line) with anti-MR1 mAbs 26.5. Isotype-matched control staining is depicted in wild type cells (light grey shadow with grey dot line), in knockout cells (H, black dashed line) or GLO1-overexpressing A375-MR1 (B, black dotted line). (C, F, I,) Western blot analysis of target protein expression in indicated cell lines. Tubulin was used as loading control. The experiments were repeated twice and one representative experiment is shown.

To explore the potential synergism in stimulating MR1T cells between MG and purine metabolism, we tested GLO1-modified A375-MR1 cells in the presence of deoxyadenosine (dAdo) (Figure 3-4 A, B). Similar to the results with MG alone, dAdo-induced stimulation was increased by GLO1-deficient THP-1 cells (Figure 3-4 A). On the contrary, dAdo was less effective when GLO1-overexpressing THP-1 cells were used as APC (Figure 3-4 B).

Next, we checked the effects of individual and combined pharmacologic inhibition of key enzymes in both glycolysis and purine pathways. The following compounds were tested: the inhibitor of GLO1, S-p-bromobenzylglutathione (BBG) [268, 269]; the inhibitor of nucleic acid synthesis, mycophenolic acid (MPA) [270]; and erythro-9-(2-Hydroxy-3-nonyl) adenine

hydrochloride (EHNA) which inhibits adenosine deaminase (ADA), thus inducing accumulation of adenosine, dAdo and cGMP [271]. To investigate the effects of these inhibitors, THP-1 cells were pulsed with inhibitors for 18 hours and washed before T cell activation (Figure 3-4 C, D). BBG in combination with MPA or EHNA showed significant increase of the IFN-γ release for both MR1T cell clone TC5A87 (Figure 3-4 C) and DGB129 (Figure 3-4 D) to THP-1 cells. Clone DGB129 was more sensitive to inhibitors as it also reacted to THP-1 cells treated with BBG, MPA or EHNA alone. In control experiments, addition of the inhibitors did not induce the stimulation of MAIT cells (Figure 3-4 E). These findings suggested that nucleosides/nucleobases and MG cooperate in generating MR1T cell antigens.
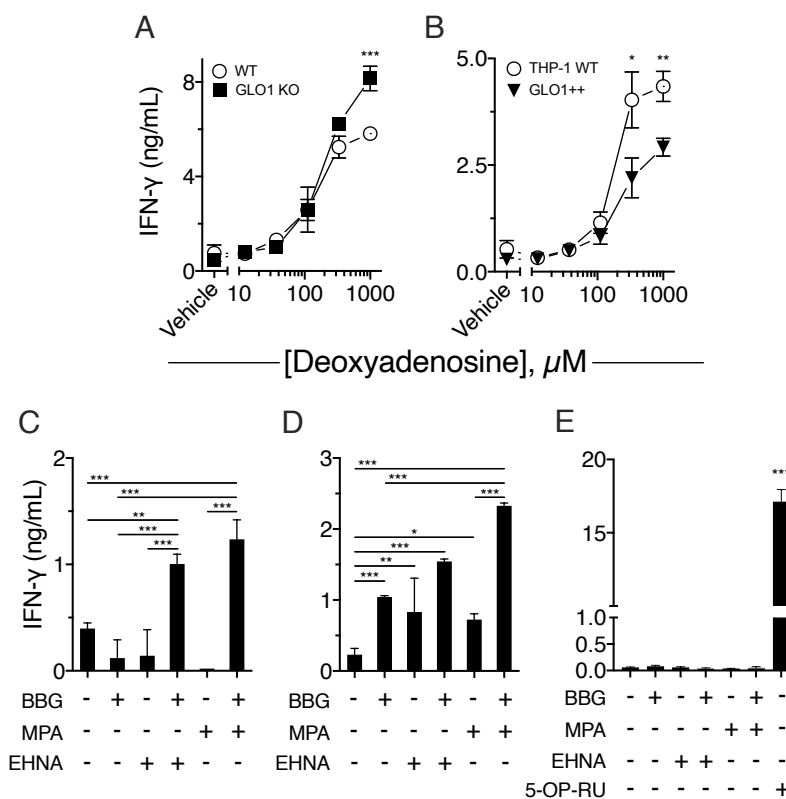
Figure 3-4. Potential synergism between MG and purine metabolic pathways for MR1T antigen accumulation.

(A and B) MR1T clone DGB129 activation in response to THP-1 cells (O), GLO1 knockout (■) and GLO1^{++} (▼) THP-1 cells, in the presence of deoxyadenosine. (C - E) Stimulation of MR1T cell clone TC5A87 (C) and DGB129 (D) and MAIT clone MRC25 (E) with THP-1 cells pre-treated with erythro-9-(2-Hydroxy-3-nonyl) adenine hydrochloride (EHNA), Mycophenolic acid (MPA) and S-Bromobenzylglutathione (BBG), alone or in combination. 5-OP-RU (2 nM) was used as positive control of MRC25. IFN-γ released is the mean ± SD of triplicate cultures. The data shown are representative of at least three independent experiments. *p<0.05 **p≤0.01 and ***p≤0.001. (A, B) Multiple t-test, (C and D) one-way ANOVA with Tukey's multiple comparison.

3.4 Multiple oxidative stress-related reactive carbonyls accumulate within tumour cells and contribute to MR1T cell stimulation

As these results confirmed the importance of purine, glycolysis and methylglyoxal pathways in MR1T cell stimulation, thus validating our CRISPR approach, we continued to investigate the role of other genes highlighted by the *in silico* analysis. Our initial CRISPR screening revealed a significant depletion of sgRNAs encoding several enzymes of the human glutathione S-transferase (GST) family. These enzymes are known to catalyse the conjugation of glutathione (GSH) for the purpose of reactive oxygen species (ROS) detoxification [227, 272]. ROS are constantly generated as natural by-products of the normal aerobic metabolism of oxygen [161]. Under normal physiological conditions, cells control ROS levels by balancing their accumulation with multiple scavenging systems [273]. When the production of peroxides and free radicals, two types of typical ROS compounds, is imbalanced and their concentrations increase, cells undergo oxidative stress, which is followed by a large number of changes inside cells, including damages of cellular components such as nucleic acids, proteins, and lipids [274]. Glutathione is very important in preventing such damages [275]. We tested several cellular oxidation related drugs, which induce accumulation of cellular ROS, for their capacity to increase the capacity of tumour cells to stimulate MR1T cells.

Paclitaxel and doxorubicin are two drugs known to promote cellular accumulation of O_2^- and H_2O_2 [276-279]. They were used to prime THP-1 cells and test enhanced MR1T cell activation. Both drugs showed significantly increased ROS accumulation (Figure 3-5 A), and also induced a strong activation of four MR1T cell clones when incubated with THP-1 cells and nucleoside compounds (Figure 3-5 B-E), mirroring the synergetic effects of BBG, MPA and EHNA (Figure 3-4 C, D). Same experiment was performed with MAIT clone MRC25 (Figure 3-8 A) and both drugs did not induce activation of MRC25. The combination of Paclitaxel and nucleosides showed significant stimulation, while the reactivity was relevantly low comparing with MR1T cell clones.
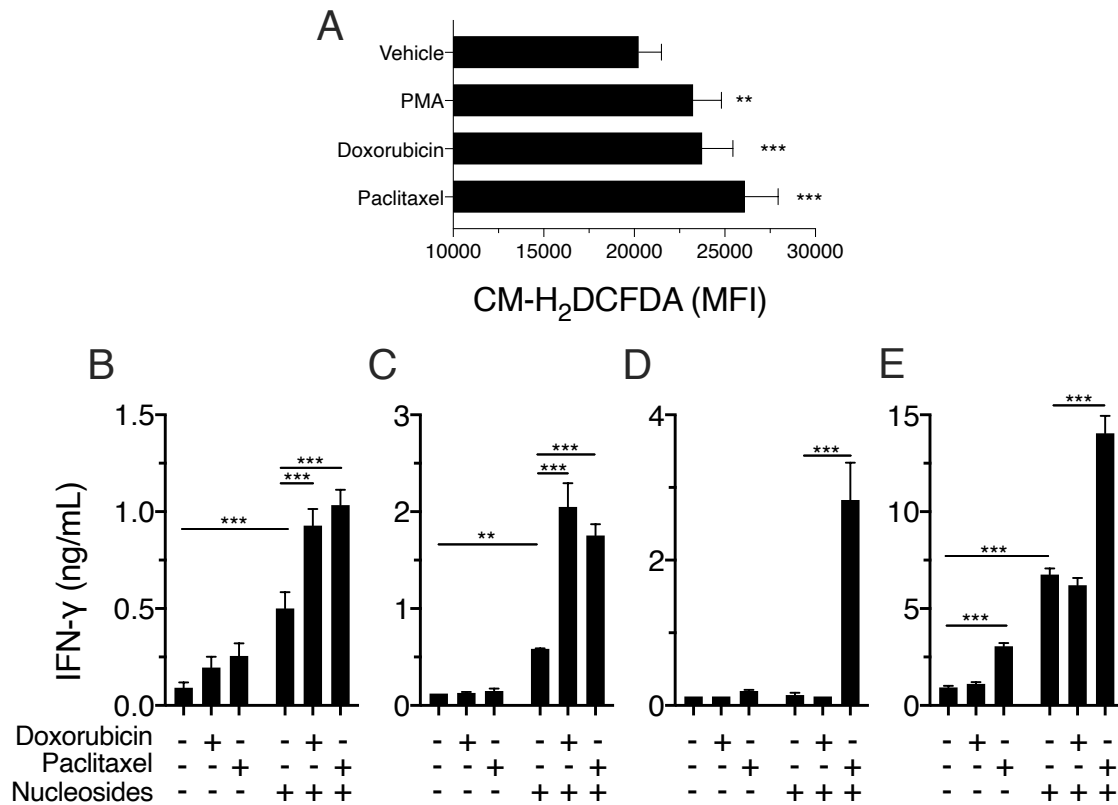
Figure 3-5. ROS and nucleosides promote MR1T antigen accumulation.

(A) Quantification of ROS produced in THP-1 cells treated with Doxorubicin, Paclitaxel or Phorbol 12-myristate 13-acetate (PMA, positive control). Results are expressed Median Fluorescence Intensity (MFI) of live cells ± SD of triplicate cultures. (B-E) Stimulation of MR1T cell clone TC5A87 (B), DGB129 (C), MCA2B1 (D) and MCA3C3 (E) with THP-1 cells pre-treated with Doxorubicin or Paclitaxel in the absence or presence of nucleosides (deoxyadenosine and guanosine). IFN-γ release is the mean ± SD of triplicate cultures. The data shown are representative of at least three independent experiments. *p<0.05, **p≤0.01 and ***p≤0.001, two-way ANOVA with Tukey's multiple comparison.

To confirm that cellular oxidation is important for MR1T antigen accumulation, several inhibitors for cellular oxidation were tested. In these experiments A375-MR1 cells were selected as stimulators, as they show a strong stimulatory capacity. A375-MR1 cells were treated separately with buthionine sulfoximine (BSO), Glutathione (GSH), N-acetylcysteine (NAC), or apocynin (APO), then fixed and washed and finally used to stimulate four MR1T cell clones (Figure 3-6) and a MAIT clone (Figure 3-8 B). Buthionine sulfoximine (BSO) is an inhibitor of GSH synthase [280]. Significant increase was observed in the stimulation of all tested MR1T clones after the pre-treatment of A375-MR1 with BSO (Figure 3-6). GSH and NAC are H_2O_2 scavengers and prevent damage to important cellular components caused by

ROS [275, 276]. When A375-MR1 cells were treated with any of these inhibitors, the release of IFN-γ was significantly reduced for all four MR1T clones (Figure 3-6). Apocynin, is a natural inhibitor of NADPH oxidase, which is one of the major sources of cellular superoxide [281]. Apocynin pre-treatment induced a significant reduction of IFN-γ release in one MR1T cell clone (Figure 3-6 A). Together, these data showed that inhibiting ROS accumulation impedes tumour cell stimulation of MR1T cells. On the other hand, blocking GSH synthesis also facilitated MR1T cell activation. However, similar effects were not observed with MAIT clone (Figure 3-8 B). Importantly, as these drugs were washed before addition of T cells, their effect has to be ascribed to their induced changes within tumour cells.

Figure 3-6. ROS scavengers inhibit MR1T antigen accumulation.

Stimulation of MR1T cell clone TC5A87 (A), DGB129 (B), MCA2B1 (C) and MCA3C3 (D) with fixed A375-MR1 cells treated with Buthionine Sulfoximine (BSO), Glutathione (GSH), N-Acetylcysteine (NAC) and Apocynin (APO). IFN-γ release is the mean $\pm$ SD of triplicate cultures. The data shown are representative of at least three independent experiments. *$p < 0.05$, **$p \leq 0.01$ and ***$p \leq 0.001$, one-way ANOVA with Dunnett's multiple comparison.

The results of Figure 3-5 and 3-6 suggested that accumulation of ROS promotes MR1T antigen formation. ROS participates in lipid peroxidation, a pathway that generates highly reactive carbonyls as end products, such as malondialdehyde (MDA), 4-hydroxy-nonenal (HNE) and 4-oxo-nonenal (ONE) [171, 282]. These compounds react with proteins, lipids and nucleobases, forming stable adducts which accumulate within tumour cells [188-190, 192, 283]. Because of these effects following ROS accumulation, we investigated the role of lipid peroxidation within tumour cells that stimulate MR1T cells. Our CRISPR/Cas9 screen showed that the sgRNA of

two genes, namely Glutathione peroxidase 1 (*GPX1)* and Glutathione peroxidase 4 (*GPX4)* were significantly less represented. GPX1 protein catalyses organic hydroperoxides reduction and H_2O_2 degradation by glutathione, whereas GPX4 has a high preference for lipid hydroperoxides promoting their degradation, thus exerting a very important effect in protecting cells against membrane lipid peroxidation and death [197]. A375-MR1 cells were pulsed with the inhibitor of GPX1, mercaptosuccinic acid (MSA) and two inhibitors of GPX4, RSL3 and ML-210 before stimulation of MR1T cell clones. In these conditions, the IFN-γ production of all tested MR1T cell clones significantly increased (Figure 3-7), but same effects were not observed with MAIT clone (Figure 3-8 C). These findings illustrated the relevance of lipid peroxidation in MR1T cell stimulation.

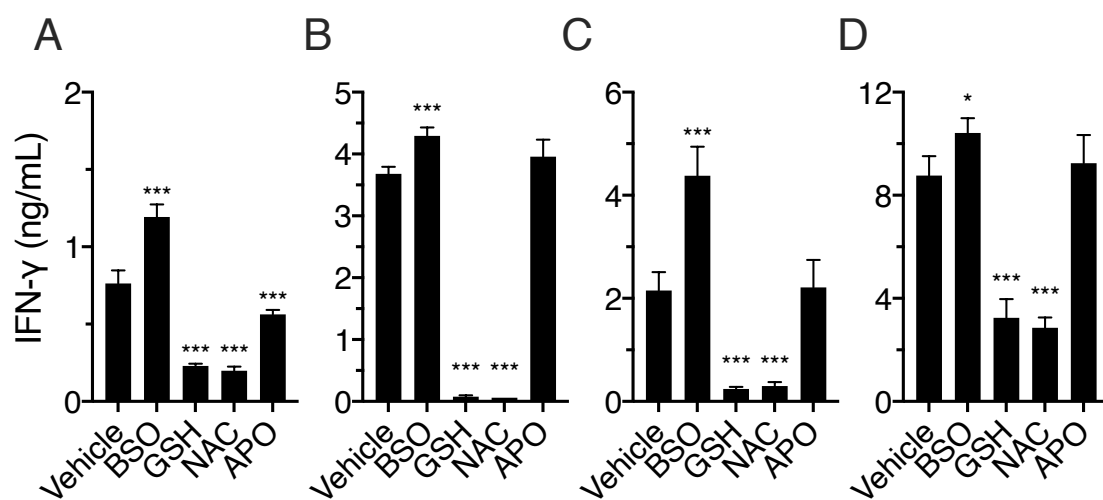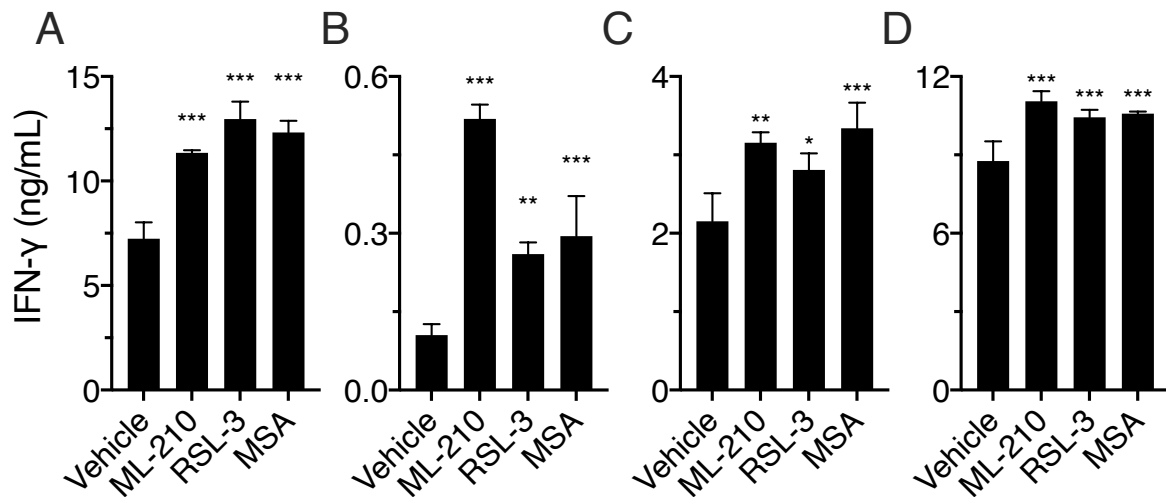**Figure 3-7. Lipid peroxidation contributes MR1T antigen accumulation.**

Stimulation of MR1T cell clone TC5A87 (A), DGB129 (B), MCA2B1 (C) and MCA3C3 (D) with fixed A375-MR1 cells treated with ML-210, RSL3 and Mercaptosuccinic acid (MSA). IFN-γ release is the mean ± SD of triplicate cultures. The data shown are representative of at least three independent experiments. *p<0.05, **p≤0.01 and ***p≤0.001, one-way ANOVA with Dunnett's multiple comparison.
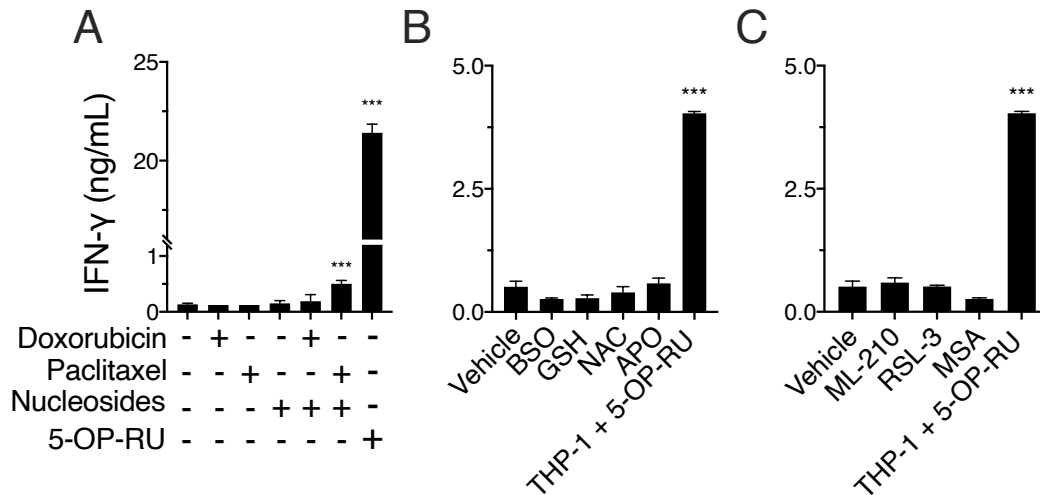
Figure 3-8. Different drugs do not influence MAIT antigen accumulation.

(A) MAIT clone MRC25 stimulated with THP-1 cells treated with indicated drugs. As control, 5-OP-RU (2 nM) was tested with MRC25 in same experiment. (B, C) MRC25 cells stimulated with A375-MR1 cells treated with BSO, GSH, NAC, APO or GPX inhibitors. As control, THP-1 cells pulsed with 5-OP-RU (100 pM) was tested with MRC25 in same experiment. IFN-γ is expressed as mean ± SD of triplicate cultures. The experiments were repeated at least twice and one representative experiment is shown. ***p≤0.001 compared to vehicle-treated cells using One-way ANOVA (A) or Two-way ANOVA (B and C) with Dunnett's multiple comparison.

To further identify the function of reactive carbonyls in MR1T antigen accumulation of tumour cells, oleanolic acid was tested to increase the endogenous level of carbonyls. Aldehyde reductase and aldo-keto reductases (AKRs) are responsible for the reduction of carbonyls to alcoholic forms [284]. AKR1B10 sgRNA was found significantly depleted in our CRISPR/Cas9 screening. This gene encodes the aldo-keto reductase family 1 member B10, an enzyme that can reduce various types of aldehyde compounds [285, 286]. AKR1B10 also plays an important role in glycolysis and detoxification of lipid peroxidation products and precursors of advanced glycation end products [287, 288]. Oleanolic acid has been found as a strong inhibitor of AKRIB10 [289]. Therefore, we tested whether oleanolic acid by blocking AKRIB10 activity influences the responsiveness of MR1T cells. THP-1 cells were incubated with oleanolic acid before incubating with MR1T cell clones (Figure 3-9 A-D). Addition of oleanolic acid significantly increased IFN-γ production of all tested MR1T cell clones. In control experiments, oleanolic acid did not influence a control MAIT-cell clone response to the microbial antigen 5-OP-RU (Figure 3-9 E). Thus, inhibition of keto reductases involved in

carbonyl degradation also contributes to increased capacity of tumour cells in MR1T cell stimulation.

In general, these data suggested that multiple oxidative stresses inducing lipid peroxidation and accumulation of related reactive carbonyls is very important. The possible mechanism is the accumulation of relevant carbonyls that reacting with nucleobases generate different types of adducts. Some of these adducts bind to MR1 and stimulate MR1T cells.
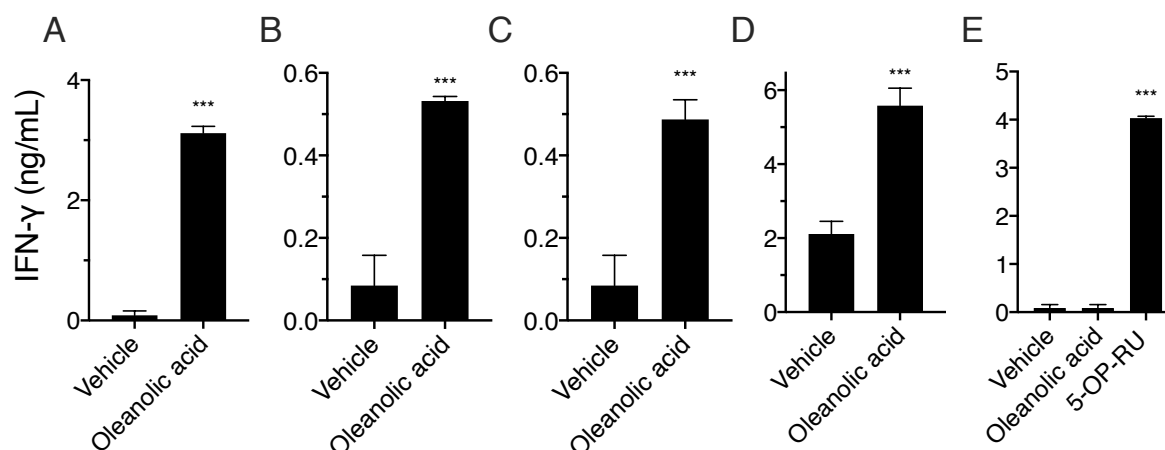
Figure 3-9. Aldehydes contribute MR1T antigen accumulation.

(A-D) Stimulation of MR1T cell clone TC5A87 (A), DGB129 (B), MCA2B1 (C), MCA3C3 (D) and MAIT clone MRC25 (E) with THP-1 cells treated with Oleanolic acid. As control, THP-1 cells pulsed with 5-OP-RU (1 nM) was tested with MRC25 in same experiment. IFN-γ release is the mean ± SD of triplicate cultures. The data shown are representative of at least two independent experiments. $*p<0.05$, $**p \leq 0.01$ and $***p \leq 0.001$, multiple t-test.

3.5 Nucleobase-MDA adducts stimulate MR1T cells

Many different types of reactive carbonyl species are present in living organisms [290]. They are involved in different diseases by generating DNA and protein adducts [291, 292]. Based on our previous results and published literatures on cellular functions of carbonyl effects, we postulated that various reactive carbonyl species form nucleobases adducts, some of which are MR1T cell antigens. To test this hypothesis, we synthesized several types of nucleobases adducts which were then tested for their capacity to stimulate MR1T cells.

In initial experiments we generated adducts of purines with MDA, a highly reactive carbonyl which accumulates in the final steps of lipid peroxidation. Adducts were first synthesized by

performing chemical reaction of different nucleobases and MDA. The reactivity of titrated adducts mixture was tested with three MR1T cell clones using THP-1 cells as APCs. Some of the synthetic mixtures showed very potent stimulation (Fig 3-10). MR1T cell clone AC1A4 (Figure 3-10 A, B) and DGB129 (Figure 3-10 C, D) reacted to different synthetic adducts in a similar manner.　They both reacted to most of the mixtures except MDA alone (Fig 3-10 A, C) and AMP-MDA (Fig 3-10 B, D). Among all adducts, adenine-MDA and deoxyadenosine (dAdo)-MDA had the highest stimulation toward DGB129 and AC1A4 MR1T cell clones. These adducts induced very potent IFN-γ release even after dilution of 10,000 times. In addition, other mixtures induced less but still very potent stimulation, in order they were adenosine-MDA, ATP-MDA, and ADP-MDA. Clone TC5A87 had the reaction profiles quite differently (Figure 3-10 E, F). They reacted to adenosine-MDA, dAdo-MDA, AMP-MDA, and MDA alone in a similar manner. Together, these results suggested that nucleobases and aldehyde MDA form adducts and stimulate MR1T cell clones in a different manner.
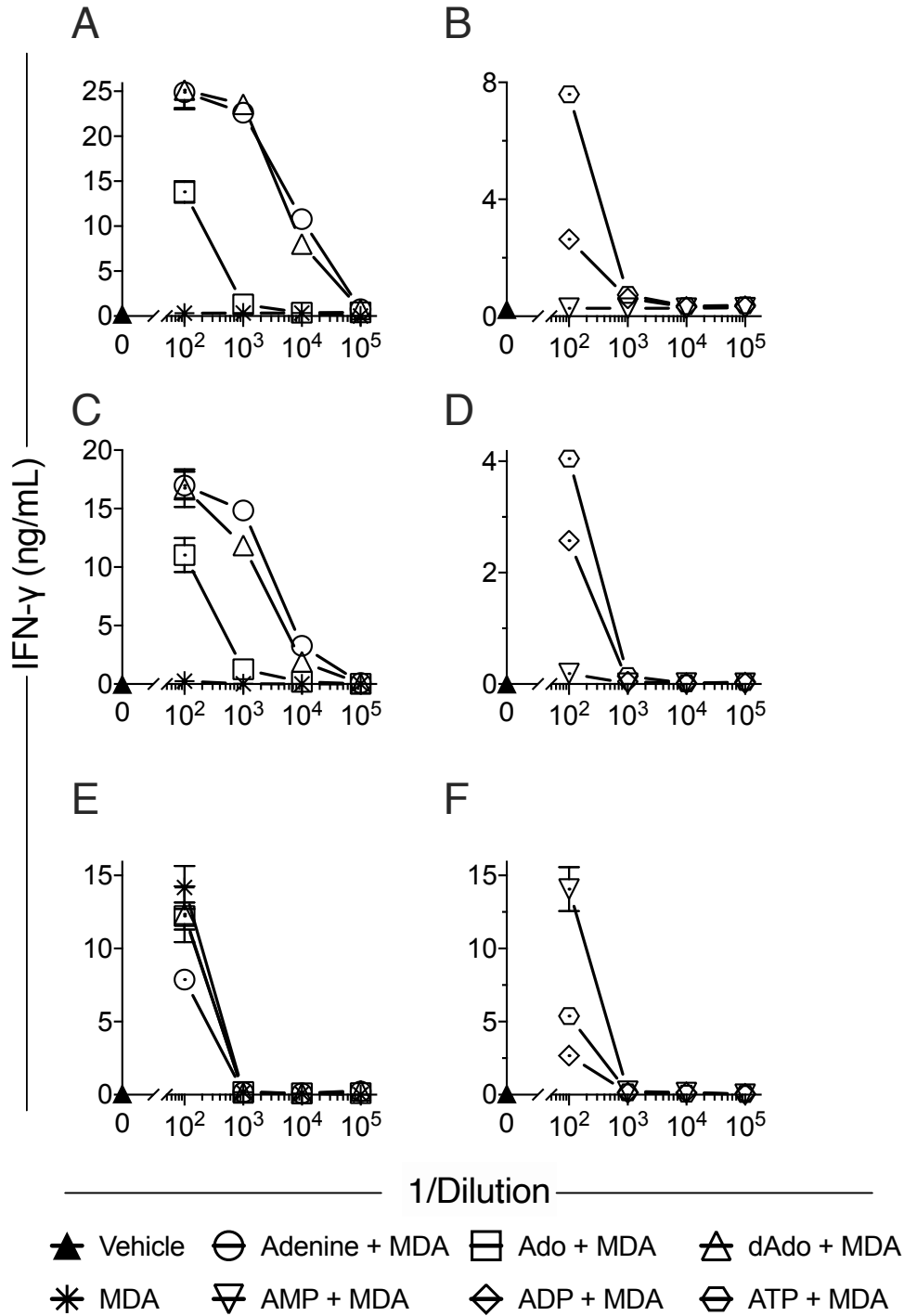
Figure 3-10. Nucleobase-MDA adducts stimulate MR1T cell clones.

Stimulation of MR1T cell clone AC1A4 (A, B), DGB129 (C, D), and TC5A87 (E, F) with THP-1 cells with series dilutions of synthetic nucleobases-MDA adducts. Solutions containing adducts of nucleobases and MDA (25 mM and 100 mM, respectively) were diluted 100x, 1,000x, 10,000x, and 100,000x times. IFN-γ release is the mean ± SD of duplicate cultures. The data shown are representative of at least two independent experiments.

3.5.1 Synthesis and purification of adenine-MDA adducts (M₃ADE)

To further identify the biological function and structures of MR1T antigens, we focused on the most potent adducts from adenine-MDA and deoxyadenosine-MDA. By following the T cell reactivity, synthetic conditions of adenine-MDA and deoxyadenosine-MDA adducts were optimized. The synthetic mixtures of adenine-MDA (Fig 3-11 A) and dAdo-MDA (Fig 3-11 B) were checked on HPLC at wavelength 254nm using an analytical C18 pyramid column. The HPLC profiles of adenine-MDA and dAdo-MDA looked very similar. Several peaks were detected on HPLC around minutes 3, 8, 15 and 19. In addition, by comparing the nucleobases and MDA alone as control, the peak detected approximately at minute 3 was identified as MDA and the peak near minute 8 as the unmodified nucleobase, adenine or dAdo. Therefore, the adducts are more hydrophobic than the unmodified nucleobase and eluted after minute 8.
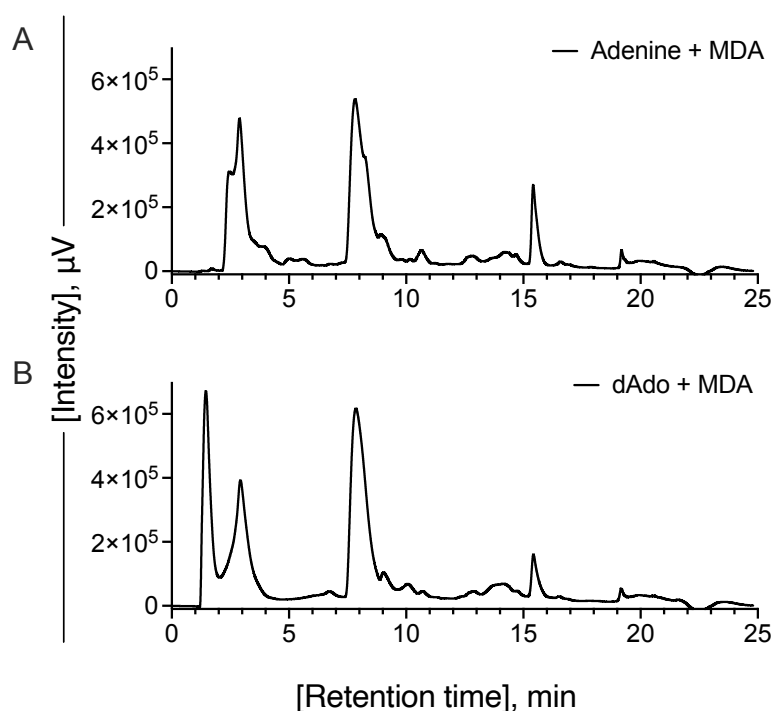
Figure 3-11. HPLC analysis of synthetic adenine-MDA and dAdo-MDA adducts.
HPLC analysis of adenine-MDA adducts (A) and dAdo-MDA adducts (B). The raw mixture was diluted 50x with H_2O and injected 50μl in HPLC (Absorbance 254 nm).

To purify the synthetic adducts, raw adenine-MDA was first loaded on solid phase extraction (SPE) C18 cartridge, washed with H_2O, and then eluted stepwise with 10%, 20% and 30% acetonitrile in H_2O. Diluted fractions of each step were run on HPLC and the different elution

profiles were compared (Figure 3-12 A-F). In parallel, each fraction was pulsed on THP-1 cells and tested for the capacity to induce IFN-γ release by the MR1T cell clones AC1A4 (Figure 3-13 A) and DGB129 (Figure 3-13 B). The cartridge flow through, and the material washed with H$_2$O mainly contained free MDA and nucleobases (peaks before min 10 on the HPLC run). As we have seen before, free MDA did not stimulate MR1T cell clone AC1A4 and DGB129 (Figure 3-10 A, C). The fraction eluted with 10% acetonitrile (peaks before minutes 15 on HPLC profile) stimulated DGB129 cells weakly, but not AC1A4. Instead, the fraction eluted with 30% acetonitrile (peaks around minute 19 on HPLC profile) stimulated AC1A4 cells weakly, but not DGB129. Fraction with 20% acetonitrile mainly contained compounds eluting near minute 15. It showed the strongest stimulation and the reactivity is similar to that of the unpurified crude adenine-MDA preparation. In general, these results suggested that SPE-purified adenine-MDA adducts stimulated both MR1T clone DGB129 and AC1A4. The fraction eluted with 20% acetonitrile had the strongest stimulation, the reactivity of fraction with 10% and 30% acetonitrile were slightly different.
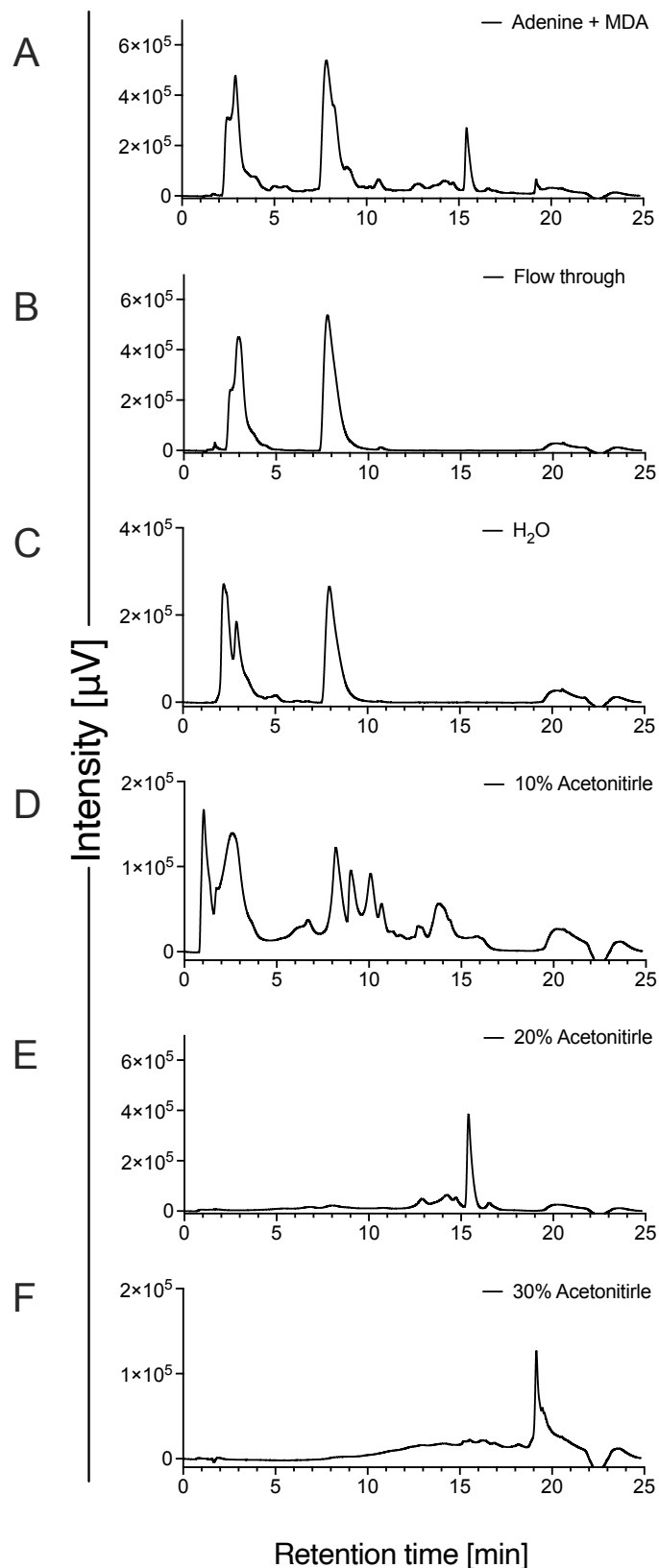
Figure 3-12. HPLC analysis of SPE purified adenine-MDA adducts.

Synthetic adducts of adenine-MDA (A), fraction of SPE flow through (B), fraction with H_2O (C), fraction with 10% acetonitrile (D), fraction with 20% acetonitrile (E), fraction with 30% acetonitrile (F). Each fraction was diluted 50x with H_2O and injected 50µl in HPLC (Absorbance 254 nm).
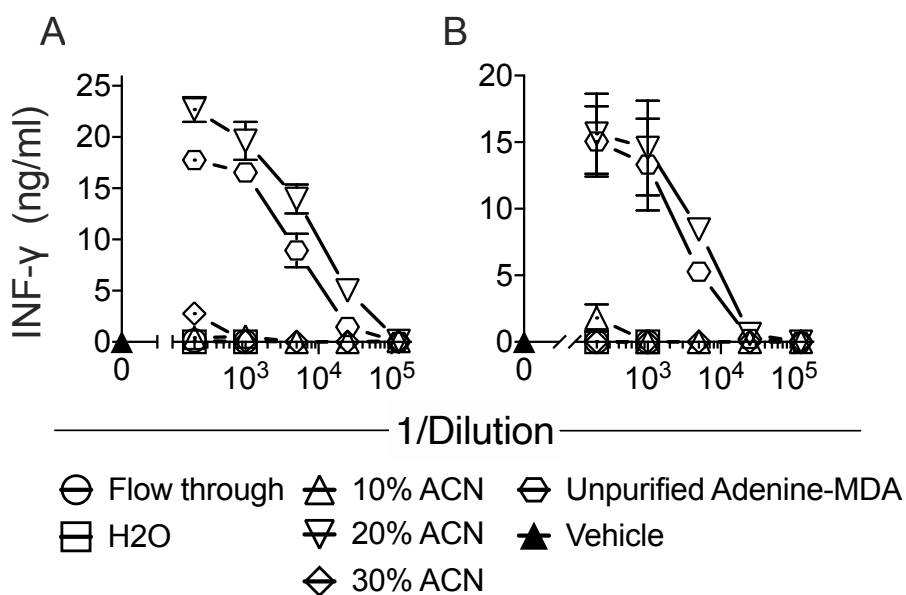
Figure 3-13. SPE purified adenine-MDA fractions stimulate MR1T cell clones.

Activation assay of SPE purified adenine-MDA adducts with MR1T cell clone AC1A4 (A) and DGB129 (B). Solutions containing adducts of nucleobases and MDA (25 mM and 100 mM, respectively) were diluted 200x, 1,000x, 5,000x, and 25,000x times. IFN-γ release is the mean $\pm$ SD of duplicate cultures. The data shown are representative of at least three independent experiments.

To further purify the stimulatory adenine-MDA adducts, the fraction eluted with 20% acetonitrile from the SPE cartridge was run on HPLC using a C18 column and eluting fractions were collected every 30 seconds. The reactivity of collected fractions was tested with both AC1A4 and DGB129 clones. The active fractions were pooled and their purity was checked on HPLC (Figure 3-14). In total, 12.5 mg reactive adducts were purified which were then used to test the biological activity and for structure identification using high-resolution electro-spray ionization mass spectrometry (HR-ESI-MS) and nuclear magnetic resonance (NMR) spectroscopy (Figure 3-15). The identified structure was 8-(9H-purin-6-yl)-2-oxa-8-azabicyclo[3.3.1]nona-3,6-diene-4,6-dicarbaldehyde, which made of adenine with three MDA molecules (M$_3$ADE, Figure 3-15 A). The same synthesis and purification procedures were also used to generate deoxyadenosine-MDA adducts. We found that also in this case M$_3$ADE was detected using HR-ESI-MS and NMR analyses, suggesting the ribose moiety of deoxyadenosine was cleaved during synthesis and is not relevant for the stimulation of the MR1T cell clones tested.
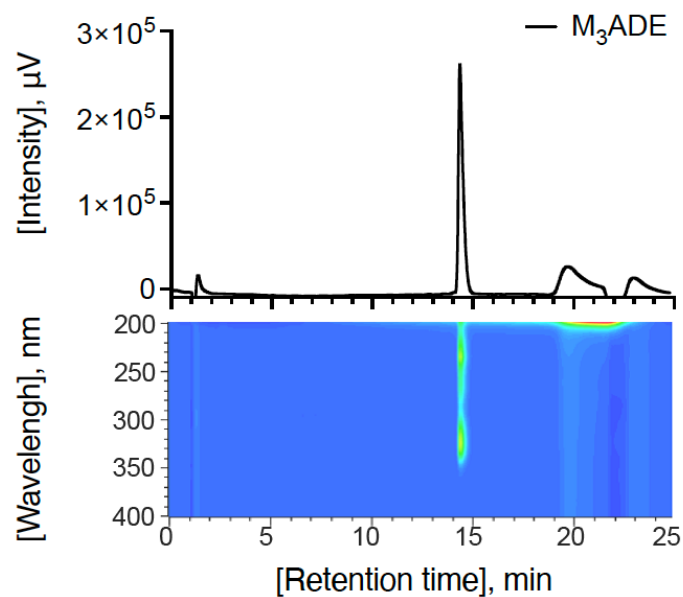
Figure 3-14. HPLC analysis of purified adenine-MDA adduct, M₃ADE.

(A) HPLC analysis of purified M₃ADE using single UV detection at absorbance 254 nm (upper) and photo diode array (PDA) detector between absorbance 200 nm to 400 nm (lower). Approximately 3μg M₃ADE was injected in HPLC.

Figure 3-15. Mass-Spectrometric and NMR analyses of synthetic M₃ADE

(A) Structure of synthetic M₃ADE, $C_{14}H_{11}N_5O_3$. (B) High Resolution Mass-Spectrometry (HRMS), top: experiment, centre & bottom: calculated, and (C) NMR analysis.

3.5.2 Synthesis and purification of other nucleobase-MDA adducts: OPdA, OPdC, and M_1G

Having identified M_3ADE as the first MR1T antigen, we generated and tested other known MDA-nucleobase adducts. N^6-(3-oxo-1-propenyl)-2'-deoxyadenosine (OPdA) [248], N^4-(3-Oxo-1-propenyl)-2'-deoxycytidine (OPdC) [293], and pyrimido[1,2-α]purin-10(3H)-one (M_1G) [294, 295] are known MDA-deoxyadenosine, MDA-deoxycytidine and MDA-guanine adducts. OPdA was detected after treatment of calf thymus DNA with 3-benzoylacrolein, a reactive equivalent of MDA [294, 296]. To test their potential reactivity towards MR1T cells, OPdA and OPdC were synthesized in the Department of Chemistry of the University of Basel following a previously described protocol with minor modifications [250]. M_1G was purified in our laboratory using the optimized method [249], it was detected from rat and human urine [297]. The purity of OPdA, OPdC and M_1G were accessed using HPLC profiles with UV spectra (Figure 3-16), HR-ESI-MS and NMR spectroscopy (Figure 3-17 - 3-19). In general, M_3ADE, OPdA, OPdC and M_1G were very stable when stored at -70 °C in H_2O. The stability and reactivity were checked monthly using HPLC profiles and biological activity with MR1T clones. These findings confirmed that nucleobase adducts formed with carbonyls may stimulate MR1T cells.
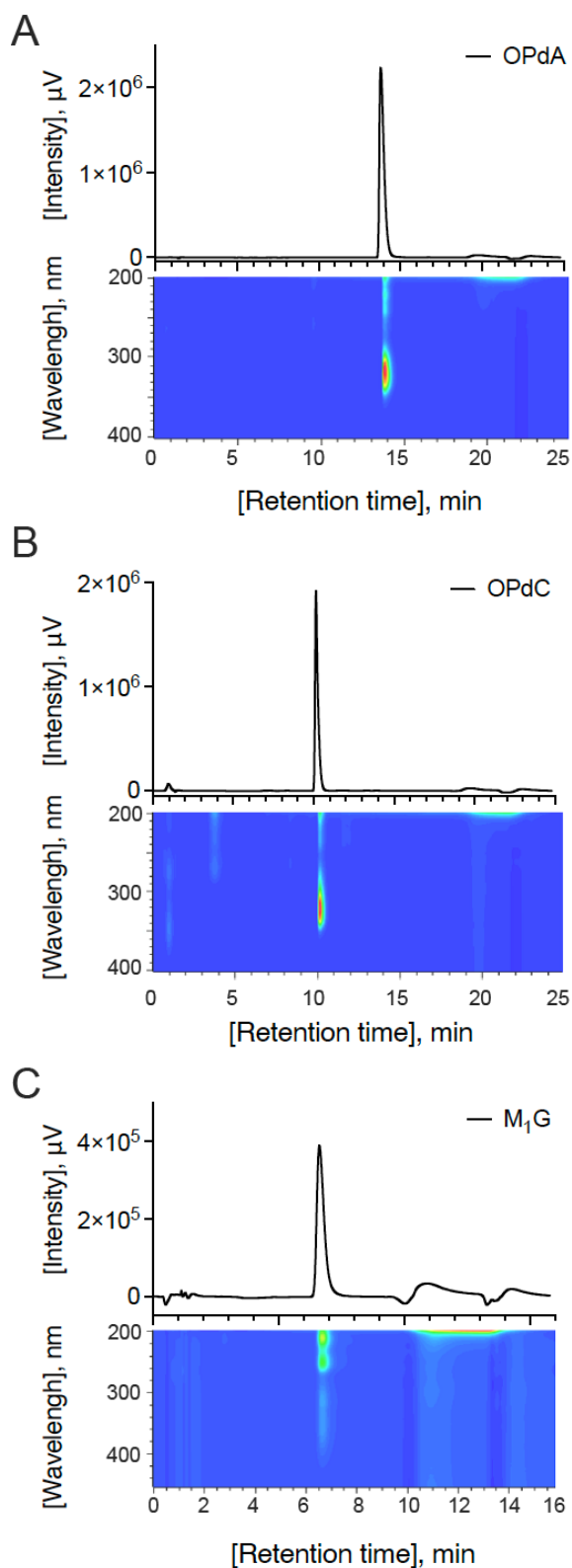
Figure 3-16. HPLC analysis of purified nucleobase-MDA adducts, OPdA, OPdC and M_1G.

(A) HPLC analysis of purified deoxyadenosine-MDA (OPdA) using single UV detection at absorbance 320 nm (upper) and photo diode array (PDA) detector between absorbance 200 nm to 400 nm (lower). (B) HPLC analysis of purified deoxyadenosine-MDA (OPdC) using single UV detection at absorbance 320 nm (upper) and photo diode array (PDA) detector between absorbance 200 nm to 400 nm (lower). (C) HPLC analysis of purified Guanine-MDA (M_1G) using single UV detection at absorbance 254 nm (upper) and photo diode array (PDA) detector between absorbance 200 nm to 400 nm (lower). Approximately 3μg of each adduct was injected in HPLC.
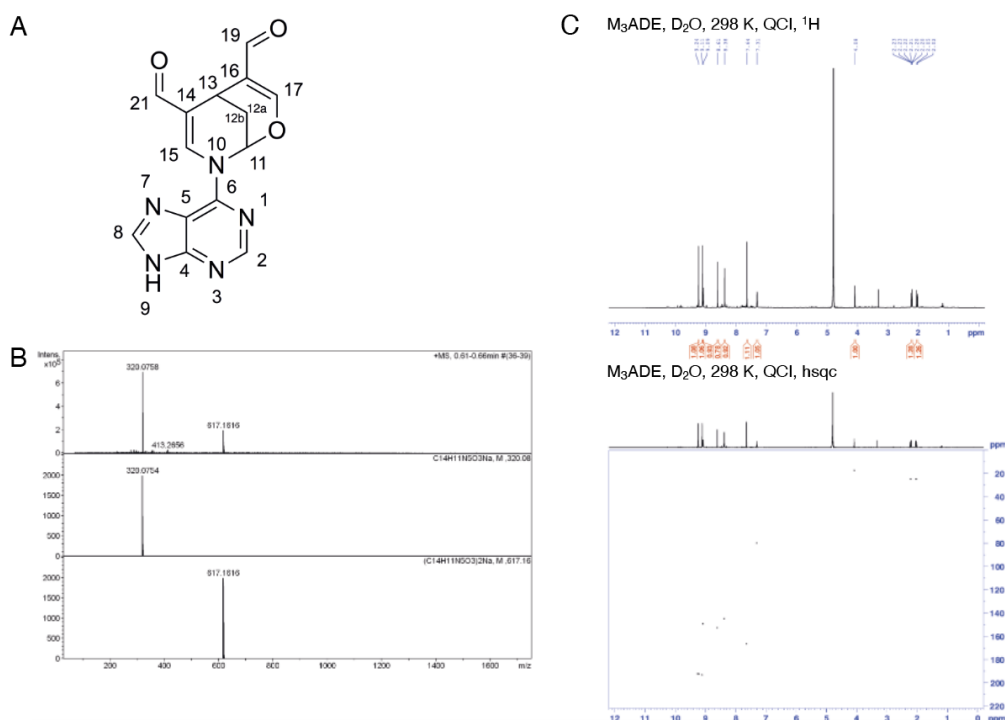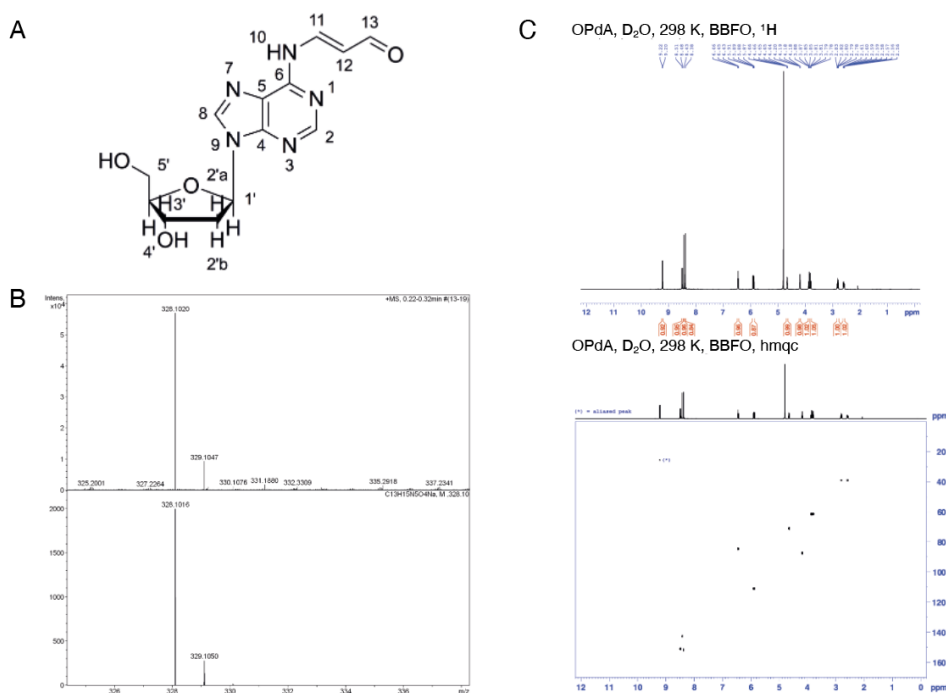
Figure 3-17. Mass-Spectrometric and NMR analyses of synthetic OPdA.

(A) Structure of synthetic OPdA, $C_{13}H_{15}N_5O_4$. (B) HRMS, top: experiment, bottom: calculated, and (C) NMR analysis.
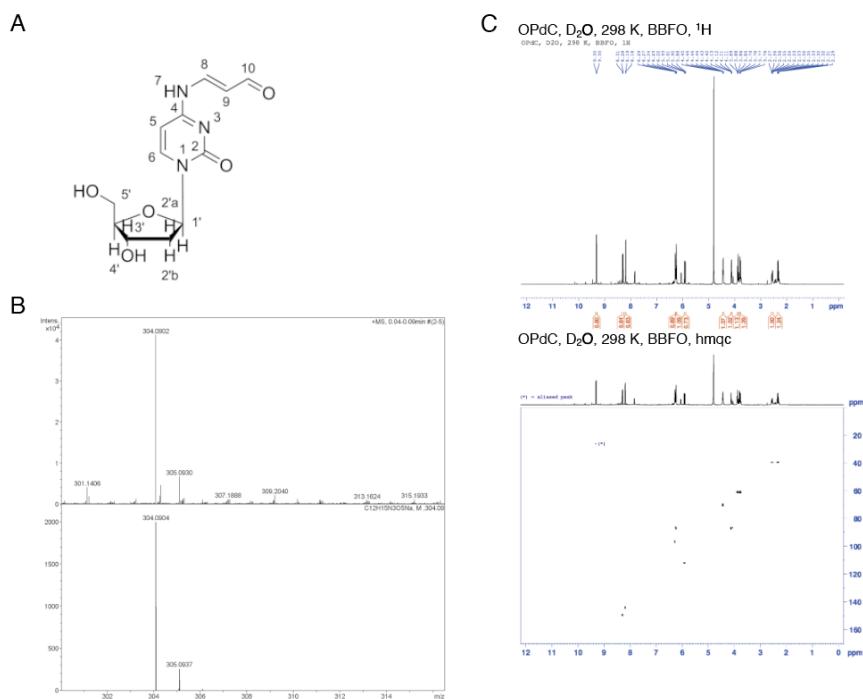
Figure 3-18. Mass-Spectrometric and NMR analyses of synthetic OPdC.

(A) Structure of synthetic OPdC, $C_{12}H_{15}N_3O_5$. (B) HRMS, top: experiment, bottom: calculated, and (C) NMR analysis.
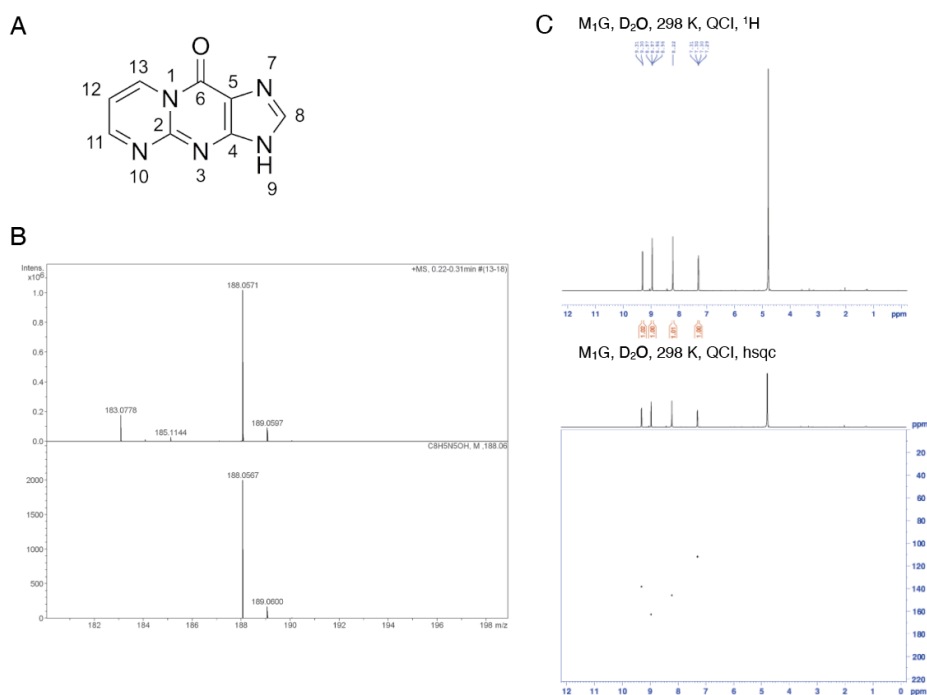
Figure 3-19. Mass-Spectrometric and NMR analyses of synthetic M₁G.

(A) Structure of synthetic M_1G, $C_8H_5N_5O$. (B) HRMS, top: experiment, bottom: calculated, and (C) NMR analysis.

3.5.3 Further antigenic activity test of purified nucleobase-MDA adducts

To investigate the antigenic activity of the four purified synthetic adducts, three types of assays were performed: MR1 upregulation, activation assay of MR1T cell clones after presentation by APC pulsed with synthetic compounds, and plate-bound assay by presenting each compound with recombinant MR1 on plastic plate.

MR1 upregulation assay was used to check whether, after binding MR1, the adducts intracellularly stabilize MR1 molecules and promote their expression on the plasma membrane. THP-1 cells, which express very low physiological amounts of MR1 on their surface, were incubated with increasing amounts of adducts and MR1 median florescence intensity (MFI) was checked by flow cytometry. After 6 hours of incubation, all four adducts induced upregulation of MR1 expression in a dose dependent manner (Figure 3-20). Antigen induced MR1 upregulation has been previously observed when cells were incubated with vitamin B–related MR1 ligands and was interpreted as MR1 stabilization capacity of those antigens [139]. In our experiments, when the four nucleobases were compared, M_3ADE was the most potent inducer of MR1 cell surface expression (~2.5-time fold increase). The same assay was also

performed with THP-1 MR1 cells, which express large amounts of MR1 on the plasma membrane in the absence of any treatment. With these cells a stronger increase of MR1 surface expression was observed, suggesting that in these cells there is an abundant reservoir of MR1 molecules which is not stably expressed on the cell surface.
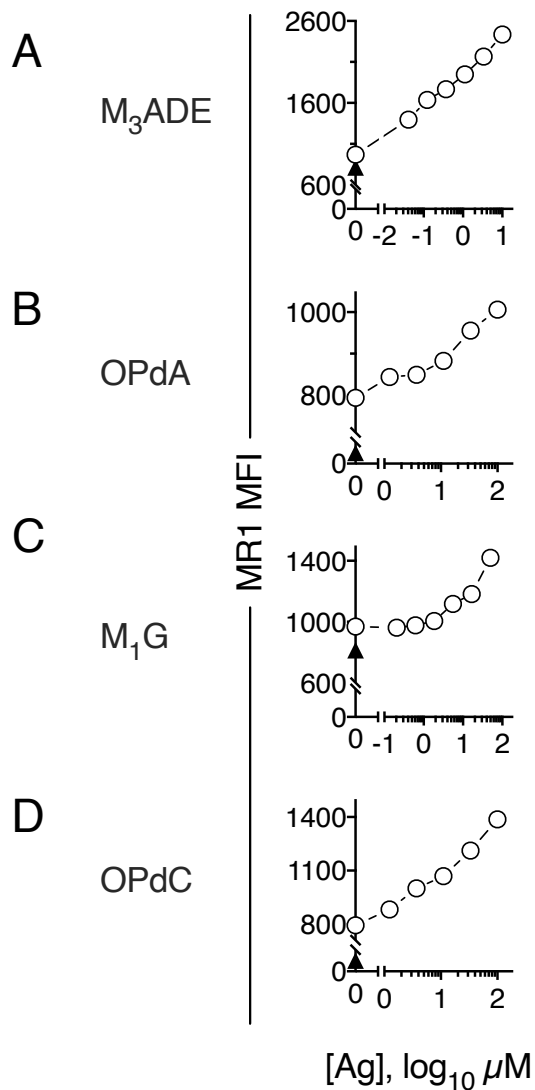
Figure 3-20. Synthetic nucleobase-MDA adducts upregulate MR1 surface expression.

Upregulation of MR1 surface expression on THP-1 cells following 6 h incubation with four synthetic adducts M_3ADE (A), OPdA (B), M_1G (C), and OPdC (D) (O), isotype control (▲). Median florescence intensity (MFI) was checked by flow cytometry. The data shown are representative of at least three independent experiments and one representative experiment is shown.

The four compounds were then tested for their capacity to stimulate MR1T cell clones. We used our collection of MR1T cells and THP1 cells as APC because they do not induce relevant MR1T stimulation in the absence of exogenous antigens. THP-1 cells were pulsed with increasing amounts of synthetic adducts and then used to stimulate different MR1T cell clones. Three types of reactivity were observed: i) Some MR1T cell clones showed reactivity only against one adduct; ii) Some clones cross-reacted with different adducts; iii) Some clones did not respond to any of the adducts. The antigen dose-dependent responses of reacting clones are

shown in (Figure 3-21). In all cases, MR1T cell activation was completely blocked by the addition of anti-MR1 mAbs, confirming the MR1 restricted activation of tested MR1T cells.
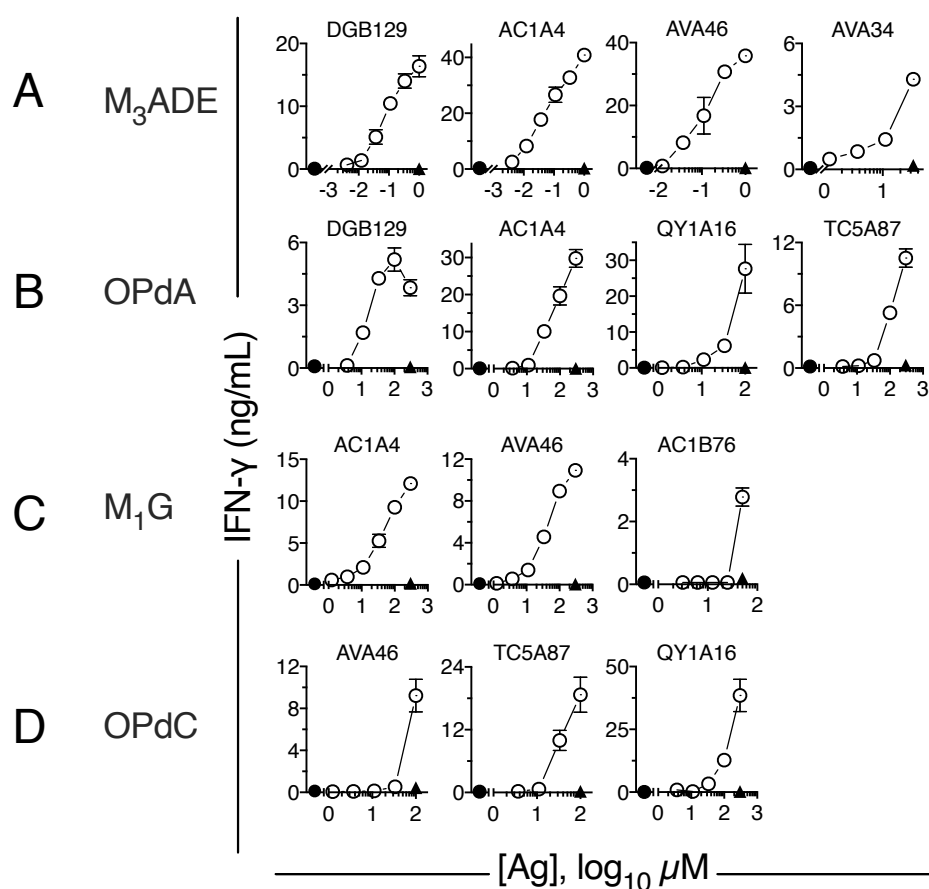
Figure 3-21. Synthetic nucleobase-MDA adducts stimulate MR1T cell clones.

IFN-γ release response of indicated MR1T cell clones co-cultured with THP-1 cells in the presence (○) or absence of adducts (●). Blocking of T-cell reactivity is shown for the highest antigen (Ag) dose using anti-MR1 mAbs (▲). IFN-γ release is the mean ± SD of triplicate cultures. The data shown are representative of at least three independent experiments and one representative experiment is shown.

In total. fourteen MR1T clones express different TCRs were selected and tested (Figure 3-22). By comparing the response of T cells, one clone (AVA46) recognized all four antigens, three clones (AC1A4, AC1B76 and QY1A16) recognized three antigens, although with different specificities, three other clones recognized two antigens (DGB129, AVA34 and TC5A47) also with different specificities, one clone reacts only one antigen (MCA2E7) and six clones were not reactive (QY1B42, LMC1D1, MCA2B1, TRA44, MCA3C3, QY1C3) (Figure 3-22).

When the stimulatory capacity of each antigen was compared instead, M_3ADE stimulated six clones, OPdA eight clones, M_1G and OPdC stimulated three clones each. Furthermore, the clone QY1C3 showed high level of reactivity to THP-1 cells in the absence of antigens and such response was significantly reduced by addition of the four antigens (Figure 3-22). The same type of competition was observed with the clone QY1B42 challenged with M_1G and OPdC antigens, and also with LMC1D1 cells challenged with M_3ADE. These latter findings suggested that added adducts may compete with endogenous MR1 antigens produced by THP-1 cells. In addition, THP-1 cells incubated with the four adducts did not stimulate the MAIT-cell clone MRC25 (Figure 3-23).
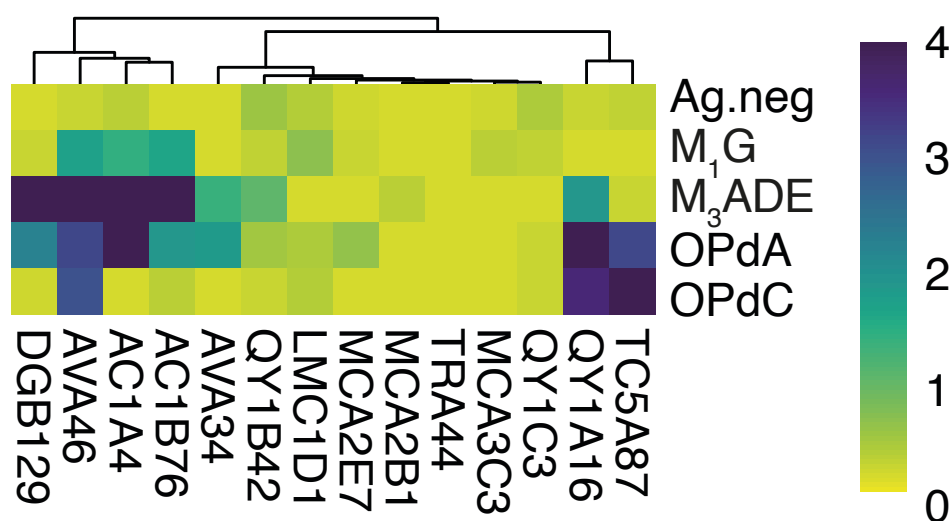
Figure 3-22. Synthetic nucleobase-MDA adducts stimulate MR1T cell clones with different reactivities.

Activation assay of 14 MR1T cell clones in the presence of THP-1 cells treated with M_3ADE, OPdA, M_1G, OPdC or vehicle. Heat-map reports the square root of mean IFN-γ concentration. Antigen response was compared to vehicle and evaluated by multiple t-test ($p < 0.05$). IFN-γ release is the mean $\pm$ SD of triplicate cultures. The data shown are representative of at least two independent experiments and one representative experiment is shown.
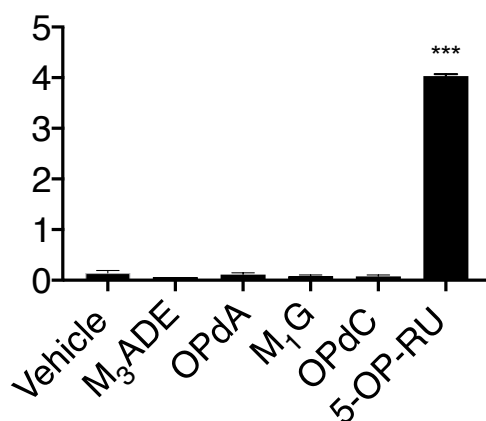
Figure 3-23. Synthetic nucleobase-MDA adducts do not stimulate MAIT cells.

MRC25 cells stimulated with THP-1 cells in the presence of M3ADE, OPdA, OPdC, M1G and 5-OP-RU (1 nM). IFN-γ is expressed as mean ± SD of triplicate cultures. The experiments were repeated at least twice and one representative experiment is shown. ***$p \leq 0.001$ compared to vehicle-treated cells using One-way ANOVA with Dunnett's multiple comparison.

We next investigated whether the four adducts undergo any modifications before MR1 binding, in analogy to processing of protein antigens which give rise to peptides binding MHC molecules. To address this issue, MR1T cell activation assays were performed using plastic-bound recombinant soluble MR1 loaded with synthetic adducts. The response of MR1T cells was evaluated by measuring INF-γ production. Recombinant soluble MR1 molecule was generated with a mutation of lysine to alanine at position 43 (K43A), which facilitates folding of recombinant MR1 [148]. All tested adducts efficiently stimulated MR1T cell clones in the plate-bound assay, thus implying that they bind to MR1 and stimulate MR1T cells without processing and modifications by APCs (Figure 3-24). These findings also confirmed that all four synthetic antigens do not require the formation of a Schiff's base, which instead is required to stimulate MAIT cells by the potent ligand 5-OP-RU [107, 108].
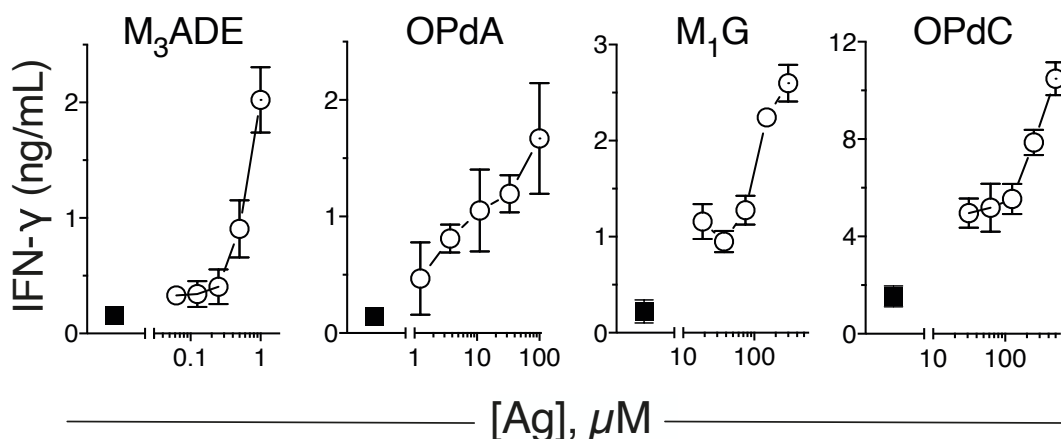
Figure 3-24. Synthetic nucleobase-MDA adducts stimulate MR1T cells with plate-bounded MR1 molecule.

Response of MR1T clones DGB129, QY1A16, AC1A4 and TC5A87, stimulated by plate-bound soluble MR1 loaded (○) respectively with M_3ADE, OPdA, M_1G and OPdC or not (■). IFN-γ release is the mean ± SD of triplicate cultures. The experiments were repeated at least twice and one representative experiment is shown.

3.5.4 Synthesis and purification of nucleobase-MG formed adducts, MGG

The previous results confirmed that MDA generates nucleobase adducts that stimulate MR1T cells. To investigate whether other reactive carbonyl species generate antigenic nucleobase adducts, additional syntheses were performed using methylglyoxal (MG) and various nucleobases. MG is formed in several metabolic pathways [298], including glycolysis, degradation of acetone and of threonine [183]. Physiological concentrations of up to 100 μM of MG have been reported from various sources [266]. Our initial experiments also showed that MG in involved in generating MR1T cell antigens (Figure 3-2). By modifying a described protocol [251], we first synthesized and purified the cyclic adducts formed by guanosine and MG (MGG). A pair of diastereoisomers (Figure 3-25 A, peak 1 and 3) were identified as a form with a methyl group at position 6 (MGG1) and a form with a methyl group at position 7 (MGG2) (Figure 3-25 B), named as 3-(β-D-erythro-pentofuranosyl)-5,7-dihydro-6,7-dihyroxy-6-methyl-imidazo[1,2-a]purine-9-one. The structures of these compounds were identified using ^{1}H-NMR spectroscopy (Figure 3-26).
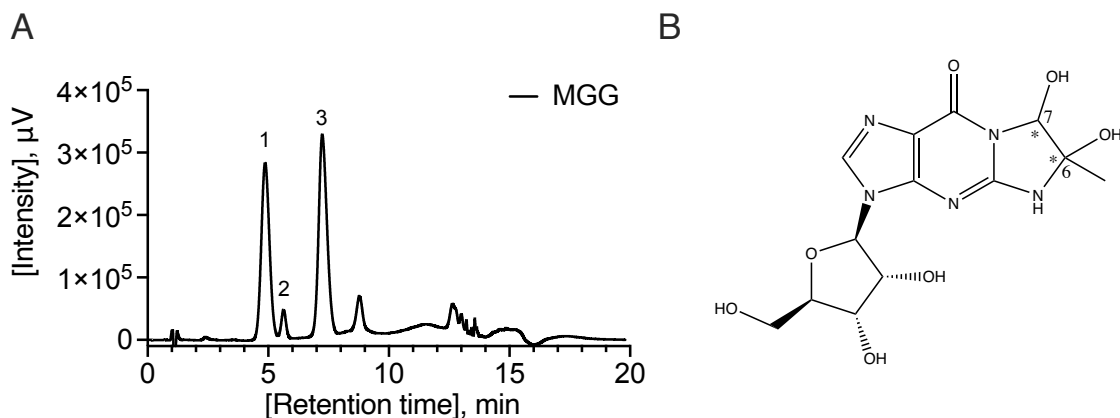
Figure 3-25. HPLC analysis and structure of MGG.

(A) HPLC chromatograms of MGG synthesis. Peak 2 is guanosine, peak 1 and 3 represent the two MGG diastereoisomers. Raw mixture was diluted 50x with H_2O and injected 50µl on HPLC (Absorbance 254 nm). (B) Identified structure of MGG, $C_{13}H_{17}N_5O_7$. The newly formed chiral carbons are indicated by asterisks.
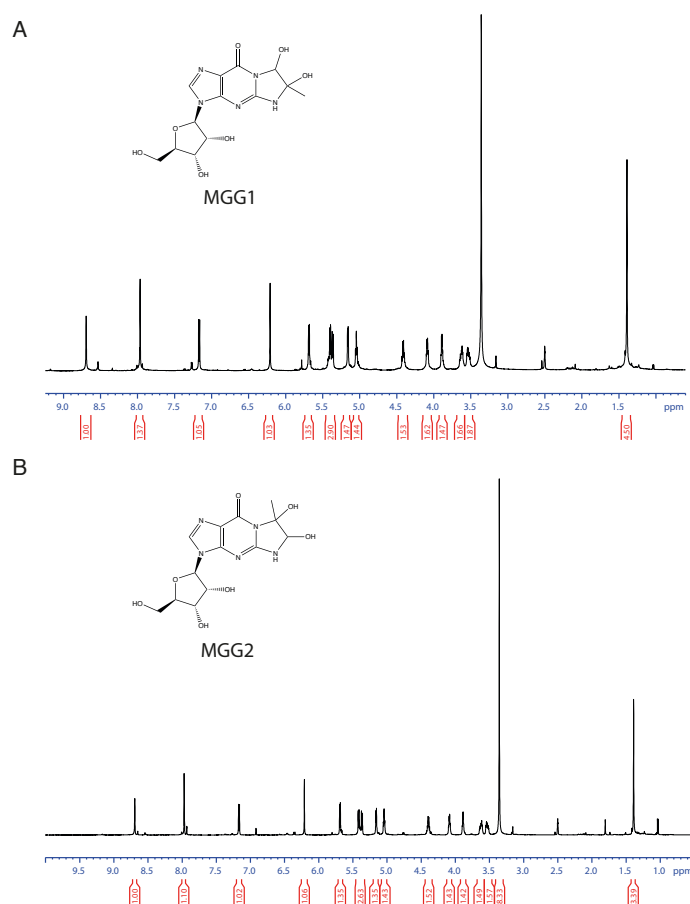
Figure 3-26. NMR analysis of synthetic MGG.

(A) ^{1}H-NMR analysis of MGG isomer 1 (A) and isomer 2 (B) with structure.

73

When the stimulatory capacity of both isomers was tested using 41 randomly selected MR1T clones, only clone DGB129 reacted, and it was activated by both isomers in a similar manner (Figure 3-27 A, B). Instead, MGG did not stimulate the MAIT-cell clone MRC25 (Figure 3-29). In addition, both isomers did not induce MR1 upregulation and were not active in MR1 plastic-bound activation assays. After purification, the MGG isomers were very unstable. Both diastereoisomers were decomposed quickly to guanosine (Figure 3-25 A, peak 2) and also transformed to each other after one hour at room temperature. This decomposition and transformation of MGG isomers was also observed in the previous report [251]. In conclusion, we were able to synthesize and purify a novel pair of MR1 ligand made of MG and guanosine. They are not stable and stimulated only one MR1T cell clone, indicating that they are not recognized by the panel of MR1T cell clones used in our experiments. However, these negative data do not exclude the possibility that other MR1T cells exist that recognize these antigens.
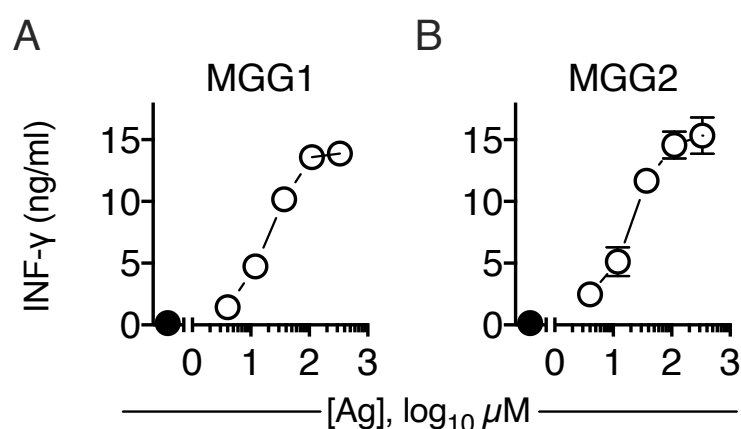
Figure 3-27. Synthetic adducts MGG1 and MGG2 stimulate MR1T cells.

IFN-γ release response of indicated MR1T cell clone DGB129 co-cultured with THP-1 cells in the presence (O) or absence of adducts (●). IFN-γ release is the mean ± SD of triplicate cultures. The data shown are representative of at least two independent experiments and one representative experiment is shown.

3.5.5 Synthesis and purification of nucleobase-MG formed adducts, MGdA

We next attempted to generate synthetic adducts made of MG and deoxyadenosine (MGdA). Using a synthesis procedure similar to that used for M_3ADE, adducts were synthesized. This procedure generated a large variety of adducts, which we attempted to purify. However, using combinations of different SPE cartridges and HPLC column, the purity and quantity of the active adducts was not sufficient for structure identification. When the raw adducts were tested

with 38 randomly selected MR1T clones with polyclonal TCRs, six clones showed MR1-dependent activation by MGdA (Figure 3-28). However, THP-1 cells incubated with MGdA did not stimulate the MAIT-cell clone MRC25 (Figure 3-29).
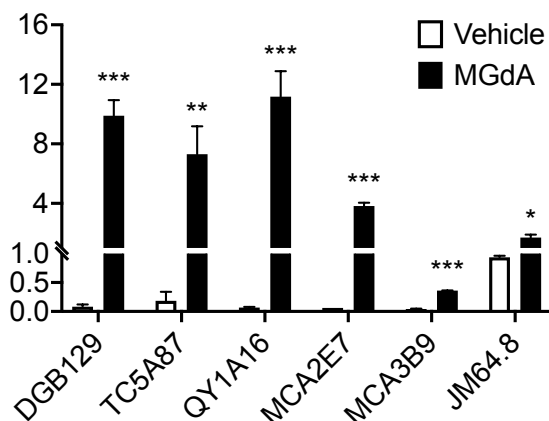
Figure 3-28. Synthetic adducts MGdA stimulate different MR1T clones.

IFN-γ release response of indicated MR1T cell clones co-cultured with THP-1 cells in the presence (black bars) or absence of MGdA (white bars). Synthetic MGdA was purified by SPE cartridges and diluted 100x for activation assay. IFN-γ release is the mean ± SD of duplicate cultures. The data shown are representative of at least two independent experiments and one representative experiment is shown. *$p<0.05$, **$p \leq 0.01$ and ***$p \leq 0.001$, multiple t-test.
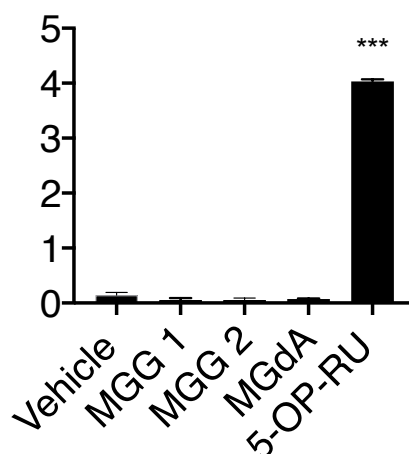
Figure 3-29. Synthetic MGG and MGdA do not stimulate MAIT cells.

MAIT clone MRC25 stimulated with THP-1 cells in the presence of MGG 1 and MGG 2 (all 100 μM), MGdA (diluted 10) and 5-OP-RU (1 nM). IFN-γ is expressed as mean ± SD of triplicate cultures. The experiments were repeated at least twice and one representative experiment is shown. ***$p \leq 0.001$ compared to vehicle-treated cells using One-way ANOVA with Dunnett's multiple comparison.

3.6 Discussion

The data presented in this Chapter highlighted that purines, pyrimidine and reactive carbonyls derived from different metabolic pathways participate in the generation of MR1T antigens, confirming the extended role of MR1 molecule beyond microbial antigen presentation [151]. Previous studies of our lab identified the novel MR1T cell population from healthy individuals [1]. MR1T cells do not react to bacteria-derived MAIT antigens, but to compounds accumulating in different tumour cells, showing their distinct antigen specificity and functional diversity in human immunity.

The unique specificity of MR1T cells is supported by a series of experiments which utilized very different approaches and techniques. When we initially performed a genome-wide CRISPR/Cas9-mediated gene disruption, we found that tumour cells survived when key genes involved in different metabolic pathways were inactivated. These initial studies on one side revealed the participation of a complex array of genes and metabolic pathways, whose roles were difficult to interpret. On the other side, the same studies showed that genes involved in cell proliferation and in the accumulation of aldehydes as side products of glucose and lipid degradation were also important. By further investigating the genes highlighted by the CRISPR/Cas9 approach, we could clearly identify the most important metabolic pathways involved in antigen generation. By following *in silico* study highlighted genes and metabolic pathways, different purine metabolisms were first found to be involved in MR1T antigen stimulation (Figure 3-1). Our CRISPR/Cas9-mediated screening indicated that accumulation of carbonyls, a consequence of altered glycolysis and lipid peroxidation in tumour cells [257] was also important. According to these analyses, we generated tumour cell lines with alterations of the glycolysis-related gene *GLO1* (GLO1 KO and GLO1-overexpressing cells), which showed alterations in the accumulation of methylglyoxal and also promoted (GLO1 KO cells) or reduced (GLO1-overexpressing cells) the activation of MR1T cells. In additional experiments, we investigated whether addition of methylglyoxal (MG) to tumour cells implements MR1T cell response (Figure 3-2). In these latter experiments, addition of MG showed significant increase of IFN-γ release by MR1T cells when GLO1-deficient tumour cells were incubated with MG. On the contrary, MG did not induce any stimulation when GLO1-overexpressing tumour cells were used. We interpreted these results as evidence of the important roles of glycolysis and methylglyoxal accumulation. However, the CRISPR/Cas9 data also indicated that the accumulation of carbonyls is not sufficient to simulate MR1T cells.

We therefore investigated the role of nucleobases and of nucleobase adducts formed upon condensation of nucleobases with different carbonyls (Figure 3-4).

We also found that other important chemical compounds in MR1T antigen accumulation are reactive oxygen species (ROS). ROS are well-known side products of oxidative phosphorylation which also accumulate during tumour cell proliferation [299]. Indeed, several ROS scavengers reduced MR1T cell activation, whereas the combination of ROS induction and nucleosides accumulation promotes MR1T antigen generation (Figure 3-5, 3-6). ROS also promote lipid peroxidation leading to carbonyl generation. These carbonyls are very reactive and have been described in literature as accumulating in tumour cells [167, 176, 183] and capable of generating DNA adducts [169-171]. ROS accumulation is limited within cells by proteins of the GPX family [197]. When we treated tumour cells with drugs inhibiting the GPX1 and GPX4 proteins, we observed an increased MR1T stimulation, which was ascribed to increased accumulation of carbonyls generated during lipid peroxidation (Figure 3-7). Carbonyl accumulation can be also consequence of other metabolic alterations. For example, carbonyls may accumulate when the enzymes involved in their degradation are not efficient [171, 199, 209]. To test this possibility, we also performed experiments in which an inhibitor of aldehyde reductase AKR1B10, oleanolic acid was used to treat tumour cells. AKR1B10 is primarily involved in reducing aldehyde compounds generated from several metabolites [287, 288]. When tumour cells were treated with these drugs, we observed an increased stimulation of MR1T cells (Figure 3-9). In conclusion, these experiments showed that tumour cells become stimulatory when several metabolic alterations occur at the same time. These alterations include: i) Accumulation of nucleobases, which are necessary to sustain tumour cell proliferation; ii) Increased generation of ROS, which is frequently observed in tumour cells; and iii) Increased accumulation of carbonyls, which are the main by-products of altered glycolysis and lipid peroxidation. Furthermore, alterations in carbonyl degradation systems are also important.

Our findings were further supported by the activity of synthetic analogues of nucleobase adducts. We synthesized an array of adducts made of nucleobases and reactive carbonyls derived from lipid peroxidation, like malondialdehyde (MDA) and glycolysis, like MG. Some of these carbonyls and nucleobase adducts naturally accumulate within tumour cells and have also been detected in cancer tissues [188-190, 294, 295]. Among our collection of adducts, four MDA-nucleobase adducts induced MR1 surface upregulation (Figure 3-20) and also showed

stimulation capacity of MR1T clones, measured as cytokine secretion after stimulation with antigen-pulsed APCs (Figure 3-21, 3-22) or with plastic plate-bound MR1 molecules (Figure 3-23). In our collection, the MG-nucleobase adducts (MGG and MGdA) showed much weaker activities. Indeed, they did not induce MR1 surface expression, weakly stimulated very few MR1T clones and we never observed significant activation using soluble MR1 plate-bound assays. These results might due to their weak stability and low purity.

Our studies also showed that free purines and pyrimidines that are naturally accumulating cellular components in highly proliferating cells, are not immunogenic as such, i.e. without carbonyl-induced modifications The fact that this class of MR1T antigens requires structural modifications characterized by generation of bigger molecules and not by partial digestion, such as the antigen processing of proteins that lead to MHC-binding short peptides is a unique feature of several MR1-binding molecules. The same occurs with some bacterial antigens (5-OP-RU) that stimulate MAIT cells, and which are derived by the condensation of MG with a Vitamin B2 precursor [108]. This similarity raises an important issue on the role of MR1-restricted T cells in immune response. Indeed, the recognition of ligands built inside target cells upon accumulation and reaction of different precursors, may indicate that MR1 is an antigen-presenting molecule preferentially presenting modified metabolites which are not usually present inside the cell.

The nucleobases adducts identified in this thesis work bind MR1 in a stable manner and in some cases are immunogenic at low nanomolar concentrations. Their structures are quite different from the ones of bacterial origin [300], thus indicating that MR1 may bind several types of molecules and probably the size and variety of the MR1T cell antigen repertoire is not limited. The existence of additional ligands which bind MR1 and are not in the list of those that we have identified and tested is strongly inferred by the fact that several MR1T cell clones react to tumour cells and not to any of the synthetic antigens. These findings also suggested that the MR1T antigens generated by tumour cells can be different and probably the antigen repertoire stimulating MR1T cells is very different. This conclusion is in line with our finding that among the MR1T TCRs there is no preferential use of any TRVA or TRVB genes, nor J gene segments and therefore the TCR repertoire appears quite heterogeneous.

In summary, the data presented in this section show that MR1T cells are activated by nucleobase adducts generated upon condensation of nucleobases with reactive carbonyls.

Several metabolic pathways participate in the generation of MR1T antigens, thus indicating that different types of metabolic alterations can lead to the accumulation of these antigens.

Chapter 4 MR1T cells recognize small metabolites derived from tumour cells

4.1 Introduction

MR1T cell clones have broad recognition of tumours derived from different tissues, and they are activated by different fractions containing small molecules purified from total tumour lysates [1, 157]. Although we identified nucleobase adducts as the antigens stimulating MR1T cell clones, the direct evidence that nucleobase adducts from tumour lysates also stimulate the same MR1T cells was still missing. To directly address this issue, we used a novel strategy. First, we generated a gene construct encoding a soluble β2m-MR1-human IgG1 fusion protein, which was transfected into CHO tumour cells. These CHO cells which produce soluble engineered MR1 (CHO sMR1) were first cloned, and the clone producing the largest amounts of protein was selected. The selected subclones were adapted to serum-free medium and used for protein production. As control, we also grew the same tumour cells in serum free medium which were not transfected and thus do not produce sMR1. All supernatants from transduced and wild type tumour cell lines were concentrated and sMR1 was purified using IgG magnetic beads followed by HPLC fractionation. The control supernatants that did not contain sMR1 were treated in the same manner. In total, supernatant with secreted sMR1 from CHO cells was used for antigen elution.

4.2 Antigen purification from CHO cells

Using a C18-pyramid column (capable of binding relative polar compounds), compounds eluted from sMR1 and controls were purified on HPLC and collected in individual fractions. The total amounts of each compound were too low to be detected on HPLC using evaporative light scattering detector (ELSD) detector or a photo diode array (PDA) detector. When each fraction was used to stimulate MR1T cell clones, several peaks from CHO sMR1 cells were identified which activated the MR1T clone TC5A87 (Figure 4-1). Two cytokines, IFN-γ (Figure 4-1 B) and IL-13 (Figure 4-1C) were evaluated to monitor T cell activation by ELISA. We found that the fractions with different hydrophilicities were able to stimulate MR1T clone TC5A87 with differing efficacy. Both cytokines IFN-γ and IL-13 were secreted by cells stimulated with the same fractions. Fractions 3 to 13 contained a weakly stimulatory and very polar compounds as they elute with ~5% acetonitrile. Fraction 17 contained a moderately hydrophobic compound which eluted with ~25% acetonitrile and which was extremely active as it induced the release of large amounts of IFN-γ. Fraction 28 to 30, 33 to 35 and 37 to 39 contained at least three different antigens and as they eluted with 100% acetonitrile, they are

more hydrophobic compounds. In general, these results indicated that several active compounds can be eluted from sMR1 molecules. In agreement with data obtained with synthetic compounds, the MR1T clone TC5A87 also cross-reacts with several antigens bound to MR1.
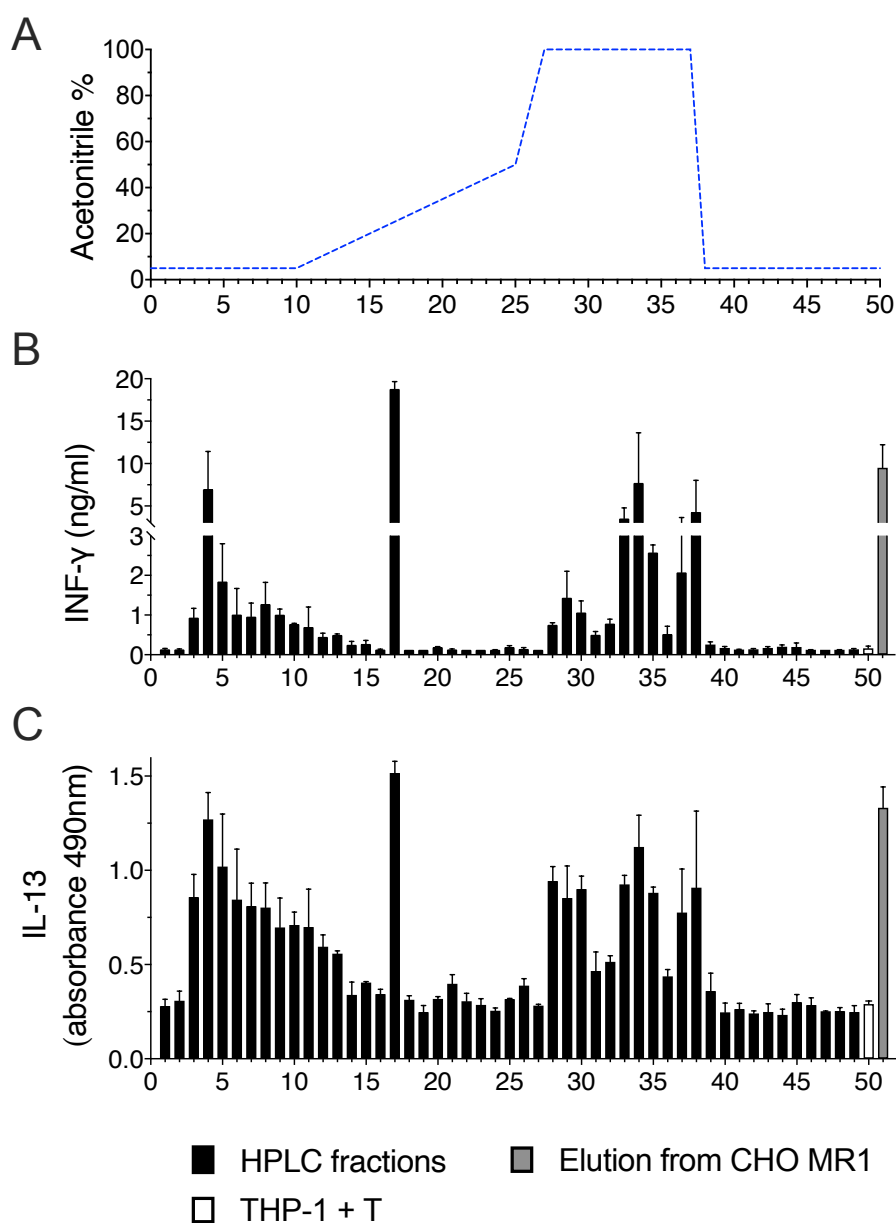
Figure 4-1. Compounds eluted from CHO sMR1 cells stimulate MR1T cells (gradient 1).

(A) Gradient of reversed phase HPLC analysis of compounds eluted from CHO sMR1 cells. Separation was carried out using an analytical 100 mm x 4 mm 5 μM NUCLEODUR C18 Pyramid HPLC column fitted with a C18 guard column. The system was operated in a binary model with a flowrate of 1 mL/min using 100% water and 100% acetonitrile. (B) IFN-γ release response to MR1T clone TC5A87 with HPLC fractions. (C) IL-13 release response to MR1T clone TC5A87 with HPLC fractions. Absorbance at 490 nm was plotted as the IL-13 standard was not working. HPLC fractions were tested per minute and shown as black bars. As control, THP-1 cells with T cells and T cells with THP-1 incubated with compounds before HPLC fractionation were shown as indicated bars. IFN-γ and IL-13 are expressed as mean ± SD of duplicate cultures. The data shown are representative of at least two independent experiments and one representative experiment is shown.

Next, we attempted to identify the nature of active compounds. However, due to the limited amounts of compounds in the HPLC fractions, no clear structures were identified using LC-MS-MS analyses. Therefore, the HPLC gradient was optimised in order to have better separation of the active molecules (Figure 4-2 A). In addition, we made a scale-up of tumour supernatants containing the sMR1. In these new series of experiments, approximately 30% of each HPLC fraction was dried under N2 and incubated with THP-1 cells as APCs upon T cells activation.

IFN-γ (Figure 4-2 B) and IL-13 (Figure 4-2 C) were evaluated to monitor T cell activation by ELISA. We found that many fractions were able to stimulate the MR1T clone TC5A87 with different efficacy. Both cytokines IFN-γ and IL-13 were secreted in a similar manner. In control experiments the same T cells did not react to material derived from wild-type tumour cells not producing sMR1, confirming the specificity of this activation (Figure 4-2 B, C). In these experiments, fractions with high reactivity were not detected, possibly because the antigens were diluted or because there was competition between the molecules co-eluting in the same fractions. The remaining 70% of each fraction was dried and used for structure identification. Same amount of HPLC purified fractions eluted from CHO WT cells were used as controls.
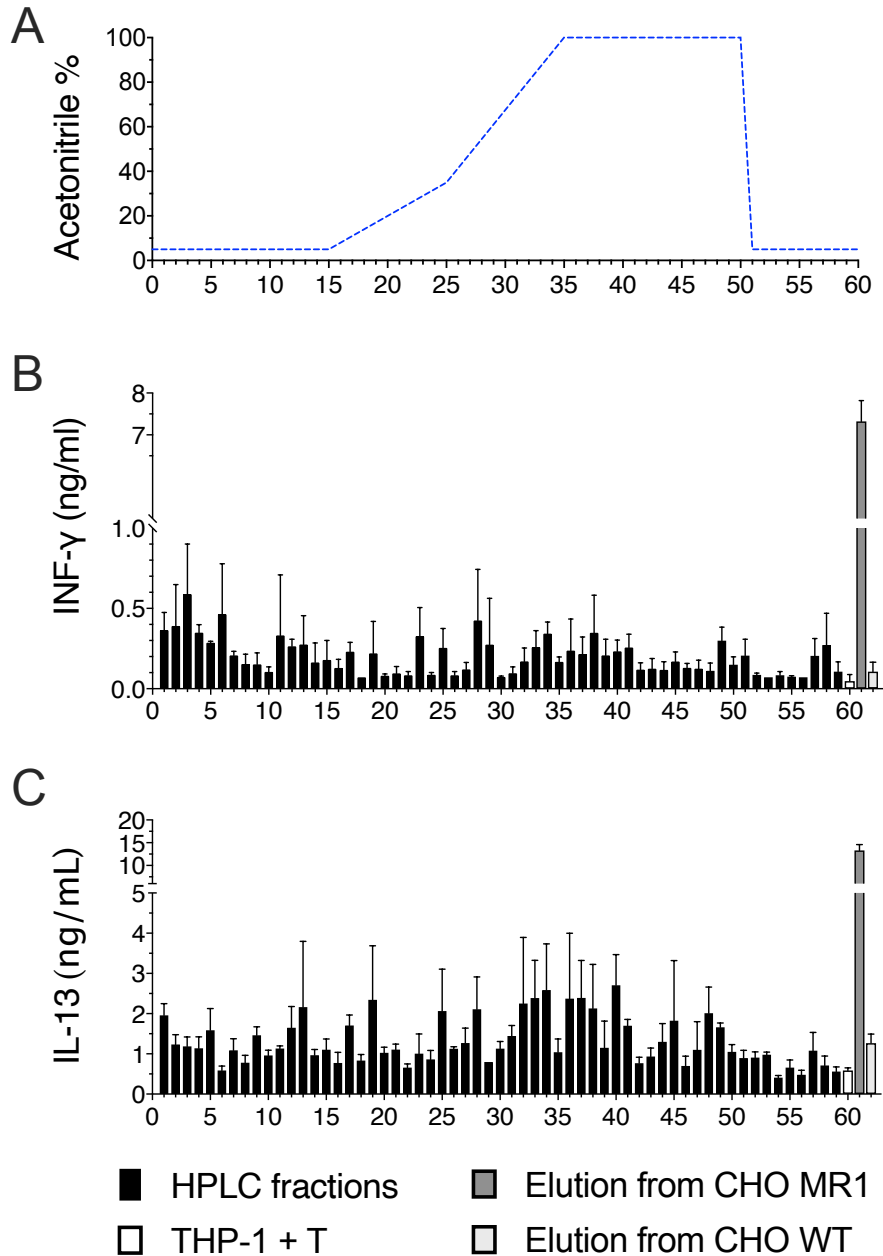
Figure 4-2. Compounds eluted from CHO sMR1 cells stimulate MR1T cells (gradient 2).

(A) Gradient of reversed phase HPLC analysis of compounds eluted from CHO sMR1 cells. Separation was carried out using an analytical 100 mm x 4 mm 5 μM NUCLEODUR C18 Pyramid HPLC column fitted with a C18 guard column. The system was operated in a binary model with a flowrate of 1 mL/min using 100% water and 100% acetonitrile. (B) IFN-γ release response to MR1T clone TC5A87 with HPLC fractions. (C) IL-13 release response to MR1T clone TC5A87 with HPLC fractions. HPLC fractions were tested per minute and shown as black bars. As control, THP-1 cells with T cells, T cells with THP-1 incubated with compounds before HPLC fractionation, and compounds eluted from the supernatant of CHO wildtype cells were shown as indicated bars. IFN-γ and IL-13 expressed as mean ± SD of triplicate cultures.

4.3 Antigen identification from CHO cells

The structure identification was performed by our collaborator using a high resolution/accurate mass data dependent-constant neutral loss-MS^3 methodology developed for DNA adductomics [252]. This method consists of three detection processes, including full scan, data dependent MS^2 acquisition (MS^2) and a neutral loss MS^3 data acquisition (NL-MS3). MS^2 analysis was performed using two strategies, untargeted analysis and targeted analysis. The identified MS^2 were compared with reference standards, with the RNA modifications database [232] and with the mzCloud compound database (https://www.mzcloud.org) in the untargeted method. Furthermore, a targeted screening was also performed using the known DNA adduct list [254] as reference. The NL-MS3 data acquisition was triggered upon observation of the constant-neutral-loss of a ribose or deoxyribose moiety.

Significantly increased detections of several masses were found in the CHO sMR1 samples when compared to CHO wildtype samples. Notably, all of the detected ions contain a purine or pyrimidine structure. Especially, high levels of adenosine and guanosine were detected from the pool of fraction 25-30 from CHO sMR1 cells but not from CHO wildtype cells (Figure 4-3). These results confirmed that purine metabolites are involved in MR1T antigen accumulation, which we previously observed in the experiments depicted in Figure 3-1 and Figure 3-3.
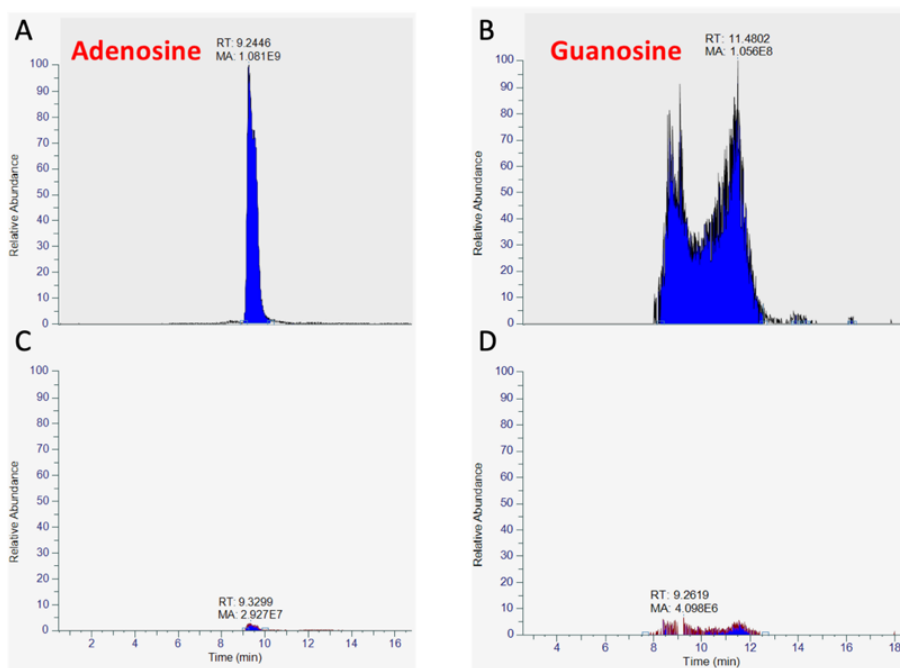
Figure 4-3. Extracted ion chromatogram of fraction 25-30 purified from CHO sMR1 and CHO wildtype cells.

(A, B) Detection of adenosine (A) and guanosine (B) from purified HPLC fraction 25-30 of CHO sMR1 cells. (C, D) Detection of adenosine (C) and guanosine (D) from purified HPLC fraction 25-30 of CHO wildtype cells.

In total, putative structures of 22 ions were assigned based on the target and untargeted analysis. The major detection was found in fractions 25-30, which contained 20 ions. Furthermore, one ion was detected in the polar fractions 11-15 and one ion was detected in the nonpolar fractions 31-35. Two compounds were confirmed by the compound database using untargeted analysis (Table 4-1, No. 1 and 2) and four compounds were confirmed using targeted approach with the known DNA adduct list (Table 4-1, No. 19 and 22). In addition, several compounds although containing nucleobase core structures, showed larger masses and their structures were not identified. The summarized identification is shown in Table 4-1.

Table 4-1. Ions detected during the MS screening by untargeted and targeted analysis.

NO.	MH$^+$	Analysis	Name or conformation	Origin in *vivo*	Molecular Formula	From fraction
1	296.1355	Untargeted	N^6, N^6-dimethyladenosine	rRNA	$C_{12}H_{18}O_4N_5$	25 to 30
2	336.167	Untargeted	N^6-isopentenyladenosine	tRNA	$C_{15}N_{22}O_4N_5$	25 to 30
3	338.1827	Untargeted	Adenine +	unknown	$C_{15}H_{24}O_4N_5$	25 to 30
4	350.1465	Untargeted	Adenine +	unknown	$C_{15}N_{20}O_5N_5$	25 to 30
5	352.1625	Untargeted	Adenine +	unknown	$C_{15}H_{22}O_5N_5$	25 to 30
6	356.132	Untargeted	Guanine +	unknown	$C_{12}H_{18}O_6N_7$	25 to 30
7	372.1519	Untargeted	Adenine +	unknown	$C_{14}H_{22}O_7N_5$	25 to 30
8	382.1478	Untargeted	Adenine +	unknown	$C_{14}H_{20}O_6N_7$	25 to 30
9	404.1241	Untargeted	Thioadenine +	unknown	$C_{14}H_{22}N_5O_7S$	25 to 30
10	407.1789	Untargeted	Adenine +	unknown	$C_{16}H_{23}O_5N_8$	25 to 30
11	425.1883	Untargeted	Adenine +	unknown	$C_{16}H_{25}O_6N_8$	25 to 30
12	436.2197	Untargeted	Adenine +	unknown	$C_{20}H_{30}O_6N_5$	25 to 30
13	437.1904	Untargeted	Adenine +	unknown	$C_{17}H_{25}O_6N_8$	25 to 30
14	438.2108	Untargeted	Guanine +	unknown	$C_{18}H_{27}O_6N_7$	25 to 30
15	452.2261	Untargeted	Guanine +	unknown	$C_{19}H_{29}O_6N_7$	25 to 30
16	452.2027	Targeted	Cytidine + DODE	unknown	$C_{21}H_{29}O_8N_3$	11 to 15
17	326.1095	Targeted	Adenosine + Glyoxal	unknown	$C_{12}H_{15}O_6N_5$	25 to 30
18	350.1459	Targeted	Adenosine + Malonaldehyde; Acetaldehyde	unknown	$C_{15}H_{19}O_5N_5$	25 to 30
19	322.1146	Targeted	Adenosine + Malonaldehyde	unknown	$C_{13}H_{15}O_5N_5$	25 to 30
20	292.104	Targeted	Adenosine + Glyoxal	unknown	$C_{12}H_{13}O_4N_5$	25 to 30
21	354.1408	Targeted	Guanosine + Crotonaldehyde	unknown	$C_{14}H_{19}O_6N_5$	25 to 30
22	380.1816	Targeted	Cytidine+ 4-oxo-2-nonenal	unknown	$C_{18}H_{25}O_6N_3$	31 to 35

4.4 Antigenic activity test of identified compounds by untargeted analysis

Based upon the ion signal intensities in the total ion chromatogram and their MS^2 and MS^3 spectra, two compounds were confirmed by comparison with synthetized standards and databases. They are N^6, N^6-dimethyladenosine (m6,6A, Figure 4-4) and N^6-isopentenyladenosine (i6A, Figure 4-5). To further investigate the antigenic activity of the detected compounds m6,6A and i6A, MR1 upregulation, activation, and competition assays were performed using synthetic compounds.

Initially, we tested whether these adducts increase MR1 cell surface expression (Figure 4-6). THP-1 cells were incubated with titrated adducts and MR1 median florescence intensity (MFI) was studied by flow cytometry. After six hours incubation, both m6,6A and i6A induced upregulation of MR1 cell surface expression in a dose dependent manner (Figure 4-7). A very efficient upregulation of surface MR1 was observed, suggesting that these transfectants contain large amounts of MR1 molecules that are stabilized by these antigens.
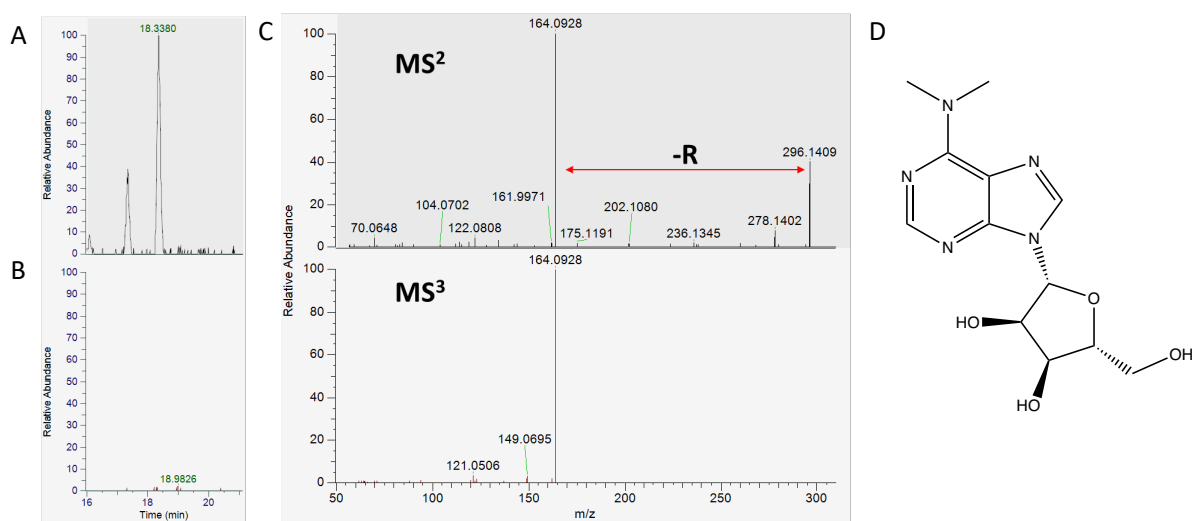
Figure 4-4. Spectra and structural assignments of N^6,N^6-dimethyladenosine (m6,6A).

(A, B) Extracted ion chromatogram of detected of N^6,N^6-dimethyladenosine (m6,6A, *m/z* 296.1355) from fraction 25-30 of CHO sMR1 cells (A) and from CHO wildtype cells (B). (C) Most intensive peaks of m6,6A detected in MS^2 and MS^3 spectra. (D) Structure of m6,6A, $C_{12}H_{17}N_5O_4$. The structure was confirmed by comparison with synthetized standards.
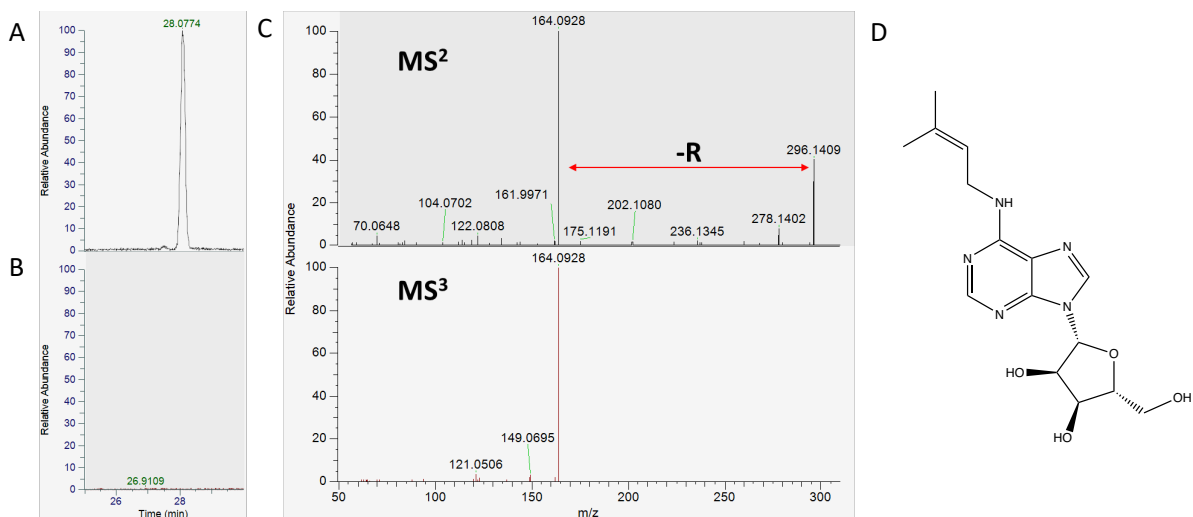
Figure 4-5. Spectra and structural assignments of N^6-isopentenyladenosine (i6A).

(A, B) Extracted ion chromatogram of detected of N^6-isopentenyladenosine (i6A, *m/z* 336.1670) from fraction 25-30 of CHO sMR1 cells (A) and from CHO wildtype cells (B). (C) Most intensive peaks of i6A detected in MS^2 and MS^3 spectra. (D) Structure of i6A, $C_{15}H_{21}N_5O_4$. The structure was confirmed by comparison with synthetic standards.
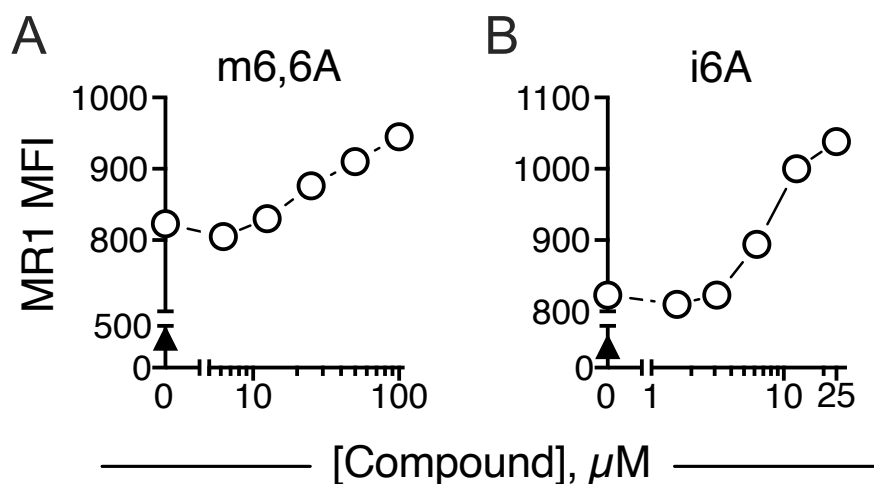
Figure 4-6. CHO sMR1 cells identified compounds m6,6A and i6A induce MR1 surface expression on THP-1 cells.

Upregulation of MR1 surface expression on THP-1 cells following 6 h incubation with i6A (A), m6,6A (B) (○), isotype control (▲). Median florescence intensity (MFI) was checked by flow cytometry. The data shown are representative of at least three independent experiments.

To check the stimulatory capacity of m6,6A and i6A, THP-1 cells were incubated with different doses of both compounds and five MR1T cell clones with distinct TCRs (Table 3-1) and a

control MAIT clone were used as responders (Figure 4-7 and 4-8). Some MR1T cell clones reacted to both compounds, some reacted to one compound or did not react (the rest clones in table 3-1). Notably, MAIT clone MRC25 did not react to any of them. In all cases MR1T cell activation was blocked by the addition of anti-MR1 mAbs, suggesting MR1 restricted recognition of both adducts.
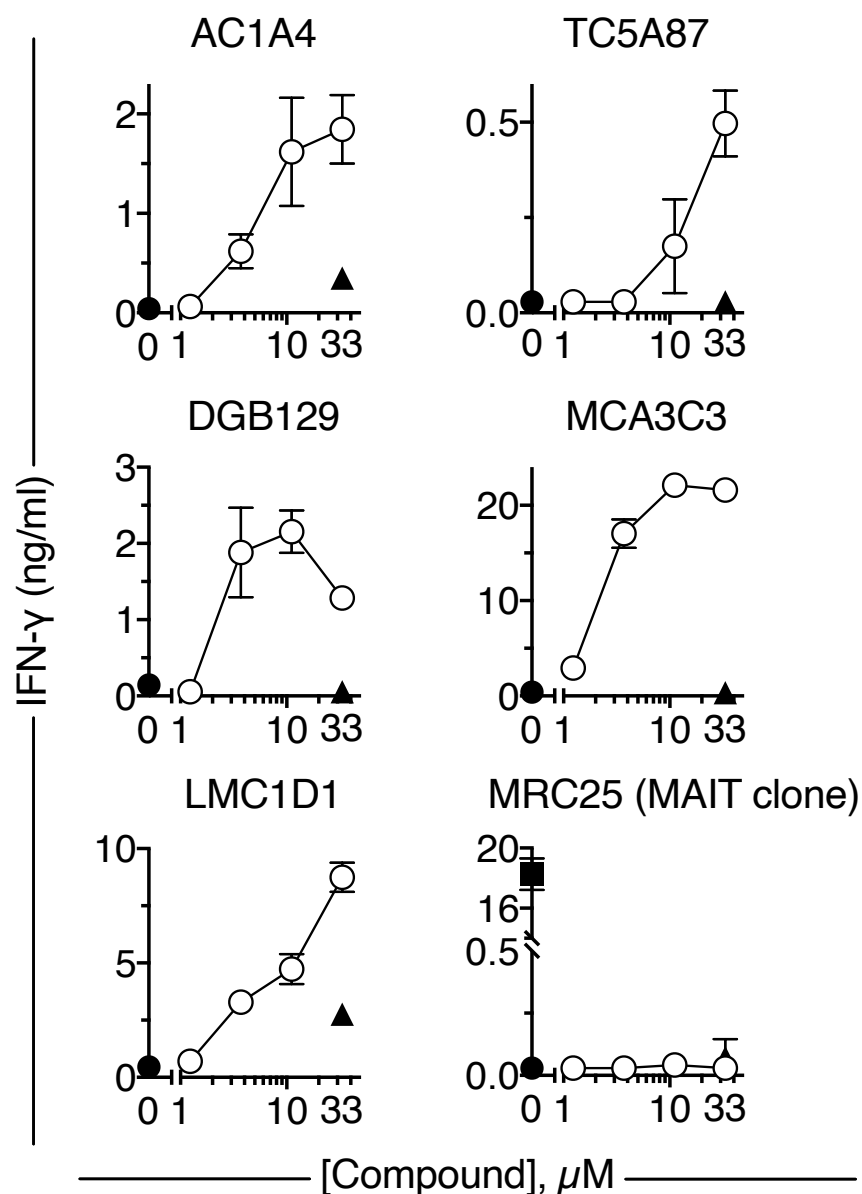
Figure 4-7. Compound m6,6A identified from CHO sMR1 cells stimulate MR1T cells.

IFN-γ release response of indicated MR1T cell clones and a MAIT clone (MRC25) co-cultured with THP-1 cells in the presence (○) or absence of m6,6A (●). Blocking of T-cell reactivity is shown for the highest and second highest dose using anti-MR1 mAbs (▲). MAIT clone co-cultured with THP-1 cells in the presence of 2 nM 5-OP-RU (■) was used as the positive control. The data shown are representative of at least two independent experiments. IFN-γ is expressed as mean ± SD of triplicate cultures.
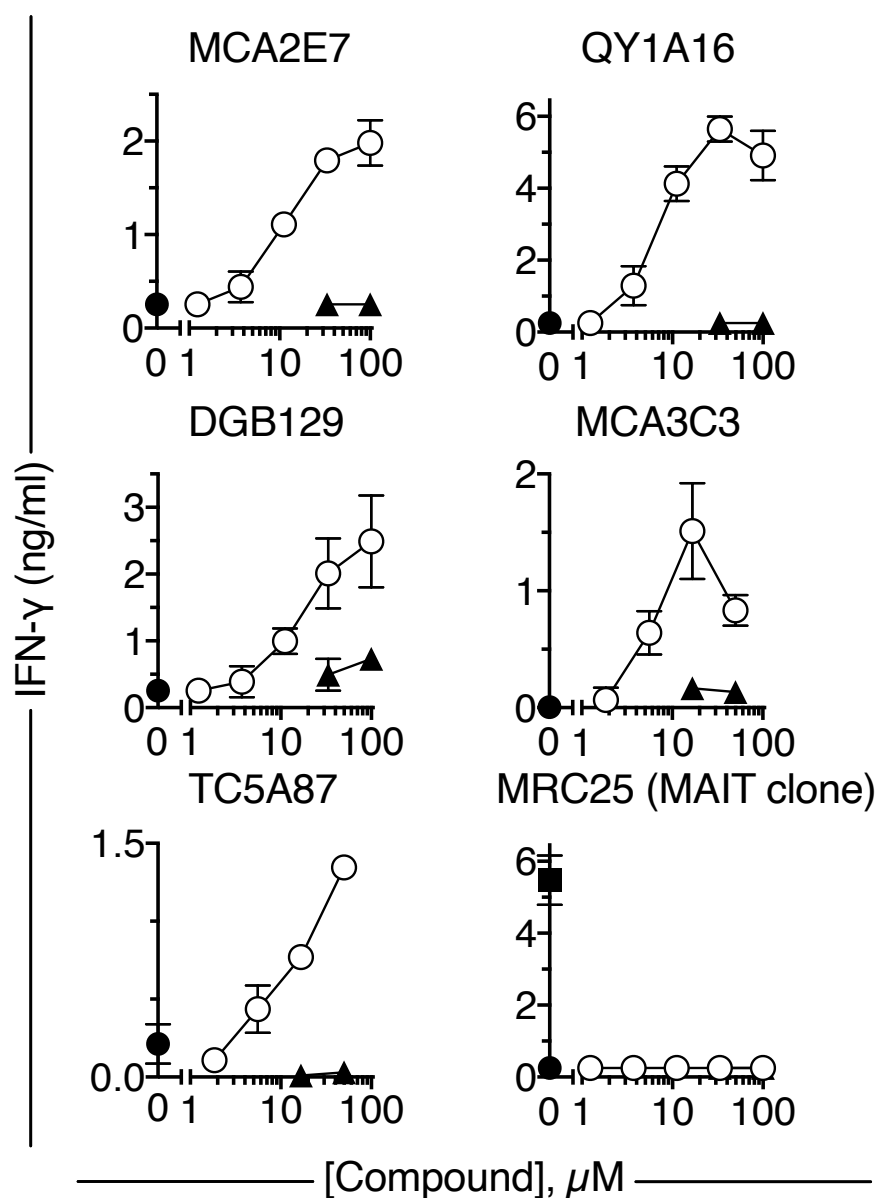
Figure 4-8. Compound i6A identified from CHO sMR1 cells stimulate MR1T cells.

IFN-γ release response of indicated MR1T cell clones and a MAIT clone (MRC25) co-cultured with THP-1 cells in the presence (O) or absence of i6A (●). Blocking of T-cell reactivity is shown for the highest and second highest dose using anti-MR1 mAbs (▲). MAIT clone co-cultured with THP-1 cells in the presence of 1 nM 5-OP-RU (■) was used as the positive control. The data shown are representative of at least two independent experiments. IFN-γ is expressed as mean ± SD of triplicate cultures.

To further prove that i6A and m6,6A bind MR1, competition assays were performed using a MR1T clone and a MAIT clone stimulated by their corresponding antigens (Figure 4-9 and 4-10). Compound i6A showed clear competition with the MR1 antigen of both MR1T- and MAIT-cell clones, suggesting that i6A when binds MR1 can displace/compete both MGdA and

92

5-OP-RU (Figure 4-9). On the contrary, addition of m6,6A, which per se stimulate weakly the MR1T cell clone DGB129 (release approximately IFN-γ 1ng/ml with 100 μM m6,6A) and does not stimulate the MAIT clone MRC25, facilitated the antigen-induced activation of both clones in a dose dependent manner (Figure 4-10). A possible explanation of this unexpected effects could be that m6,6A does not compete for MR1 binding with both M$_3$ADE and 5-OP-RU, and instead it promotes MR1 surface expression and thus it facilitates antigen stimulation of MR1-restricted T cells.

Collectively, these data confirmed that two molecules eluted from MR1 when they are added as synthetic analogues, can bind MR1 facilitating its stabilization and surface expression. They also stimulate different MR1T cells and while i6A competes with other antigens, m6,6A facilitates the MR1 presentation by other antigens.

These compounds are modified nucleosides generated endogenously, however, they are present in tRNAs and are not formed by condensation of carbonyls with nucleosides. To investigate whether this class of nucleobase adducts are also present in the MR1-eluted compounds further experiments were performed.
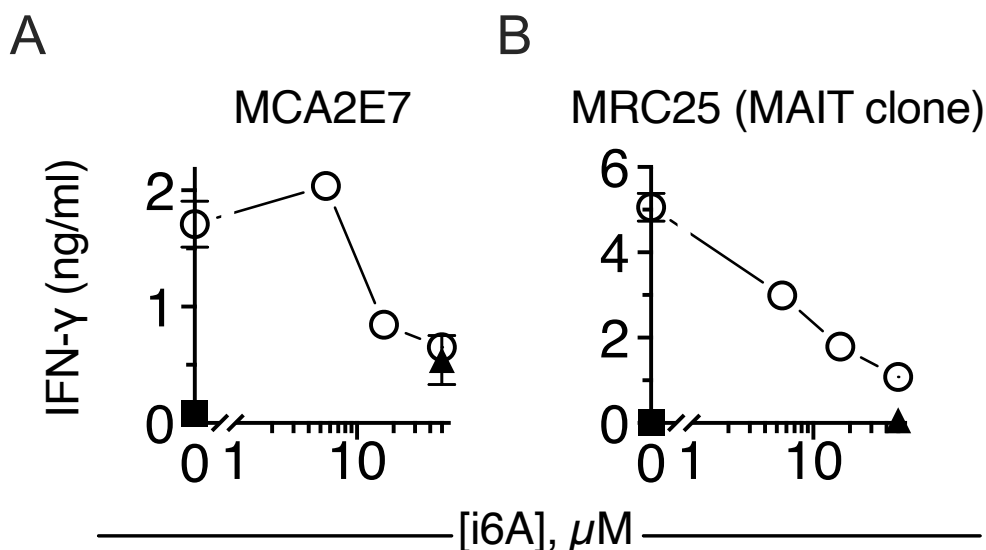
Figure 4-9. i6A competes MR1 binding with the known MR1 antigens.

MR1T cell clone MCA2E7 (A) and MAIT clone MRC25 (B) were first co-cultured with THP-1 cells in the presence of titrated competitor i6A for 3 h, then adding a fixed dose of known antigen MGdA for MCA2E7 and 5-OP-RU for MRC25 (O) or without adding antigen (▲) or in the absence of competitor and antigen (■). The data shown are representative of at least two independent experiments. IFN-γ is expressed as mean ± SD of triplicate cultures.
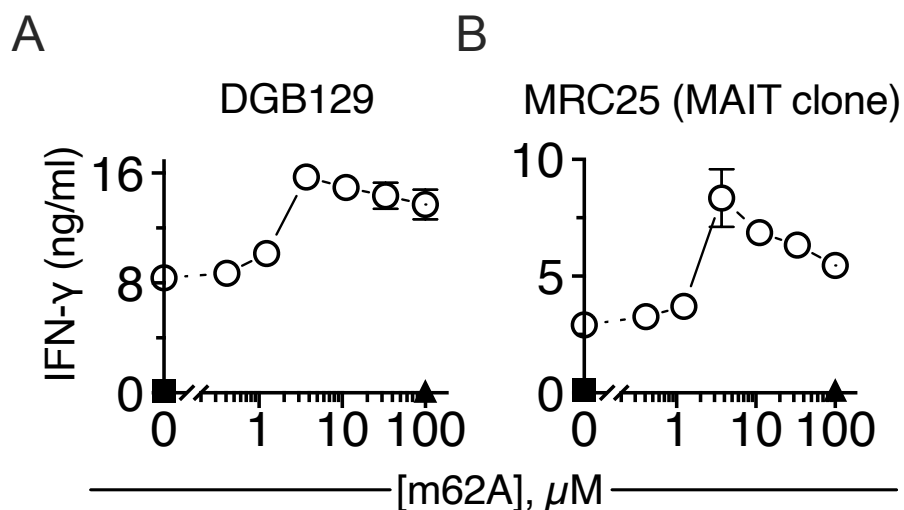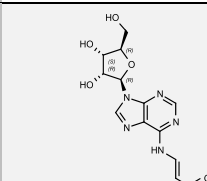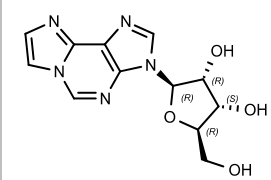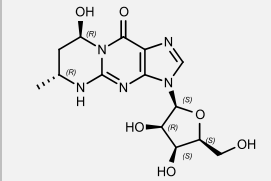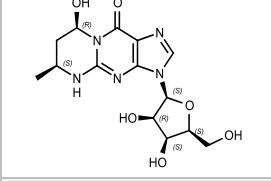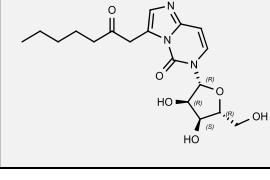
Figure 4-10. M6,6A does not compete MR1 binding with the known MR1 antigens.

MR1T cell clone DGB129 (A) and MAIT clone MRC25 (B) were first co-cultured with THP-1 cells in the presence of titrated competitor m6,6A for 3 h, then adding the same dose of known antigen M$_3$ADE for DGB129 and 5-OP-RU for MRC25 (O) or without adding antigen (▲) or in the absence of competitor and antigen (■). The data shown are representative of at least two independent experiments. IFN-γ is expressed as mean ± SD of triplicate cultures.

4.5 Antigenic activity test of identified compounds by targeted analysis

In addition of the identified MR1 antigens by untargeted analysis, seven RNA-aldehyde adducts were detected using targeted screening with known DNA adduct list as a reference library (Table 4-1). Four out of total seven identified compounds (Table 4-2) were successfully synthesized. In addition, two isomers of Guanosine-Crotonaldehyde adducts named Guanosine-Crotonaldehyde isomer 1 (Crot-G 1) and Guanosine-Crotonaldehyde isomer 2 (Crot-G 2) were tested. Two different assays were used: i) evaluation of MR1 upregulation, and ii) activation of MR1T cell clones.

Table 4-2. MS identified compounds with their chemical structures.

NO. in Table 4-1	Name	Short name	Structure
19	N^6-(3-oxo-1-propenyl)-adenosine	M1A	
20	(2R,3R,4S,5R)-2-(1,3,4,5a,8-Pentaaza-3H-as-indacen-3-yl)-5-(hydroxymethyl)tetrahydrofuran-3,4-diol	Etheno-A	
21	Pyrimido[1,2-a]purin-10(3H)-one, 4,6,7,8-tetrahydro-8-hydroxy-6-methyl-3-β-D-ribofuranosyl	Crot-G 1	
21	Pyrimido[1,2-a]purin-10(3H)-one, 4,6,7,8-tetrahydro-8-hydroxy-6-methyl-3-β-D-ribofuranosyl	Crot-G 2	
22	Imidazo[1,2-c]pyrimidin-5(6H)-one, 6-(β-D-erythro-pentofuranosyl)-3-(1,2-dihydroxyheptyl)	ONEC	

The MR1 upregulation assay was used to check whether the adducts stabilize MR1 molecules and promote their expression on the plasma membrane. When THP-1 cells overexpressing MR1 (THP-1 MR1) were incubated with the synthetic adducts, we found that they all induced an increase of the MR1 expression levels on the cell surface (Figure 4-11), as found with the other nucleoside-aldehyde adducts (Figure 3-20). When the five compounds were compared, M1A was the most potent inducer of MR1 cell surface upregulation (~7-time fold increase vs. control not-treated cells). The other compounds showed ~1.5-2 times fold increase with the highest doses. The same assay was also performed with THP-1 wildtype cells, which express physiological low levels of MR1 on the plasma membrane. Using these cells, a very weak increase of MR1 surface expression was observed with all five compounds except M1A (~2-time fold increase), confirming that these four compounds are much less active in this assay.
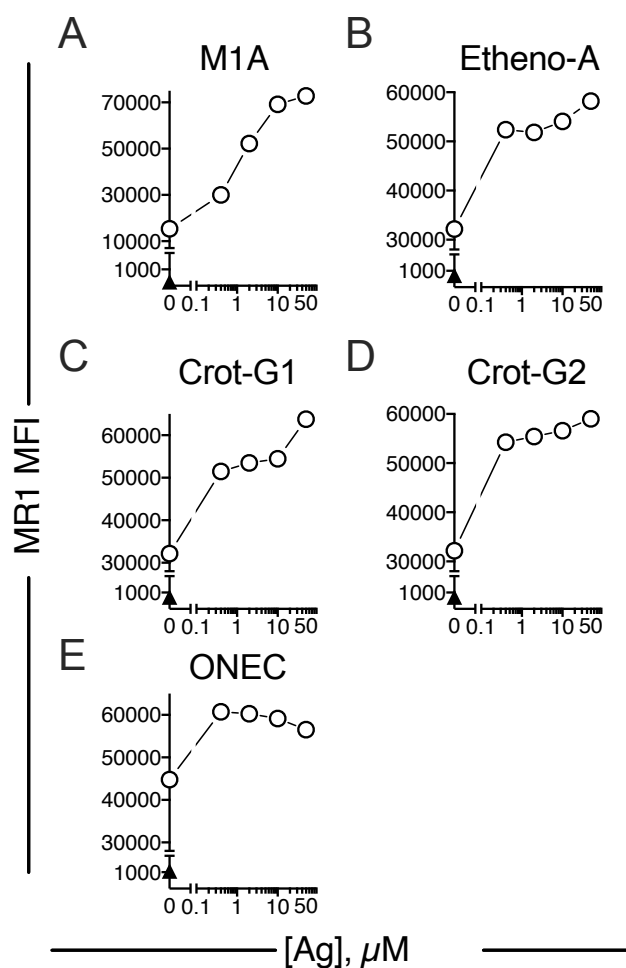
Figure 4-11. Synthetic nucleoside-aldehyde adducts upregulate MR1 surface expression.
Upregulation of MR1 surface expression on THP-1 MR1 cells following 6 h incubation with five synthetic adducts M1A (A), Etheno-A (B), Crot-G1 (C), Crot-G2 (D) and ONEC (E) (O), isotype control (▲). Median florescence intensity (MFI) was checked by flow cytometry. The data shown are representative of at least two independent experiments and one representative experiment is shown.

The compounds were then tested for their capacity to stimulate MR1T cell clones (Figure 4-12). In total fourteen MR1T clones and a MAIT clone were tested (Table 3-1). THP-1 cells were pulsed with synthetic adducts and then used to stimulate different each T cell clone. Two cytokines IFN-γ and IL-13 were monitored in each experiment. As some clones showed very low IFN-γ secretion, IL-13 is shown in Figure 4-12. By comparing the stimulatory capacity of each antigen, M1A stimulated eight MR1T clones out of fourteen, Etheno-A did not stimulate any MR1T clone, Crot-G1 and Crot-G2 stimulated same clones (QY1C3, MCA3C3, QY1A16) and ONEC stimulated only one clone (QY1A16). On the other hand, most MR1T cell clones

showed reactivity against only one adduct, while clone MCA3C3 and QY1A16 cross-reacted with three adducts. In all cases, MR1T cell activation was blocked by the addition of anti-MR1 mAbs, confirming the MR1 restricted activation of tested MR1T cells. Notably, all of the compounds did not react with MAIT clone MRC25 (Figure 4-13), suggesting the compounds derived from tumour cells are MR1T cell specific antigens.
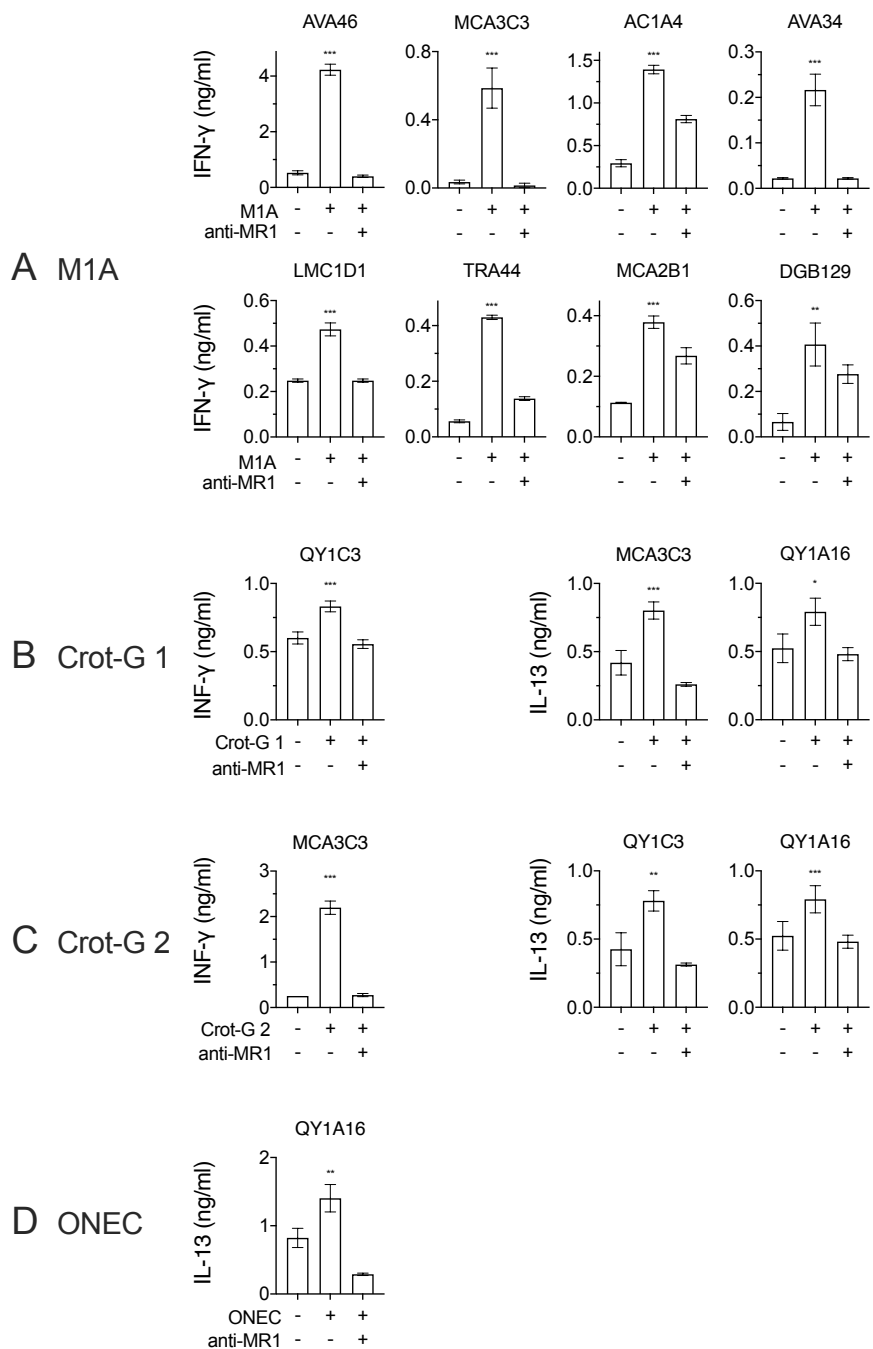
Figure 4-12. Synthetic nucleoside-aldehyde adducts stimulate MR1T cell clones.

Cytokine release response of indicated MR1T cell clones and co-cultured with THP-1 cells in the presence or absence of five synthetic adducts (all 50 μM) M1A (A), Crot-G1 (B), Crot-G2 (C) and ONEC (D). Blocking of T-cell reactivity is shown using anti-MR1 mAbs. IFN-γ or IL-13 release is the mean ± SD of triplicate cultures. The data shown are representative of at least two independent experiments and one representative experiment is shown. ***p≤0.001 compared to vehicle-treated cells using One-way ANOVA with Dunnett's multiple comparison.
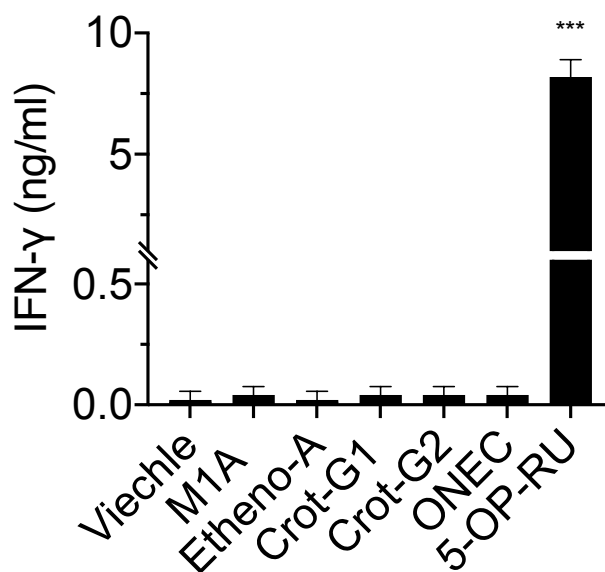
Figure 4-13. Synthetic nucleoside-aldehyde adducts do not stimulate MAIT cells.

MAIT clone MRC25 stimulated with THP-1 cells in the presence of five synthetic adducts (all 50 μM) M1A (A), Etheno-A (B), Crot-G1 (C), Crot-G2 (D) and ONEC (E) and 5-OP-RU (2 nM). IFN-γ is expressed as mean ± SD of triplicate cultures. The experiments were repeated at least twice and one representative experiment is shown. ***p≤0.001 compared to vehicle-treated cells using One-way ANOVA with Dunnett's multiple comparison.

4.6 Discussion

The results presented in this Chapter provide direct experimental evidence of which compounds isolated from tumour cells stimulate MR1T cells. Compounds from soluble MR1 derived from tumour cells were purified by HPLC (Figure 4-1, 4-2) and their structures were identified by mass spectrometry analysis using various compound databases as references [232, 254]. We confirmed the previous finding that MR1T cells are activated by different fractions containing small molecules purified from different tumour cells [1]. The first important finding was that compounds eluted from soluble MR1 showed large amounts of purine analogues (Figure 4-3). These results confirmed the previous ones described in Chapter 3 (Figure 3-1 and 3-3) which indicated that purine metabolites are involved in MR1T cell stimulation. The second finding was that several compounds, although containing nucleobase core structures, showed larger masses and their structures were not identified (Table 4-1). These results indicated that many different adducts, whose structures remain unknown, can accumulate within tumour cells and bind MR1. The third important finding was that most of the identified molecules contained a ribose, thus indicating that they were derived from RNAs. The implications of these latter findings remain to be investigated with *ad hoc* experiments.

Two modified RNAs, N^6, N^6-dimethyladenosine (m6,6A, Figure 4-4) and N^6-isopentenyladenosine (i6A, Figure 4-5) were identified in the sMR1 purified fractions and showed strong signals in the spectrometer. These two modified nucleosides are present within cells, including those of eukaryotic, microbial and plant origin. The fact that these two molecules were abundant in soluble MR1, opened the possibility that other molecules derived from modified RNAs might bind MR1 and be immunogenic. More than 100 RNA modifications have been identified in human cells [232-235], some of them being involved in various human diseases, including cancer [236-238].

i6A appears at position 37 in many tRNA molecules [301]. In Eubacteria and Eukaryotes, the synthesis of i6A is accomplished by conjugating an adenosine with an isopentenyl pyrophosphate (IPP) molecule to the human TRIT1 enzyme [301]. i6A is associated with several human diseases. In the past decades, i6A was tested as a potential antitumour cytokinin [302] and it inhibits the growth of the MCF breast cancer cell line. i6A may also activate the oxidative stress response [302, 303], and can associated with mitochondrial respiratory chain defects [304]. The generation of i6A requires IPP, which is the known antigen of $V_\gamma 9 V_\delta 2$ T cells [74, 75]. Therefore, the accumulation of these MR1T cell antigens in tumour cells might

be associated with the accumulation of other antigens that stimulate the TCR γδ population expressing the TCR $V_γ9V_δ2$.

Another identified RNA was m6,6A, which is found in rRNA of Eukaryotes, and in tRNA of Eubacteria. m6,6A represents an important component of rRNA [305] and it is involved in the assembly of minimal functional ribosomes [306]. The function of i6A and m6,6A in the immune response remains unclear. Our data provided clear evidence that these modified RNAs accumulate in tumour cells, upregulate MR1 surface expression (Figure 4-6), and stimulate individual MR1T clones in a MR1 dependent manner (Figure 4-7, 4-8).

In addition to modified RNAs, some nucleoside-aldehyde adducts were also identified by targeted analysis (Table 4-1). Similar to the adducts described in Chapter 3, four adducts and one isomer were synthesized for different functional assays (Table 4-2). All of them upregulated MR1 surface expression and some stimulated the selected MR1T cell clones (Figure 4-12) but not MAIT clone (Figure 4-13).

Taken together, these data extended our knowledge on the antigen that stimulate MR1T cells. They are modified RNAs and nucleosides adducts generated and accumulating in tumour cells. Future studies will address the mechanisms and metabolic alterations that lead to the accumulation of these antigens, whether different tumours preferentially accumulate some antigens, and which of them will represent the most suitable target antigen in novel and broader strategies in cancer cell immunotherapy.

Chapter 5 The repertoire of MR1T cell antigens comprises other types of modified nucleosides

5.1 Introduction

The studies described in Chapter 3 and 4 showed that MR1T cell antigens are nucleoside-aldehyde adducts and modified nucleosides. So far, we only identified nucleoside adducts containing ribose, implying that RNA is the source of these antigens. The fact that this novel class of molecules is actively involved in stimulating specific T cells opened the possibility that other molecules with similar structural features might bind MR1 and stimulate MR1T cells. To investigate the immunogenic potential of other nucleoside adducts, we selected 30 compounds (Table 5-1). The majority of these selected compounds contain the ribose sugar, some contain a deoxyribose, and some others are modified nucleosides known to be generated in different metabolic pathways. Most of the compounds are generated endogenously by mammalian cells and a few are produced by bacteria and plants. With each compound, we performed MR1 upregulation, activation, and competition assays using MR1T clones TC5A87, DGB129, AC1A4, MCA2E7 with various TCRs and a MAIT clone MRC25, which expresses a canonical non-invariant TCR Vα7.2/Ja33 TCR (Table 3-1). A summary of these findings is shown in Table 5-2. The detailed results of each assay are shown in Figure 5-1, 5-2, and 5-3.

Table 5-1. List of modified nucleobases for MR1T antigenic assays.

Short Name	Full name	Found in	Involved as	Ref.
m1A	1-methyladenosine	Archaea, Eubacteria, Eukaryota	rRNA, tRNA	[235, 307, 308]
m2A	2-methyladenosine	Eubacteria	rRNA, tRNA	[229, 232]
Am	2′-O-methyladenosine	Eubacteria, Eukaryota	rRNA, snRNA, snoRNA, tRNA	[229, 232]
t6A	N^6-threonylcarbamoyladenosine	Eubacteria, Eukaryota	tRNA	[229, 232]
io6A	N^6-(cis-hydroxyisopentenyl) adenosine	Eubacteria	tRNA	[229, 232]
ms2io6A	2-methylthio-N^6-(cis-hydroxyisopentenyl) adenosine	Eubacteria	tRNA	[229, 232]
ms2i6A	2-methylthio-N^6-isopentenyladenosine	Eubacteria	tRNA	[229, 232]
m6t6A	N^6-methyl-N^6-threonylcarbamoyladenosine	Eubacteria	tRNA	[229, 232]
Ar(p)	2′-O-ribosyladenosine (phosphate)	Eukaryota	tRNA	[229, 232]
me1G	N^1-Methylguanosine	Archaea, Eubacteria, Eukaryota	rRNA, tRNA	[229, 232]
m2G	N^2-methylguanosine	Archaea, Eubacteria, Eukaryota	rRNA, snRNA, tRNA	[229, 232]

Short Name	Full name	Found in	Involved as	Ref.
m7G	7-Methylguanosine	Eubacteria, Eukaryota	rRNA, tRNA	[229, 232]
Gm	2'-O-Methylguanosine	Eubacteria, Eukaryota	rRNA, snRNA, tRNA	[229, 232]
m2,2G	N^2, N^2-dimethylguanosine	Archaea, Eubacteria, Eukaryota	rRNA, tRNA	[229, 232]
Gr	2′-O-ribosylguanosine (phosphate)	Eukaryota	tRNA	[309]
m6dA	N^6-Methyl-2′-deoxyadenosine	Archaea, Eubacteria, Eukaryota	DNA modification	[310-312]
i6Ade	N^6-(delta2-Isopentenyl)adenine	Eukaryota	DNA, Cytokinins	[313, 314]
6DMAP	6-(Dimethylamino)purine	Eukaryota	cellular metabolite	[315]
MTA	Methylthioadenosine	Eubacteria, Eukaryota	cellular metabolite	[316]
Cm	2′-O-methylcytidine	Archaea, Eubacteria, Eukaryota	rRNA, snRNA, tRNA	[229, 232]
m3U	3-methyluridine	Eubacteria	rRNA	[229, 232]
m5U	5-Methyluridine	Archaea, Eubacteria, Eukaryota	rRNA, tRNA	[229, 232]
m3Um	5-methyluridine	Archaea, Eubacteria, Eukaryota	rRNA, tRNA	[229, 232]
Q	Queuosine	Eubacteria, Eukaryota	tRNA	[229, 232]
yW	Wybutosine	Eukaryota	rRNA, tRNA	[229, 232]
OHyW	Hydroxywybutosine	Eukaryota	tRNA	[317]
Psi	Pseudouridine	Archaea, Eubacteria, Eukaryota	rRNA, snRNA, snoRNA, tRNA	[229, 232]
N2MedG	N^2-Methyl-2'-deoxyguanosine	Eukaryota	aldehyde-derived DNA adducts	[318-320]
m6A	N^6-methyladenosine	Eubacteria, Eukaryota	mRNA, rRNA, snRNA, tRNA	[229, 232]
MeP	6-methylpurine	Archaea, Eubacteria, Eukaryota	cellular metabolite	[229, 232]

Table 5-2. Overview of MR1T antigenic assays with modified nucleobases.

Short Name	MR1 upregulation	Reactive T cells isolated	Competition with MR1T clone	Competition with MAIT clone (MRC25)
m1A	YES	NOT FOUND	TC5A87, DGB129, MCA2E7	NO COMPETITION
m2A	YES	NOT FOUND	TC5A87, DGB129, MCA2E7	NOT DONE
Am	YES	TC5A87	NO COMPETITION	NO COMPETITION
t6A	YES	TC5A87	DGB129	NO COMPETITION
io6A	NO	NO	TC5A87	NOT DONE
ms2io6A	NO	TC5A87, DGB129, MCA2E7	TC5A87	NOT DONE
ms2i6A	NO	NOT FOUND	TC5A87, DGB129, MCA2E7	NOT DONE
m6t6A	YES	TC5A87	DGB129	NOT DONE
Ar(p)	YES	NOT FOUND	DGB129	NOT DONE
me1G	NO	TC5A87	DGB129, MCA2E7	NO COMPETITION
m2G	NO	NOT FOUND	TC5A87, DGB129, MCA2E7	NOT DONE
m7G	NO	TC5A87	DGB129, MCA2E7	NO COMPETITION
Gm	YES	NOT FOUND	MCA2E7	NOT DONE
m2,2G	YES	MCA2E7	DGB129	NOT DONE
Gr	YES	TC5A87	MCA2E7	NOT DONE
N6MedAdo	NO	MCA3C3	NOT DONE	NOT DONE
i6Ade	NO	NOT FOUND	MCA2E7, DGB129, AC1A4	YES
6DMAP	YES	NOT FOUND	MCA2E7, DGB129, AC1A4	YES
MTA	YES	NOT FOUND	DGB129, AC1A4	YES
Cm	YES	NOT FOUND	MCA2E7	NOT DONE
m3U	YES	TC5A87	DGB129	NOT DONE
m5U	YES	NOT FOUND	DGB129, MCA2E7	NOT DONE
m3Um	YES	NOT FOUND	DGB129, MCA2E7	NOT DONE
Q	YES	NOT FOUND	TC5A87, DGB129, MCA2E7	NOT DONE
yW	YES	NOT FOUND	DGB129, MCA2E7	NOT DONE
OHyW	YES	NOT FOUND	DGB129, MCA2E7	NOT DONE
Psi	YES	NOT FOUND	DGB129	NOT DONE
N2MedG	YES	NOT FOUND	NO COMPETITION	NO COMPETITION
m6A	YES	NOT FOUND	MCA2E7	NO COMPETITION
MeP	NO	NOT FOUND	MCA2E7	YES

5.2 MR1 upregulation

Initially we performed MR1 upregulation assays to investigate whether each compound may stabilize MR1 on the plasma membrane, as initial evidence of interaction with MR1. THP-1 wildtype or THP-1 MR1 cells were incubated with different compounds and the MR1 median florescence intensity (MFI) was checked by flow cytometry. After six hours of incubation, 21 compounds out of the total 30 compounds, induced a significant although small upregulation of MR1 in a dose dependent manner (Figure 5-1). In each experiment, the potent MR1 ligand Ac-6-FP was used as positive control. Methylthioadenosine (MTA) showed the highest upregulation of MR1 (> 2-time fold increase), which is similar as the synthetic MR1T antigen M_3ADE (Figure 3-20) and M1A (Figure 4-11), whereas the others induced less or very weak MR1 upregulation.
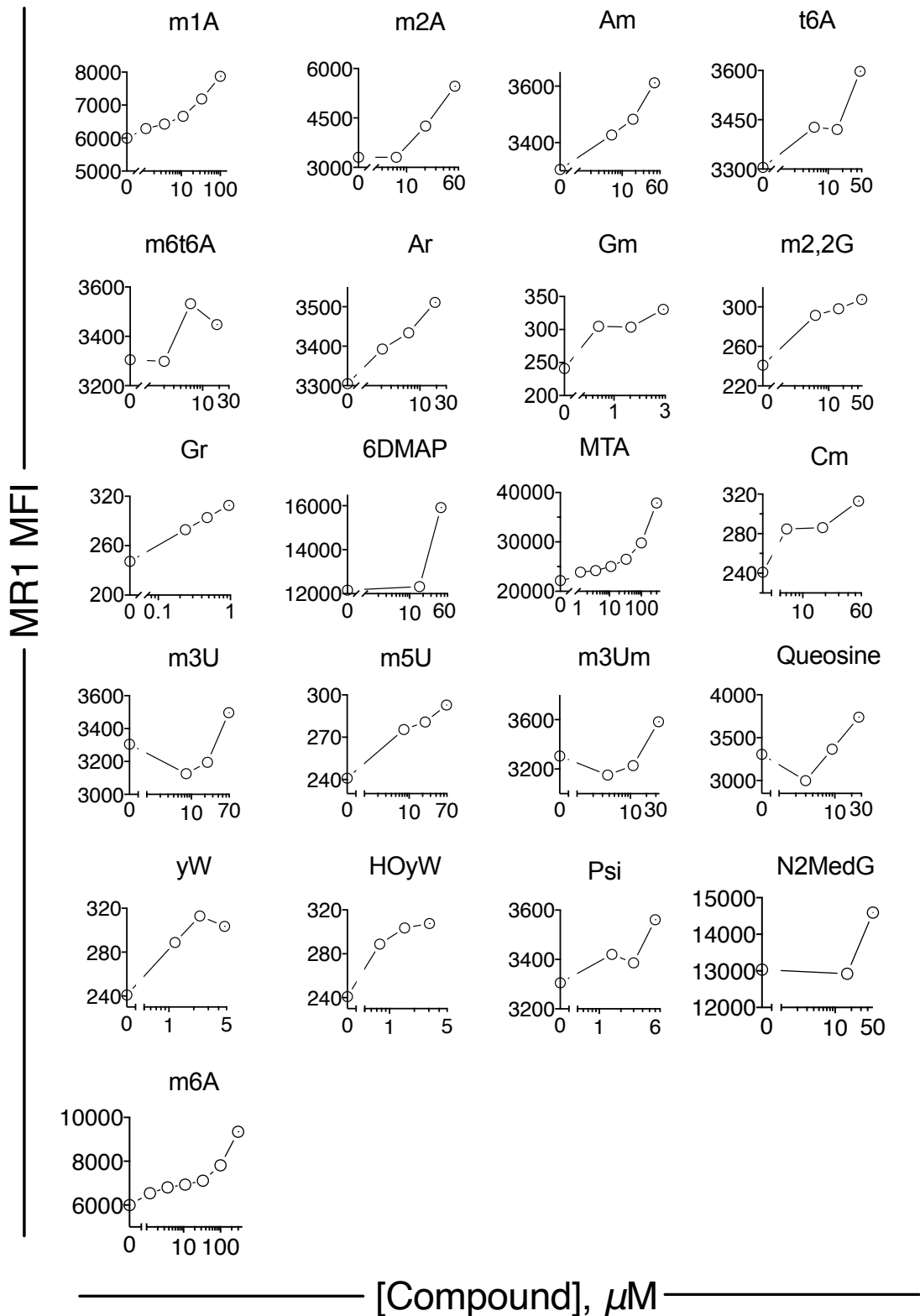
Figure 5-1. Modified nucleobases induce MR1 surface expression on THP-1 cells.

Upregulation of MR1 surface expression on THP-1 wildtype or THP-1 MR1 cells following 6h incubation with different compounds (O). Median florescence intensity (MFI) was checked by flow cytometry. The data shown are representative of at least two independent experiments and one representative experiment is shown.

5.3 Activation assays

Next, we tested the capacity of selected compounds to stimulate the four MR1T cell clones TC5A87, DGB129, AC1A4, and MCA2E7, which were selected because they express different TCR and showed distinct reactivity in previous experiments. In total, 11 compounds stimulated one or several MR1T clones (Figure 5-2), while, none of them stimulated MAIT clone. The compound N^6-threonylcarbamoyladenosine (t6A), 2-methylthio-N^6-(cis-hydroxyisopentenyl) adenosine (ms2io6A), and N^6-Methyl-2′-deoxyadenosine (N6MedAdo) showed the highest stimulatory activity (> 1 ng/ml IFN-γ). The IFN-γ release of the 10 reactive compounds are shown in Figure 5-2.
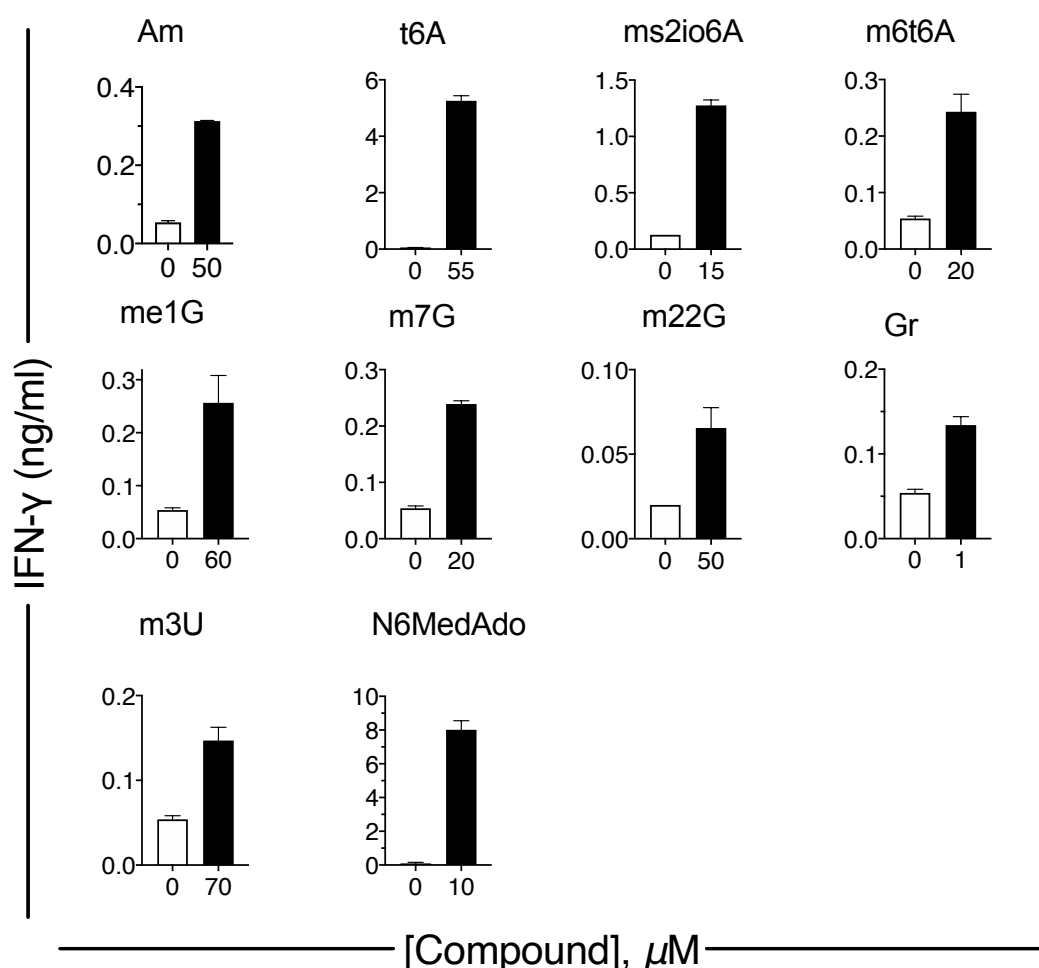
Figure 5-2. Modified nucleobases stimulate MR1T cells.

IFN-γ release response of indicated MR1T cell clones co-cultured with THP-1 cells in the presence (black bar) and absence of compounds (white bar). IFN-γ release is the mean ± SD of duplicate cultures. The data shown are representative of at least two independent experiments and one representative experiment is shown.

5.4 Competition assays

To investigate whether the selected compounds bind MR1 and compete with other antigens, competition assays were performed using non-responder MR1T clones which react to other synthetic antigens. The competitor was added first to the APC and after 6 hours the stimulatory antigen was also added at suboptimal doses. In these competition experiments, we used the MR1T cell clones DGB129 (stimulated with synthetic compound M_3ADE or MGdA), the clone AC1A4 (stimulated with the synthetic compound M_1G), the clone MCA2E7 (stimulated with synthetic mixture MGdA), and the MAIT clone MRC25 (stimulated with MAIT antigen 5-OP-RU). The compounds showed efficient competition with several clones (Table 5-2). The results of one clone are shown in Figure 5-3. In total, 27 modified nucleobases showed clear competition with the MR1 antigen, suggesting that they might be presented by MR1 and probably compete for binding in the same MR1 pocket with tested antigens.
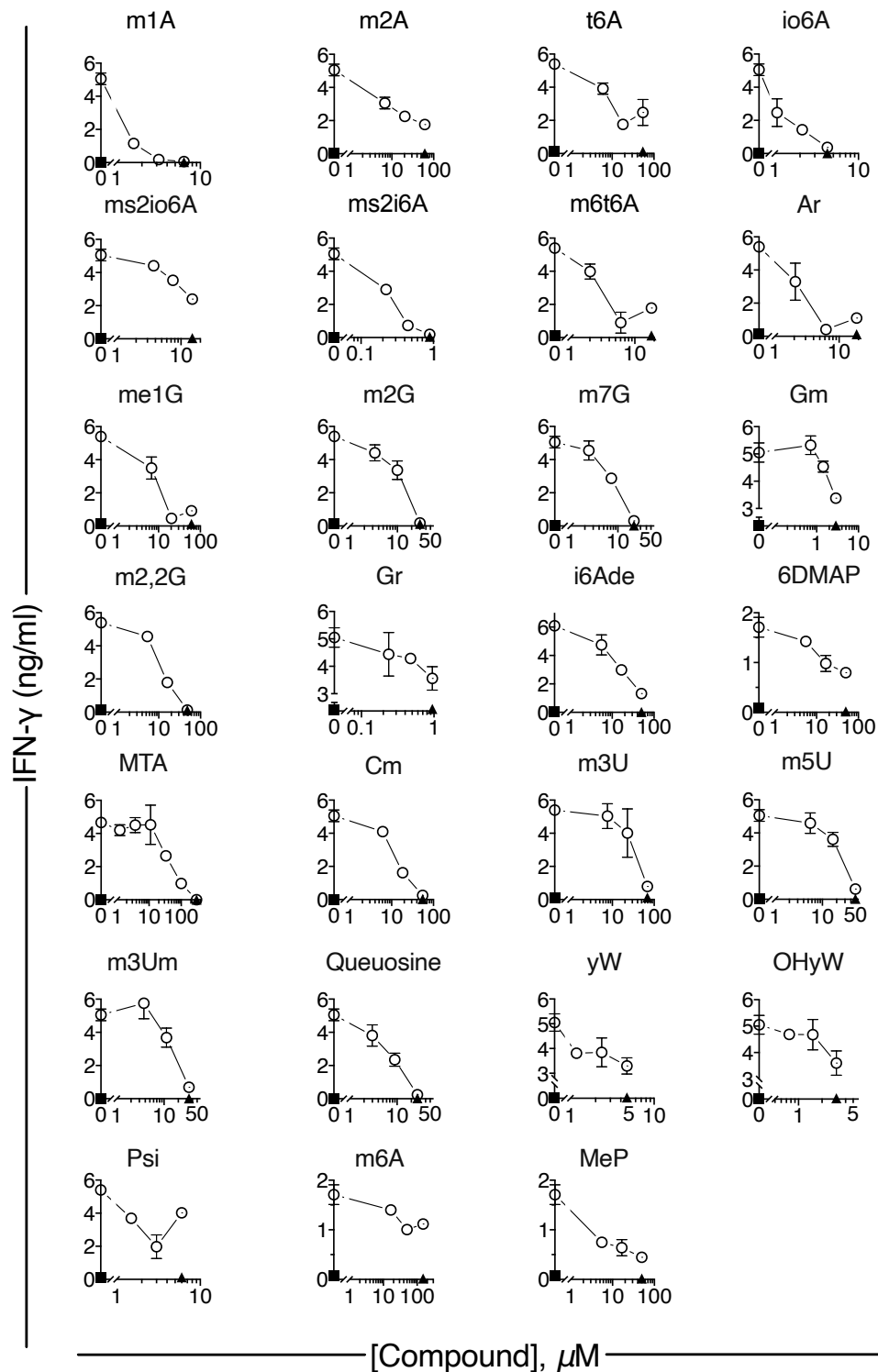
Figure 5-3. Modified nucleobases compete MR1 binding with the known MR1T antigens.

MR1T cell clones were first co-cultured with THP-1 cells in the presence of titrated compounds as competitors for 3 h, then adding a fixed dose of known antigen (○) or without adding antigen (▲) or in the absence of competitor and antigen (■). IFN-γ release is the mean ± SD of duplicate cultures. The data shown are representative of at least two independent experiments and one representative experiment is shown.

5.5 Discussion

The results presented in this Chapter provided information on additional 30 modified nucleosides that may bind MR1 and thus represent potential MR1T antigens. Most of them are modified RNA-derived nucleosides and some are cellular metabolites. Using the same *in vitro* assays described in previous Chapters, most of the modified RNAs promote MR1 surface expression (Figure 5-1), stimulate selected MR1T cell clones (Figure 5-2), and compete for MR1 binding (Figure 5-3). Therefore, these naturally occurring compounds accumulate in tumour cells and show efficient binding to the MR1 pocket. Whether they indeed associate with MR1 inside tumour cells remains to be investigates. In that case, they will represent novel MR1 ligands.

Another compound, 5'-Methylthioadenosine (MTA) attracted our attention. MTA is a natural sulfur-containing nucleoside found in numerous species. At least five independent pathways participate in MTA generation in mammals and it is an important intermediate in methionine pathway, polyamine biosynthesis, and purine salvage pathway [316, 321]. Many studies showed that MTA suppresses tumour growth by inhibiting tumour cell proliferation, invasion and inducing cell apoptosis. In healthy people, MTA remains at low levels between 10 nM to 20 nM in the skin. However, in melanoma patients, the MTA levels are approximately 7 to 14 times higher [322]. Moreover, many tumour cells express low levels of methylthioadenosine phosphorylase (MTAP) gene or show loss of MTAP activity [323], which is the main enzyme that degrades adenine and methionine [324]. It remains unclear whether MTA represents an additional antigen stimulating MR1T cells. However, MTA accumulating in tumour cells might also directly increase the surface expression of the MR1 molecule, thus facilitating presentation of other MR1T-stimulatory antigens.

In conclusion, a large variety of modified nucleosides stimulate MR1T cells, thus showing that MR1 binding can be implemented by different chemical residues attached to nucleobases. In some instance the ribose moiety is not necessary for MR1 binding, thus illustrating an unexpected capacity of MR1T cells to interact with several compounds retained in the MR1 antigen-binding pocket.

Chapter 6 General conclusions

In a seminal paper in 1993, the presence of a unique T cell population was found in circulating blood, expressing a semi-invariant TCR with a fixed use of the human TRAV 1.2 gene [96]. The cells expressing these receptors were later isolated and named mucosal-associated invariant T (MAIT) cells, as they were more abundant in mucosal tissue [99]. MAIT cells recognize microbial ligands presented by MR1 and participate in different phases of immune response during infections. Our laboratory identified a novel population of MR1-restricted T cells, that we called MR1T cells, which do not recognize MAIT antigens and instead react to different tumour-associated antigens [1]. During my PhD, I have been working on the identification and characterization of the tumour-associated antigens that stimulate MR1T cells. We found various structurally-diverse nucleobase adducts that are generated within tumours cells, form stable complexes with MR1 and interact with the T cell receptors of MR1T cells inducing their activation.

Several metabolic pathways are important in MR1T antigen accumulation in tumour cells. These pathways are correlated with tumour cell division and growth, and include the pathways leading to the synthesis and accumulation of purines and pyrimidines, to increased glycolysis, to accumulation of reactive oxygen species, and changes associated with reduced activity of carbonyl degradation systems. The regulation of these pathways and the accumulation of relevant antigen precursors is often altered within tumour cells. These alterations lead to the accumulation of nucleobase adducts, that otherwise are readily disposed by normal cells, and these changes are efficiently sensed by MR1T-cells. The preferential accumulation of these metabolites and nucleobase adducts in rapidly proliferating and transformed cells, explains why MR1T cells preferentially recognize tumour cells and not normal cells [1]. The generation and accumulation of these metabolites is highly regulated in normal cells [325-327]. In contrast, tumour cells have important alterations of those pathways, because they are required to sustain uncontrolled and rapid cell division [328]. Such high cellular demand of purine and pyrimidine accumulation, together with the unusual increase of a variety of toxic carbonyls leads to the accumulation of high levels of nucleobase adducts formed upon nucleoside oxidation following interaction with products of oxidative and carbonyl stress [329]. These findings suggest that MR1T cell-stimulatory antigens represent products accumulating in metabolically altered cells, that the immune system is prone to eliminate.

Mass spectrometry studies performed by other investigators showed that the MR1-eluted compounds have a large range of sizes between 280 and 1200 Daltons [160]. The MR1-T

stimulatory antigens identified in our study showed masses in the range of 300-350 Daltons. These findings together illustrate that a large variety of compounds can form complexes with MR1. However, the MAIT- and MR1T-stimulatory compounds are all in a rather low range of masses. These findings suggest that these compounds probably only occupy one antigen binding pocket of MR1, resembling the microbial antigens which are located in the A' pocket of MR1 [151]. However, it is not excluded that other bigger compounds may occupy also the F' pocket and thus may stimulate MR1T cells with other specificities.

MR1 is a highly conserved non-polymorphic molecule ubiquitously expressed at low levels on human cells [137, 138]. These unique MR1 features might be instrumental to design novel types of a cancer cell therapy which overcomes the problem of HLA restriction, thus allowing the establishment of immunotherapies applicable to the entire population of cancer patients. This possibility is also supported by the finding that MR1T cell antigens accumulate in cancer cells, which cannot escape nucleobase and carbonyl accumulation. In addition, the accumulation of different nucleobase adducts might be beneficial to MR1T cell stimulation also through another mechanism, which is not observed with other antigen-presenting molecules. This mechanism relies on the usual very low expression of MR1 on the cell surface, and its stabilization and surface upregulation when proper MR1-binding molecules accumulate. Such upregulation leads to more efficient MR1 antigen presentation, which in turn facilitates the engagement of MR1T TCRs. Using drugs that tune the generation and accumulation of MR1T cell antigens in tumour cells might be a further strategy to increase the quantity of MR1T cell antigens in tumour cells. Finally, the large availability of such MR1T cell-stimulatory antigens might also provide new pathways to cancer vaccination to prime and expand tumour-reactive MR1T cells in either preventive or therapeutic vaccination strategies.

An important question raised by our studies is what is the physiological role of MR1T cells. In the blood of healthy donors, MR1T cell population is maintained at low levels (0.02-0.04% of total T cells) [1], which is the same range of T cells specific for individual peptides. Our preferred hypothesis is that MR1T cells might have a potential role in surveying the abnormal accumulation of metabolites within all cells of the body. When DNA or RNA synthesis is abnormal and unbalanced production of reactive carbonyls occurs inside cells, stimulatory nucleobase adducts are formed in large amounts, they accumulate and become available to form complexes with MR1. In such conditions, cells with these metabolic alterations may trigger the response of MR1T cells, which in turn, according to their functional capabilities,

initiate different types of immune responses. The fact that several MR1T TCRs cross-react with different nucleobase adducts, also suggest that this patrolling system is tuned to react to a variety of alterations using the same TCRs. Another important aspect is that the stimulatory nucleobase adducts may be generated in many different types of malignant cells. MR1 ubiquitous expression is another aspect that may facilitate the recognition of tumour cells of different tissue origin. These findings were readily observed in or studies using a large variety of tumour cells. Taken together, all these features indicate that MR1T cell immunity may represent a successful novel approach to cancer cell therapy independently of type of tumour and patient HLA haplotype.

The immune system of tumour-reactive MR1T cells continues to surprise us with its wide recognition of diverse antigens. This dissertation provides the first insight of the type and structure of MR1T cell-stimulatory antigens. Their physiological roles, immunological functions, selective recognition by MR1T TCRs, and potential application in cancer cell therapy will be subject of intense and relevant future studies.

References

1. Lepore, M., et al., *Functionally diverse human T cells recognize non-microbial antigens presented by MR1.* Elife, 2017. **6.**

2. Murphy, K.P., et al., *Janeway's Immunobiology.* 2016: Garland Science.

3. Mayer, G., *Immunolgy - Innate(non-specific) immunity,* in *Immunology Section of Microbiology and Immunology On-line.* 2017: University of South Carolina.

4. Kumar, H., T. Kawai, and S. Akira, *Pathogen recognition by the innate immune system.* Int Rev Immunol, 2011. **30**(1): p. 16-34.

5. Akira, S., S. Uematsu, and O. Takeuchi, *Pathogen recognition and innate immunity.* Cell, 2006. **124**(4): p. 783-801.

6. Lin, W.W. and M. Karin, *A cytokine-mediated link between innate immunity, inflammation, and cancer.* J Clin Invest, 2007. **117**(5): p. 1175-83.

7. Premack, B.A. and T.J. Schall, *Chemokine receptors: gateways to inflammation and infection.* Nat Med, 1996. **2**(11): p. 1174-8.

8. Sarma, J.V. and P.A. Ward, *The complement system.* Cell Tissue Res, 2011. **343**(1): p. 227-35.

9. Parkin, J. and B. Cohen, *An overview of the immune system.* Lancet, 2001. **357**(9270): p. 1777-89.

10. Market, E. and F.N. Papavasiliou, *V(D)J recombination and the evolution of the adaptive immune system.* PLoS Biol, 2003. **1**(1): p. E16.

11. Schatz, D.G., M.A. Oettinger, and D. Baltimore, *The V(D)J recombination activating gene, RAG-1.* Cell, 1989. **59**(6): p. 1035-48.

12. Ruddle, N.H. and E.M. Akirav, *Secondary lymphoid organs: responding to genetic and environmental cues in ontogeny and the immune response.* J Immunol, 2009. **183**(4): p. 2205-12.

13. Guermonprez, P., et al., *Antigen presentation and T cell stimulation by dendritic cells.* Annu Rev Immunol, 2002. **20**: p. 621-67.

14. Mempel, T.R., S.E. Henrickson, and U.H. Von Andrian, *T-cell priming by dendritic cells in lymph nodes occurs in three distinct phases.* Nature, 2004. **427**(6970): p. 154-9.

15. Obst, R., *The Timing of T Cell Priming and Cycling.* Front Immunol, 2015. **6**: p. 563.

16. Batista, F.D. and N.E. Harwood, *The who, how and where of antigen presentation to B cells.* Nat Rev Immunol, 2009. **9**(1): p. 15-27.

17. Shapiro-Shelef, M. and K. Calame, *Regulation of plasma-cell development.* Nat Rev Immunol, 2005. **5**(3): p. 230-42.

18. Stavnezer, J., *Antibody class switching.* Adv Immunol, 1996. **61**: p. 79-146.

19. Ahmed, R. and D. Gray, *Immunological memory and protective immunity: understanding their relation.* Science, 1996. **272**(5258): p. 54-60.

20. Ada, G.L., *The immunological principles of vaccination.* Lancet, 1990. **335**(8688): p. 523-6.

21. Takahama, Y., *Journey through the thymus: stromal guides for T-cell development and selection.* Nat Rev Immunol, 2006. **6**(2): p. 127-35.

22. Starr, T.K., S.C. Jameson, and K.A. Hogquist, *Positive and negative selection of T cells.* Annu Rev Immunol, 2003. **21**: p. 139-76.

23. von Andrian, U.H. and T.R. Mempel, *Homing and cellular traffic in lymph nodes.* Nat Rev Immunol, 2003. **3**(11): p. 867-78.

24. Arden, B., et al., Human T-cell receptor variable gene segment families. Immunogenetics, 1995. **42**(6): p. 455-500.

25. Corr, M., et al., T cell receptor-MHC class I peptide interactions: affinity, kinetics, and specificity. Science, 1994. **265**(5174): p. 946-9.

26. Pamer, E. and P. Cresswell, Mechanisms of MHC class I--restricted antigen processing. Annu Rev Immunol, 1998. **16**: p. 323-58.

27. Cresswell, P., Assembly, transport, and function of MHC class II molecules. Annu Rev Immunol, 1994. **12**: p. 259-93.

28. Neefjes, J., et al., Towards a systems understanding of MHC class I and MHC class II antigen presentation. Nat Rev Immunol, 2011. **11**(12): p. 823-36.

29. Swain, S.L., T cell subsets and the recognition of MHC class. Immunol Rev, 1983. **74**: p. 129-42.

30. Watts, T.H. and M.A. DeBenedette, T cell co-stimulatory molecules other than CD28. Curr Opin Immunol, 1999. **11**(3): p. 286-93.

31. Schwartz, R.H., T cell anergy. Annu Rev Immunol, 2003. **21**: p. 305-34.

32. Kagi, D., et al., Fas and perforin pathways as major mechanisms of T cell-mediated cytotoxicity. Science, 1994. **265**(5171): p. 528-30.

33. Kaufmann, S.H.E., CD8+ T lymphocytes in intracellular microbial infections. Immunology Today, 1988. **9**(6): p. 168-174.

34. Abbas, A.K., K.M. Murphy, and A. Sher, Functional diversity of helper T lymphocytes. Nature, 1996. **383**(6603): p. 787-93.

35. Zhu, J., H. Yamane, and W.E. Paul, Differentiation of effector CD4 T cell populations (*). Annu Rev Immunol, 2010. **28**: p. 445-89.

36. Schoenberger, S.P., et al., T-cell help for cytotoxic T lymphocytes is mediated by CD40-CD40L interactions. Nature, 1998. **393**(6684): p. 480-3.

37. Huang, C.T., et al., Role of LAG-3 in regulatory T cells. Immunity, 2004. **21**(4): p. 503-13.

38. Yu, X., et al., The surface protein TIGIT suppresses T cell activation by promoting the generation of mature immunoregulatory dendritic cells. Nat Immunol, 2009. **10**(1): p. 48-57.

39. Tang, Q. and J.A. Bluestone, The Foxp3+ regulatory T cell: a jack of all trades, master of regulation. Nat Immunol, 2008. **9**(3): p. 239-44.

40. De Libero, G. and L. Mori, The T-Cell Response to Lipid Antigens of Mycobacterium tuberculosis. Front Immunol, 2014. **5**: p. 219.

41. Skold, M. and S.M. Behar, The role of group 1 and group 2 CD1-restricted T cells in microbial immunity. Microbes Infect, 2005. **7**(3): p. 544-51.

42. Lepore, M., L. Mori, and G. De Libero, The Conventional Nature of Non-MHC-Restricted T Cells. Front Immunol, 2018. **9**: p. 1365.

43. Beckman, E.M., et al., Recognition of a lipid antigen by CD1-restricted alpha beta+ T cells. Nature, 1994. **372**(6507): p. 691-4.

44. Kinjo, Y., et al., Natural killer T cells recognize diacylglycerol antigens from pathogenic bacteria. Nat Immunol, 2006. **7**(9): p. 978-86.

45. Brennan, P.J., M. Brigl, and M.B. Brenner, Invariant natural killer T cells: an innate activation scheme linked to diverse effector functions. Nat Rev Immunol, 2013. **13**(2): p. 101-17.

46. Bendelac, A., P.B. Savage, and L. Teyton, The biology of NKT cells. Annu Rev Immunol, 2007. **25**: p. 297-336.

47. Treiner, E. and O. Lantz, CD1d- and MR1-restricted invariant T cells: of mice and men. Curr Opin Immunol, 2006. **18**(5): p. 519-26.

48. Kawano, T., et al., CD1d-restricted and TCR-mediated activation of valpha14 NKT cells by glycosylceramides. Science, 1997. **278**(5343): p. 1626-9.

49. Mattner, J., et al., Exogenous and endogenous glycolipid antigens activate NKT cells during microbial infections. Nature, 2005. **434**(7032): p. 525-9.

50. Godfrey, D.I. and M. Kronenberg, Going both ways: immune regulation via CD1d-dependent NKT cells. J Clin Invest, 2004. **114**(10): p. 1379-88.

51. Angenieux, C., et al., The cellular pathway of CD1e in immature and maturing dendritic cells. Traffic, 2005. **6**(4): p. 286-302.

52. de la Salle, H., et al., Assistance of microbial glycolipid antigen processing by CD1e. Science, 2005. **310**(5752): p. 1321-4.

53. Facciotti, F., et al., Fine tuning by human CD1e of lipid-specific immune responses. Proc Natl Acad Sci U S A, 2011. **108**(34): p. 14228-33.

54. Brigl, M. and M.B. Brenner, CD1: antigen presentation and T cell function. Annu Rev Immunol, 2004. **22**: p. 817-90.

55. Barral, D.C. and M.B. Brenner, CD1 antigen presentation: how it works. Nature Reviews Immunology, 2007. **7**(12): p. 929-941.

56. Mori, L., M. Lepore, and G. De Libero, The Immunology of CD1- and MR1-Restricted T Cells. Annu Rev Immunol, 2016. **34**: p. 479-510.

57. Freigang, S., L. Kain, and L. Teyton, Transport and uptake of immunogenic lipids. Mol Immunol, 2013. **55**(2): p. 179-81.

58. Freigang, S., et al., Fatty acid amide hydrolase shapes NKT cell responses by influencing the serum transport of lipid antigen in mice. J Clin Invest, 2010. **120**(6): p. 1873-84.

59. Freigang, S., et al., Scavenger receptors target glycolipids for natural killer T cell activation. J Clin Invest, 2012. **122**(11): p. 3943-54.

60. Zhou, D., et al., Editing of CD1d-bound lipid antigens by endosomal lipid transfer proteins. Science, 2004. **303**(5657): p. 523-7.

61. Borg, N.A., et al., CD1d-lipid-antigen recognition by the semi-invariant NKT T-cell receptor. Nature, 2007. **448**(7149): p. 44-9.

62. Girardi, E., et al., Type II natural killer T cells use features of both innate-like and conventional T cells to recognize sulfatide self antigens. Nat Immunol, 2012. **13**(9): p. 851-6.

63. Patel, O., et al., Recognition of CD1d-sulfatide mediated by a type II natural killer T cell antigen receptor. Nat Immunol, 2012. **13**(9): p. 857-63.

64. Birkinshaw, R.W., et al., alphabeta T cell antigen receptor recognition of CD1a presenting self lipid ligands. Nat Immunol, 2015. **16**(3): p. 258-66.

65. Hinz, T., et al., Identification of the complete expressed human TCR V gamma repertoire by flow cytometry. Int Immunol, 1997. **9**(8): p. 1065-72.

66. Porcelli, S., M.B. Brenner, and H. Band, Biology of the human gamma delta T-cell receptor. Immunol Rev, 1991. **120**: p. 137-83.

67. Kabelitz, D., M. Lettau, and O. Janssen, Immunosurveillance by human gammadelta T lymphocytes: the emerging role of butyrophilins. F1000Res, 2017. **6**.

68. Kalyan, S. and D. Kabelitz, Defining the nature of human gammadelta T cells: a biographical sketch of the highly empathetic. Cell Mol Immunol, 2013. **10**(1): p. 21-9.

69. Agea, E., et al., Human CD1-restricted T cell recognition of lipids from pollens. J Exp Med, 2005. **202**(2): p. 295-308.

70. Uldrich, A.P., et al., CD1d-lipid antigen recognition by the gammadelta TCR. Nat Immunol, 2013. **14**(11): p. 1137-45.

71. Xu, B., et al., Crystal structure of a gammadelta T-cell receptor specific for the human MHC class I homolog MICA. Proc Natl Acad Sci U S A, 2011. **108**(6): p. 2414-9.

72. Wu, Y.L., et al., gammadelta T cells and their potential for immunotherapy. Int J Biol Sci, 2014. **10**(2): p. 119-35.

73. Hintz, M., et al., Identification of (E)-4-hydroxy-3-methyl-but-2-enyl pyrophosphate as a major activator for human gammadelta T cells in Escherichia coli. FEBS Lett, 2001. **509**(2): p. 317-22.

74. Burk, M.R., L. Mori, and G. De Libero, Human V gamma 9-V delta 2 cells are stimulated in a cross-reactive fashion by a variety of phosphorylated metabolites. Eur J Immunol, 1995. **25**(7): p. 2052-8.

75. Tanaka, Y., et al., Natural and synthetic non-peptide antigens recognized by human gamma delta T cells. Nature, 1995. **375**(6527): p. 155-8.

76. Harly, C., et al., Key implication of CD277/butyrophilin-3 (BTN3A) in cellular stress sensing by a major human gammadelta T-cell subset. Blood, 2012. **120**(11): p. 2269-79.

77. Vavassori, S., et al., Butyrophilin 3A1 binds phosphorylated antigens and stimulates human gammadelta T cells. Nat Immunol, 2013. **14**(9): p. 908-16.

78. Rigau, M., et al., Butyrophilin 2A1 is essential for phosphoantigen reactivity by gammadelta T cells. Science, 2020. **367**(6478).

79. Holtmeier, W. and D. Kabelitz, gammadelta T cells link innate and adaptive immune responses. Chem Immunol Allergy, 2005. **86**: p. 151-183.

80. Wu, Y., et al., Human gamma delta T cells: a lymphoid lineage cell capable of professional phagocytosis. J Immunol, 2009. **183**(9): p. 5622-9.

81. Li, H., K. Luo, and C.D. Pauza, TNF-alpha is a positive regulatory factor for human Vgamma2 Vdelta2 T cells. J Immunol, 2008. **181**(10): p. 7131-7.

82. van den Broek, M.F., et al., Immune defence in mice lacking type I and/or type II interferon receptors. Immunol Rev, 1995. **148**: p. 5-18.

83. Mikulak, J., et al., NKp46-expressing human gut-resident intraepithelial Vdelta1 T cell subpopulation exhibits high antitumor activity against colorectal cancer. JCI Insight, 2019. **4**(24).

84. Wrobel, P., et al., Lysis of a broad range of epithelial tumour cells by human gamma delta T cells: involvement of NKG2D ligands and T-cell receptor- versus NKG2D-dependent recognition. Scand J Immunol, 2007. **66**(2-3): p. 320-8.

85. Braza, M.S. and B. Klein, Anti-tumour immunotherapy with Vgamma9Vdelta2 T lymphocytes: from the bench to the bedside. Br J Haematol, 2013. **160**(2): p. 123-32.

86. Buccheri, S., et al., Efficacy and safety of gammadeltaT cell-based tumor immunotherapy: a meta-analysis. J Biol Regul Homeost Agents, 2014. **28**(1): p. 81-90.

87. Zou, C., et al., gammadelta T cells in cancer immunotherapy. Oncotarget, 2017. **8**(5): p. 8900-8909.

88. Blazquez, J.L., et al., New Insights Into the Regulation of gammadelta T Cells by BTN3A and Other BTN/BTNL in Tumor Immunity. Front Immunol, 2018. **9**: p. 1601.

89. De Libero, G., S.Y. Lau, and L. Mori, Phosphoantigen Presentation to TCR gammadelta Cells, a Conundrum Getting Less Gray Zones. Front Immunol, 2014. **5**: p. 679.

90. Jeong, J., et al., The PRY/SPRY/B30.2 domain of butyrophilin 1A1 (BTN1A1) binds to xanthine oxidoreductase: implications for the function of BTN1A1 in the mammary gland and other tissues. J Biol Chem, 2009. **284**(33): p. 22444-56.

91. Sandstrom, A., et al., The intracellular B30.2 domain of butyrophilin 3A1 binds phosphoantigens to mediate activation of human Vgamma9Vdelta2 T cells. Immunity, 2014. **40**(4): p. 490-500.

92. Di Marco Barros, R., et al., Epithelia Use Butyrophilin-like Molecules to Shape Organ-Specific gammadelta T Cell Compartments. Cell, 2016. **167**(1): p. 203-218 e17.

93. Lebrero-Fernandez, C., et al., Altered expression of Butyrophilin (BTN) and BTN-like (BTNL) genes in intestinal inflammation and colon cancer. Immun Inflamm Dis, 2016. **4**(2): p. 191-200.

94. Arnett, H.A., et al., BTNL2, a butyrophilin/B7-like molecule, is a negative costimulatory molecule modulated in intestinal inflammation. J Immunol, 2007. **178**(3): p. 1523-33.

95. Nguyen, T., et al., BTNL2, a butyrophilin-like molecule that functions to inhibit T cell activation. J Immunol, 2006. **176**(12): p. 7354-60.

96. Porcelli, S., et al., Analysis of T cell antigen receptor (TCR) expression by human peripheral blood CD4-8- alpha/beta T cells demonstrates preferential use of several V beta genes and an invariant TCR alpha chain. J Exp Med, 1993. **178**(1): p. 1-16.

97. Tilloy, F., et al., An invariant T cell receptor alpha chain defines a novel TAP-independent major histocompatibility complex class Ib-restricted alpha/beta T cell subpopulation in mammals. J Exp Med, 1999. **189**(12): p. 1907-21.

98. Gherardin, N.A., et al., Human blood MAIT cell subsets defined using MR1 tetramers. Immunol Cell Biol, 2018. **96**(5): p. 507-525.

99. Treiner, E., et al., Selection of evolutionarily conserved mucosal-associated invariant T cells by MR1. Nature, 2003. **422**(6928): p. 164-9.

100. Hinks, T.S., Mucosal-associated invariant T cells in autoimmunity, immune-mediated diseases and airways disease. Immunology, 2016. **148**(1): p. 1-12.

101. Tang, X.Z., et al., IL-7 licenses activation of human liver intrasinusoidal mucosal-associated invariant T cells. J Immunol, 2013. **190**(7): p. 3142-52.

102. Lepore, M., et al., Parallel T-cell cloning and deep sequencing of human MAIT cells reveal stable oligoclonal TCRbeta repertoire. Nat Commun, 2014. **5**: p. 3866.

103. Dusseaux, M., et al., Human MAIT cells are xenobiotic-resistant, tissue-targeted, CD161hi IL-17-secreting T cells. Blood, 2011. **117**(4): p. 1250-9.

104. Teunissen, M.B.M., et al., The IL-17A-producing CD8+ T-cell population in psoriatic lesional skin comprises mucosa-associated invariant T cells and conventional T cells. J Invest Dermatol, 2014. **134**(12): p. 2898-2907.

105. Sharma, P.K., et al., High expression of CD26 accurately identifies human bacteria-reactive MR1-restricted MAIT cells. Immunology, 2015. **145**(3): p. 443-53.

106. Martin, E., et al., Stepwise development of MAIT cells in mouse and human. PLoS Biol, 2009. **7**(3): p. e54.

107. Kjer-Nielsen, L., et al., MR1 presents microbial vitamin B metabolites to MAIT cells. Nature, 2012. **491**(7426): p. 717-23.

108. Corbett, A.J., et al., T-cell activation by transitory neo-antigens derived from distinct microbial pathways. Nature, 2014. **509**(7500): p. 361-5.

109. Chiba, A., et al., Mucosal-associated invariant T cells promote inflammation and exacerbate disease in murine models of arthritis. Arthritis Rheum, 2012. **64**(1): p. 153-61.

110. Kwon, Y.S., et al., Mucosal-associated invariant T cells are numerically and functionally deficient in patients with mycobacterial infection and reflect disease activity. Tuberculosis (Edinb), 2015. **95**(3): p. 267-74.

111. Ruijing, X., et al., Jalpha33+ MAIT cells play a protective role in TNBS induced intestinal inflammation. Hepatogastroenterology, 2012. **59**(115): p. 762-7.

112. Hiejima, E., et al., Reduced Numbers and Proapoptotic Features of Mucosal-associated Invariant T Cells as a Characteristic Finding in Patients with Inflammatory Bowel Disease. Inflamm Bowel Dis, 2015. **21**(7): p. 1529-40.

113. Serriari, N.E., et al., Innate mucosal-associated invariant T (MAIT) cells are activated in inflammatory bowel diseases. Clin Exp Immunol, 2014. **176**(2): p. 266-74.

114. Ling, L., et al., Circulating and tumor-infiltrating mucosal associated invariant T (MAIT) cells in colorectal cancer patients. Sci Rep, 2016. **6**: p. 20358.

115. Zabijak, L., et al., Increased tumor infiltration by mucosal-associated invariant T cells correlates with poor survival in colorectal cancer patients. Cancer Immunol Immunother, 2015. **64**(12): p. 1601-8.

116. Peterfalvi, A., et al., Invariant Valpha7.2-Jalpha33 TCR is expressed in human kidney and brain tumors indicating infiltration by mucosal-associated invariant T (MAIT) cells. Int Immunol, 2008. **20**(12): p. 1517-25.

117. Won, E.J., et al., Clinical relevance of circulating mucosal-associated invariant T cell levels and their anti-cancer activity in patients with mucosal-associated cancer. Oncotarget, 2016. **7**(46): p. 76274-76290.

118. Ussher, J.E., et al., CD161++ CD8+ T cells, including the MAIT cell subset, are specifically activated by IL-12+IL-18 in a TCR-independent manner. Eur J Immunol, 2014. **44**(1): p. 195-203.

119. Jo, J., et al., Toll-like receptor 8 agonist and bacteria trigger potent activation of innate immune cells in human liver. PLoS Pathog, 2014. **10**(6): p. e1004210.

120. Loh, L., et al., Human mucosal-associated invariant T cells contribute to antiviral influenza immunity via IL-18-dependent activation. Proc Natl Acad Sci U S A, 2016. **113**(36): p. 10133-8.

121. Wilson, R.P., et al., STAT3 is a critical cell-intrinsic regulator of human unconventional T cell numbers and function. J Exp Med, 2015. **212**(6): p. 855-64.

122. van Wilgenburg, B., et al., MAIT cells are activated during human viral infections. Nat Commun, 2016. **7**: p. 11653.

123. Boehm, U., et al., Cellular responses to interferon-gamma. Annu Rev Immunol, 1997. **15**: p. 749-95.

124. Schroder, K., et al., Interferon-gamma: an overview of signals, mechanisms and functions. J Leukoc Biol, 2004. **75**(2): p. 163-89.

125. Ellerin, T., R.H. Rubin, and M.E. Weinblatt, Infections and anti-tumor necrosis factor alpha therapy. Arthritis Rheum, 2003. **48**(11): p. 3013-22.

126. Korn, T., et al., IL-17 and Th17 Cells. Annu Rev Immunol, 2009. **27**: p. 485-517.

127. Walker, L.J., et al., Human MAIT and CD8alphaalpha cells develop from a pool of type-17 precommitted CD8+ T cells. Blood, 2012. **119**(2): p. 422-33.

128. Leeansyah, E., et al., Acquisition of innate-like microbial reactivity in mucosal tissues during human fetal MAIT-cell development. Nature Communications, 2014. **5**(1): p. 3143.

129. Le Bourhis, L., et al., MAIT cells detect and efficiently lyse bacterially-infected epithelial cells. PLoS Pathog, 2013. **9**(10): p. e1003681.

130. Kurioka, A., et al., MAIT cells are licensed through granzyme exchange to kill bacterially sensitized targets. Mucosal Immunol, 2015. **8**(2): p. 429-40.

131. Gherardin, N.A., et al., Enumeration, functional responses and cytotoxic capacity of MAIT cells in newly diagnosed and relapsed multiple myeloma. Sci Rep, 2018. **8**(1): p. 4159.

132. Leeansyah, E., et al., Arming of MAIT Cell Cytolytic Antimicrobial Activity Is Induced by IL-7 and Defective in HIV-1 Infection. PLoS Pathog, 2015. **11**(8): p. e1005072.

133. Rouxel, O., et al., Cytotoxic and regulatory roles of mucosal-associated invariant T cells in type 1 diabetes. Nat Immunol, 2017. **18**(12): p. 1321-1331.

134. Hashimoto, K., M. Hirai, and Y. Kurosawa, A gene outside the human MHC related to classical HLA class I genes. Science, 1995. **269**(5224): p. 693-5.

135. Morton, C.C., et al., Orientation of loci within the human major histocompatibility complex by chromosomal in situ hybridization. Proc Natl Acad Sci U S A, 1984. **81**(9): p. 2816-20.

136. Riegert, P., V. Wanner, and S. Bahram, Genomics, isoforms, expression, and phylogeny of the MHC class I-related MR1 gene. J Immunol, 1998. **161**(8): p. 4066-77.

137. Miley, M.J., et al., Biochemical features of the MHC-related protein 1 consistent with an immunological function. J Immunol, 2003. **170**(12): p. 6090-8.

138. Huang, S., et al., MR1 uses an endocytic pathway to activate mucosal-associated invariant T cells. J Exp Med, 2008. **205**(5): p. 1201-11.

139. McWilliam, H.E., et al., The intracellular pathway for the presentation of vitamin B-related antigens by the antigen-presenting molecule MR1. Nat Immunol, 2016. **17**(5): p. 531-7.

140. McWilliam, H.E.G., et al., Endoplasmic reticulum chaperones stabilize ligand-receptive MR1 molecules for efficient presentation of metabolite antigens. Proc Natl Acad Sci U S A, 2020. **117**(40): p. 24974-24985.

141. McWilliam, H.E., et al., MR1 presentation of vitamin B-based metabolite ligands. Curr Opin Immunol, 2015. **34**: p. 28-34.

142. Harriff, M.J., et al., Endosomal MR1 Trafficking Plays a Key Role in Presentation of Mycobacterium tuberculosis Ligands to MAIT Cells. PLoS Pathog, 2016. **12**(3): p. e1005524.

143. Le Bourhis, L., et al., Antimicrobial activity of mucosal-associated invariant T cells. Nat Immunol, 2010. **11**(8): p. 701-8.

144. Gold, M.C., et al., Human mucosal associated invariant T cells detect bacterially infected cells. PLoS Biol, 2010. **8**(6): p. e1000407.

145. McWilliam, H.E.G. and J.A. Villadangos, How MR1 Presents a Pathogen Metabolic Signature to Mucosal-Associated Invariant T (MAIT) Cells. Trends Immunol, 2017. **38**(9): p. 679-689.

146. Eckle, S.B., et al., A molecular basis underpinning the T cell receptor heterogeneity of mucosal-associated invariant T cells. J Exp Med, 2014. **211**(8): p. 1585-600.

147. Soudais, C., et al., In Vitro and In Vivo Analysis of the Gram-Negative Bacteria-Derived Riboflavin Precursor Derivatives Activating Mouse MAIT Cells. J Immunol, 2015. **194**(10): p. 4641-9.

148. Reantragoon, R., et al., Antigen-loaded MR1 tetramers define T cell receptor heterogeneity in mucosal-associated invariant T cells. J Exp Med, 2013. **210**(11): p. 2305-20.

149. *Novak, E.J., et al., MHC class II tetramers identify peptide-specific human CD4(+) T cells proliferating in response to influenza A antigen. J Clin Invest, 1999.* **104**(12): p. R63-7.

150. *Soen, Y., et al., Detection and characterization of cellular immune responses using peptide-MHC microarrays. PLoS Biol, 2003.* **1**(3): p. E65.

151. *Keller, A.N., et al., Drugs and drug-like molecules can modulate the function of mucosal-associated invariant T cells. Nat Immunol, 2017.* **18**(4): p. 402-411.

152. *Reantragoon, R., et al., Structural insight into MR1-mediated recognition of the mucosal associated invariant T cell receptor. J Exp Med, 2012.* **209**(4): p. 761-74.

153. *Keller, A.N., et al., MAIT cells and MR1-antigen recognition. Curr Opin Immunol, 2017.* **46**: p. 66-74.

154. *Lopez-Sagaseta, J., et al., MAIT recognition of a stimulatory bacterial antigen bound to MR1. J Immunol, 2013.* **191**(10): p. 5268-77.

155. *Gherardin, N.A., et al., Diversity of T Cells Restricted by the MHC Class I-Related Molecule MR1 Facilitates Differential Antigen Recognition. Immunity, 2016.* **44**(1): p. 32-45.

156. *Meermeier, E.W., et al., Human TRAV1-2-negative MR1-restricted T cells detect S. pyogenes and alternatives to MAIT riboflavin-based antigens. Nat Commun, 2016.* **7**: p. 12506.

157. *Crowther, M.D., et al., Genome-wide CRISPR-Cas9 screening reveals ubiquitous T cell cancer targeting via the monomorphic MHC class I-related protein MR1. Nat Immunol, 2020.* **21**(2): p. 178-185.

158. *Godfrey, D.I., et al., The biology and functional importance of MAIT cells. Nat Immunol, 2019.* **20**(9): p. 1110-1128.

159. *Salio, M., et al., Ligand-dependent downregulation of MR1 cell surface expression. Proc Natl Acad Sci U S A, 2020.* **117**(19): p. 10465-10475.

160. *Harriff, M.J., et al., MR1 displays the microbial metabolome driving selective MR1-restricted T cell receptor usage. Sci Immunol, 2018.* **3**(25).

161. *Devasagayam, T.P., et al., Free radicals and antioxidants in human health: current status and future prospects. J Assoc Physicians India, 2004.* **52**: p. 794-804.

162. *Halliwell, B., Role of free radicals in the neurodegenerative diseases: therapeutic implications for antioxidant treatment. Drugs Aging, 2001.* **18**(9): p. 685-716.

163. *Hayyan, M., M.A. Hashim, and I.M. AlNashef, Superoxide Ion: Generation and Chemical Implications. Chem Rev, 2016.* **116**(5): p. 3029-85.

164. *Robertson, R.P., Chronic Oxidative Stress as a Central Mechanism for Glucose Toxicity in Pancreatic Islet Beta Cells in Diabetes *. Journal of Biological Chemistry, 2004.* **279**(41): p. 42351-42354.

165. *Touyz, R.M., Reactive oxygen species, vascular oxidative stress, and redox signaling in hypertension: what is the clinical significance? Hypertension, 2004.* **44**(3): p. 248-52.

166. *Padurariu, M., et al., The oxidative stress hypothesis in Alzheimer's disease. Psychiatr Danub, 2013.* **25**(4): p. 401-9.

167. *Tan, S.L.W., et al., A Class of Environmental and Endogenous Toxins Induces BRCA2 Haploinsufficiency and Genome Instability. Cell, 2017.* **169**(6): p. 1105-1118 e15.

168. *Niki, E., Lipid peroxidation: physiological levels and dual biological effects. Free Radic Biol Med, 2009.* **47**(5): p. 469-84.

169. *Semchyshyn, H.M., Reactive carbonyl species in vivo: generation and dual biological effects. ScientificWorldJournal, 2014.* **2014**: p. 417842.

170. Burcham, P.C., Genotoxic lipid peroxidation products: their DNA damaging properties and role in formation of endogenous DNA adducts. Mutagenesis, 1998. **13**(3): p. 287-305.

171. O'Brien, P.J., A.G. Siraki, and N. Shangari, Aldehyde sources, metabolism, molecular toxicity mechanisms, and possible effects on human health. Crit Rev Toxicol, 2005. **35**(7): p. 609-62.

172. Uribarri, J., et al., Circulating glycotoxins and dietary advanced glycation endproducts: two links to inflammatory response, oxidative stress, and aging. J Gerontol A Biol Sci Med Sci, 2007. **62**(4): p. 427-33.

173. Colombo, G., et al., Water-Soluble alpha,beta-unsaturated aldehydes of cigarette smoke induce carbonylation of human serum albumin. Antioxid Redox Signal, 2010. **12**(3): p. 349-64.

174. Dini, L., Phagocytosis of dying cells: influence of smoking and static magnetic fields. Apoptosis, 2010. **15**(9): p. 1147-64.

175. Robert, L., A.M. Robert, and J. Labat-Robert, The Maillard reaction--illicite (bio)chemistry in tissues and food. Pathol Biol (Paris), 2011. **59**(6): p. 321-8.

176. Ellis, E.M., Reactive carbonyls and oxidative stress: potential for therapeutic intervention. Pharmacol Ther, 2007. **115**(1): p. 13-24.

177. Metz, T.O., et al., Pyridoxamine, an inhibitor of advanced glycation and lipoxidation reactions: a novel therapy for treatment of diabetic complications. Arch Biochem Biophys, 2003. **419**(1): p. 41-9.

178. Kalapos, M.P., Where does plasma methylglyoxal originate from? Diabetes Res Clin Pract, 2013. **99**(3): p. 260-71.

179. Onyango, A.N., Small reactive carbonyl compounds as tissue lipid oxidation products; and the mechanisms of their formation thereby. Chem Phys Lipids, 2012. **165**(7): p. 777-86.

180. McPherson, J.D., B.H. Shilton, and D.J. Walton, Role of fructose in glycation and cross-linking of proteins. Biochemistry, 1988. **27**(6): p. 1901-7.

181. Orosz, F., J. Olah, and J. Ovadi, Triosephosphate isomerase deficiency: new insights into an enigmatic disease. Biochim Biophys Acta, 2009. **1792**(12): p. 1168-74.

182. Richard, J.P., Kinetic parameters for the elimination reaction catalyzed by triosephosphate isomerase and an estimation of the reaction's physiological significance. Biochemistry, 1991. **30**(18): p. 4581-5.

183. Bellier, J., et al., Methylglyoxal, a potent inducer of AGEs, connects between diabetes and cancer. Diabetes Res Clin Pract, 2019. **148**: p. 200-211.

184. Vistoli, G., et al., Advanced glycoxidation and lipoxidation end products (AGEs and ALEs): an overview of their mechanisms of formation. Free Radic Res, 2013. **47 Suppl 1**: p. 3-27.

185. Yan, S.F., et al., Receptor for Advanced Glycation Endproducts (RAGE): a formidable force in the pathogenesis of the cardiovascular complications of diabetes & aging. Curr Mol Med, 2007. **7**(8): p. 699-710.

186. Esterbauer, H., et al., Separation and characterization of the aldehydic products of lipid peroxidation stimulated by ADP-Fe2+ in rat liver microsomes. Biochem J, 1982. **208**(1): p. 129-40.

187. Esterbauer, H., R.J. Schaur, and H. Zollner, Chemistry and biochemistry of 4-hydroxynonenal, malonaldehyde and related aldehydes. Free Radic Biol Med, 1991. **11**(1): p. 81-128.

188.   Gentile, F., et al., DNA damage by lipid peroxidation products: implications in cancer, inflammation and autoimmunity. AIMS Genet, 2017. **4**(2): p. 103-137.

189.   Munnia, A., M.E. Amasio, and M. Peluso, Exocyclic malondialdehyde and aromatic DNA adducts in larynx tissues. Free Radic Biol Med, 2004. **37**(6): p. 850-8.

190.   Peluso, M., et al., Breast fine-needle aspiration malondialdehyde deoxyguanosine adduct in breast cancer. Free Radic Res, 2011. **45**(4): p. 477-82.

191.   Lee, S.H., et al., Cyclooxygenase-2-mediated DNA damage. J Biol Chem, 2005. **280**(31): p. 28337-46.

192.   Matsuda, T., et al., Lipid peroxidation-induced DNA adducts in human gastric mucosa. Carcinogenesis, 2013. **34**(1): p. 121-7.

193.   Lee, H.W., et al., Acrolein- and 4-Aminobiphenyl-DNA adducts in human bladder mucosa and tumor tissue and their mutagenicity in human urothelial cells. Oncotarget, 2014. **5**(11): p. 3526-40.

194.   Feng, Z., et al., Acrolein is a major cigarette-related lung cancer agent: Preferential binding at p53 mutational hotspots and inhibition of DNA repair. Proc Natl Acad Sci U S A, 2006. **103**(42): p. 15404-9.

195.   Seiler, A., et al., Glutathione peroxidase 4 senses and translates oxidative stress into 12/15-lipoxygenase dependent- and AIF-mediated cell death. Cell Metab, 2008. **8**(3): p. 237-48.

196.   Yant, L.J., et al., The selenoprotein GPX4 is essential for mouse development and protects from radiation and oxidative damage insults. Free Radic Biol Med, 2003. **34**(4): p. 496-502.

197.   Brigelius-Flohe, R. and L. Flohe, Regulatory Phenomena in the Glutathione Peroxidase Superfamily. Antioxid Redox Signal, 2020. **33**(7): p. 498-516.

198.   Ellis, E.M., Reactive carbonyls and oxidative stress: Potential for therapeutic intervention. Pharmacology & Therapeutics, 2007. **115**(1): p. 13-24.

199.   Crabb, D.W., et al., Overview of the role of alcohol dehydrogenase and aldehyde dehydrogenase and their variants in the genesis of alcohol-related pathology. Proc Nutr Soc, 2004. **63**(1): p. 49-63.

200.   Mitchell, D.Y. and D.R. Petersen, The oxidation of α-β unsaturated aldehydic products of lipid peroxidation by rat liver aldehyde dehydrogenases. Toxicology and Applied Pharmacology, 1987. **87**(3): p. 403-410.

201.   Vasiliou, V., A. Pappa, and T. Estey, Role of Human Aldehyde Dehydrogenases in Endobiotic and Xenobiotic Metabolism. Drug Metabolism Reviews, 2004. **36**(2): p. 279-299.

202.   Jackson, B., et al., Update on the aldehyde dehydrogenase gene (ALDH) superfamily. Hum Genomics, 2011. **5**(4): p. 283-303.

203.   Ohsawa, I., et al., Deficiency in a mitochondrial aldehyde dehydrogenase increases vulnerability to oxidative stress in PC12 cells. J Neurochem, 2003. **84**(5): p. 1110-7.

204.   Guengerich, F.P., Cytochrome p450 and chemical toxicology. Chem Res Toxicol, 2008. **21**(1): p. 70-83.

205.   Berka, K., et al., Membrane position of ibuprofen agrees with suggested access path entrance to cytochrome P450 2C9 active site. J Phys Chem A, 2011. **115**(41): p. 11248-55.

206.   Gallego, O., et al., Comparative functional analysis of human medium-chain dehydrogenases, short-chain dehydrogenases/reductases and aldo-keto reductases with retinoids. Biochem J, 2006. **399**(1): p. 101-9.

207. Farres, J., et al., Alcohol dehydrogenase of class IV (sigma sigma-ADH) from human stomach. cDNA sequence and structure/function relationships. Eur J Biochem, 1994. **224**(2): p. 549-57.

208. O'Brien, P.J., A.G. Siraki, and N. Shangari, Aldehyde Sources, Metabolism, Molecular Toxicity Mechanisms, and Possible Effects on Human Health. Critical Reviews in Toxicology, 2005. **35**(7): p. 609-662.

209. Edenberg, H.J. and J.N. McClintick, Alcohol Dehydrogenases, Aldehyde Dehydrogenases, and Alcohol Use Disorders: A Critical Review. Alcohol Clin Exp Res, 2018. **42**(12): p. 2281-2297.

210. Kallberg, Y., et al., Short-chain dehydrogenases/reductases (SDRs). Eur J Biochem, 2002. **269**(18): p. 4409-17.

211. Matsuura, K., et al., Pulmonary carbonyl reductase: metabolism of carbonyl products in lipid peroxidation. Prog Clin Biol Res, 1989. **290**: p. 335-49.

212. Doorn, J.A., et al., Human carbonyl reductase catalyzes reduction of 4-oxonon-2-enal. Biochemistry, 2004. **43**(41): p. 13106-14.

213. Forrest, G.L. and B. Gonzalez, Carbonyl reductase. Chem Biol Interact, 2000. **129**(1-2): p. 21-40.

214. Wermuth, B., et al., Human carbonyl reductase. Nucleotide sequence analysis of a cDNA and amino acid sequence of the encoded protein. J Biol Chem, 1988. **263**(31): p. 16185-8.

215. Wirth, H. and B. Wermuth, Immunohistochemical localization of carbonyl reductase in human tissues. J Histochem Cytochem, 1992. **40**(12): p. 1857-63.

216. Jin, Y. and T.M. Penning, Aldo-Keto Reductases and Bioactivation/Detoxication. Annual Review of Pharmacology and Toxicology, 2007. **47**(1): p. 263-292.

217. Bohren, K.M., et al., The aldo-keto reductase superfamily. cDNAs and deduced amino acid sequences of human aldehyde and aldose reductases. J Biol Chem, 1989. **264**(16): p. 9547-51.

218. Burczynski, M.E., et al., The reactive oxygen species--and Michael acceptor-inducible human aldo-keto reductase AKR1C1 reduces the alpha,beta-unsaturated aldehyde 4-hydroxy-2-nonenal to 1,4-dihydroxy-2-nonene. J Biol Chem, 2001. **276**(4): p. 2890-7.

219. Srivastava, S., et al., Lipid peroxidation product, 4-hydroxynonenal and its conjugate with GSH are excellent substrates of bovine lens aldose reductase. Biochem Biophys Res Commun, 1995. **217**(3): p. 741-6.

220. Rizner, T.L. and T.M. Penning, Role of aldo-keto reductase family 1 (AKR1) enzymes in human steroid metabolism. Steroids, 2014. **79**: p. 49-63.

221. Burczynski, M.E., R.G. Harvey, and T.M. Penning, Expression and characterization of four recombinant human dihydrodiol dehydrogenase isoforms: oxidation of trans-7, 8-dihydroxy-7,8-dihydrobenzo[a]pyrene to the activated o-quinone metabolite benzo[a]pyrene-7,8-dione. Biochemistry, 1998. **37**(19): p. 6781-90.

222. Atalla, A., U. Breyer-Pfaff, and E. Maser, Purification and characterization of oxidoreductases-catalyzing carbonyl reduction of the tobacco-specific nitrosamine 4-methylnitrosamino-1-(3-pyridyl)-1-butanone (NNK) in human liver cytosol. Xenobiotica, 2000. **30**(8): p. 755-69.

223. Palackal, N.T., et al., Activation of polycyclic aromatic hydrocarbon trans-dihydrodiol proximate carcinogens by human aldo-keto reductase (AKR1C) enzymes and their functional overexpression in human lung carcinoma (A549) cells. J Biol Chem, 2002. **277**(27): p. 24799-808.

224. Kozma, E., et al., The high resolution crystal structure of rat liver AKR7A1: understanding the substrate specificites of the AKR7 family. Chem Biol Interact, 2003. **143-144**: p. 289-97.

225. Hyndman, D., et al., The aldo-keto reductase superfamily homepage. Chem Biol Interact, 2003. **143-144**: p. 621-31.

226. Esterbauer, H., H. Zollner, and N. Scholz, Reaction of glutathione with conjugated carbonyls. Z Naturforsch C Biosci, 1975. **30**(4): p. 466-73.

227. Hayes, J.D., J.U. Flanagan, and I.R. Jowsey, Glutathione transferases. Annu Rev Pharmacol Toxicol, 2005. **45**: p. 51-88.

228. Hayes, J.D. and D.J. Pulford, The glutathione S-transferase supergene family: regulation of GST and the contribution of the isoenzymes to cancer chemoprotection and drug resistance. Crit Rev Biochem Mol Biol, 1995. **30**(6): p. 445-600.

229. McCown, P.J., et al., Naturally occurring modified ribonucleosides. Wiley Interdiscip Rev RNA, 2020. **11**(5): p. e1595.

230. Mattick, J.S., RNA as the substrate for epigenome-environment interactions: RNA guidance of epigenetic processes and the expansion of RNA editing in animals underpins development, phenotypic plasticity, learning, and cognition. Bioessays, 2010. **32**(7): p. 548-52.

231. Mattick, J.S., The central role of RNA in human development and cognition. FEBS Lett, 2011. **585**(11): p. 1600-16.

232. Boccaletto, P., et al., MODOMICS: a database of RNA modification pathways. 2017 update. Nucleic Acids Res, 2018. **46**(D1): p. D303-D307.

233. Cantara, W.A., et al., The RNA modification database, RNAMDB: 2011 update. Nucleic Acids Research, 2010. **39**(suppl_1): p. D195-D201.

234. Lorenz, C., C.E. Lunse, and M. Morl, tRNA Modifications: Impact on Structure and Thermal Adaptation. Biomolecules, 2017. **7**(2).

235. Jonkhout, N., et al., The RNA modification landscape in human disease. RNA, 2017. **23**(12): p. 1754-1769.

236. Delaunay, S., et al., Elp3 links tRNA modification to IRES-dependent translation of LEF1 to sustain metastasis in breast cancer. J Exp Med, 2016. **213**(11): p. 2503-2523.

237. Yi, J., et al., Overexpression of NSUN2 by DNA hypomethylation is associated with metastatic progression in human breast cancer. Oncotarget, 2017. **8**(13): p. 20751-20765.

238. Rodriguez, V., et al., Chromosome 8 BAC array comparative genomic hybridization and expression analysis identify amplification and overexpression of TRMT12 in breast cancer. Genes Chromosomes Cancer, 2007. **46**(7): p. 694-707.

239. Lemmens, R., et al., RNA metabolism and the pathogenesis of motor neuron diseases. Trends Neurosci, 2010. **33**(5): p. 249-58.

240. Bednarova, A., et al., Lost in Translation: Defects in Transfer RNA Modifications and Neurological Disorders. Front Mol Neurosci, 2017. **10**: p. 135.

241. Blanco, S., et al., Aberrant methylation of tRNAs links cellular stress to neuro-developmental disorders. EMBO J, 2014. **33**(18): p. 2020-39.

242. Zhao, B.S., I.A. Roundtree, and C. He, Post-transcriptional gene regulation by mRNA modifications. Nat Rev Mol Cell Biol, 2017. **18**(1): p. 31-42.

243. Yan, M. and Q. Zhai, Sperm tsRNAs and acquired metabolic disorders. J Endocrinol, 2016. **230**(3): p. F13-8.

244. Franke, B., et al., *An association study of 45 folate-related genes in spina bifida: Involvement of cubilin (CUBN) and tRNA aspartic acid methyltransferase 1 (TRDMT1).* Birth Defects Res A Clin Mol Teratol, 2009. **85**(3): p. 216-26.

245. Martinez, F.J., et al., *Whole exome sequencing identifies a splicing mutation in NSUN2 as a cause of a Dubowitz-like syndrome.* J Med Genet, 2012. **49**(6): p. 380-5.

246. Fahiminiya, S., et al., *Whole exome sequencing unravels disease-causing genes in consanguineous families in Qatar.* Clin Genet, 2014. **86**(2): p. 134-41.

247. Doll, A. and K.H. Grzeschik, *Characterization of two novel genes, WBSCR20 and WBSCR22, deleted in Williams-Beuren syndrome.* Cytogenet Cell Genet, 2001. **95**(1-2): p. 20-7.

248. Stone, K., M.B. Ksebati, and L.J. Marnett, *Investigation of the adducts formed by reaction of malondialdehyde with adenosine.* Chem Res Toxicol, 1990. **3**(1): p. 33-8.

249. Seto, H., et al., *Reaction of malonaldehyde with nucleic acid. III. Studies of the fluorescent substances released by enzymatic digestion of nucleic acids modified with malonaldehyde.* Chem Pharm Bull (Tokyo), 1986. **34**(12): p. 5079-85.

250. Szekely, J., et al., *"One-pot" syntheses of malondialdehyde adducts of nucleosides.* Nucleosides Nucleotides Nucleic Acids, 2008. **27**(2): p. 103-9.

251. Lai, C., et al., *Absolute configurations and stability of cyclic guanosine mono-adducts with glyoxal and methylglyoxal.* Chirality, 2011. **23**(7): p. 487-94.

252. Stornetta, A., et al., *Screening for DNA Alkylation Mono and Cross-Linked Adducts with a Comprehensive LC-MS(3) Adductomic Approach.* Anal Chem, 2015. **87**(23): p. 11706-13.

253. Wilson, M.R., et al., *The human gut bacterial genotoxin colibactin alkylates DNA.* Science, 2019. **363**(6428).

254. Carra, A., et al., *Targeted High Resolution LC/MS(3) Adductomics Method for the Characterization of Endogenous DNA Damage.* Front Chem, 2019. **7**: p. 658.

255. Tennant, D.A., R.V. Duran, and E. Gottlieb, *Targeting metabolic transformation for cancer therapy.* Nat Rev Cancer, 2010. **10**(4): p. 267-77.

256. Cairns, R.A., I.S. Harris, and T.W. Mak, *Regulation of cancer cell metabolism.* Nat Rev Cancer, 2011. **11**(2): p. 85-95.

257. Phan, L.M., S.C. Yeung, and M.H. Lee, *Cancer metabolic reprogramming: importance, main features, and potentials for precise targeted anti-cancer therapies.* Cancer Biol Med, 2014. **11**(1): p. 1-19.

258. Shalem, O., et al., *Genome-scale CRISPR-Cas9 knockout screening in human cells.* Science, 2014. **343**(6166): p. 84-87.

259. Ashburner, M., et al., *Gene ontology: tool for the unification of biology. The Gene Ontology Consortium.* Nat Genet, 2000. **25**(1): p. 25-9.

260. The Gene Ontology, C., *The Gene Ontology Resource: 20 years and still GOing strong.* Nucleic Acids Res, 2019. **47**(D1): p. D330-D338.

261. Brunk, E., et al., *Recon3D enables a three-dimensional view of gene variation in human metabolism.* Nat Biotechnol, 2018. **36**(3): p. 272-281.

262. Thornalley, P.J., *The glyoxalase system: new developments towards functional characterization of a metabolic pathway fundamental to biological life.* Biochem J, 1990. **269**(1): p. 1-11.

263. Thornalley, P.J., *The glyoxalase system in health and disease.* Mol Aspects Med, 1993. **14**(4): p. 287-371.

264.   Thornalley, P.J., *Protecting the genome: defence against nucleotide glycation and emerging role of glyoxalase I overexpression in multidrug resistance in cancer chemotherapy.* Biochem Soc Trans, 2003. **31**(Pt 6): p. 1372-7.

265.   Mannervik, B., *Molecular enzymology of the glyoxalase system.* Drug Metabol Drug Interact, 2008. **23**(1-2): p. 13-27.

266.   Frischmann, M., et al., *Identification of DNA adducts of methylglyoxal.* Chem Res Toxicol, 2005. **18**(10): p. 1586-92.

267.   Distler, M.G. and A.A. Palmer, *Role of Glyoxalase 1 (Glo1) and methylglyoxal (MG) in behavior: recent advances and mechanistic insights.* Front Genet, 2012. **3**: p. 250.

268.   Thornalley, P.J., et al., *Antitumour activity of S-p-bromobenzylglutathione cyclopentyl diester in vitro and in vivo. Inhibition of glyoxalase I and induction of apoptosis.* Biochem Pharmacol, 1996. **51**(10): p. 1365-72.

269.   Al-Timari, A. and K.T. Douglas, *Inhibition of mammalian glyoxalase I (lactoylglutathione lyase) by N-acylated S-blocked glutathione derivatives as a probe for the role of the N-site of glutathione in glyoxalase I mechanism.* Biochim Biophys Acta, 1986. **870**(1): p. 160-8.

270.   Franklin, T.J. and J.M. Cook, *The inhibition of nucleic acid synthesis by mycophenolic acid.* Biochem J, 1969. **113**(3): p. 515-24.

271.   Podzuweit, T., P. Nennstiel, and A. Muller, *Isozyme selective inhibition of cGMP-stimulated cyclic nucleotide phosphodiesterases by erythro-9-(2-hydroxy-3-nonyl) adenine.* Cell Signal, 1995. **7**(7): p. 733-8.

272.   Allocati, N., et al., *Glutathione transferases: substrates, inihibitors and pro-drugs in cancer and neurodegenerative diseases.* Oncogenesis, 2018. **7**(1): p. 8.

273.   Edreva, A., *Generation and scavenging of reactive oxygen species in chloroplasts: a submolecular approach.* Agriculture, Ecosystems & Environment, 2005. **106**(2): p. 119-133.

274.   Li, H.C., et al., *Imbalanced free radicals and antioxidant defense systems in schizophrenia: a comparative study.* J Zhejiang Univ Sci B, 2006. **7**(12): p. 981-6.

275.   Pompella, A., et al., *The changing faces of glutathione, a cellular protagonist.* Biochem Pharmacol, 2003. **66**(8): p. 1499-503.

276.   Alexandre, J., et al., *Accumulation of hydrogen peroxide is an early and crucial step for paclitaxel-induced cancer cell death both in vitro and in vivo.* Int J Cancer, 2006. **119**(1): p. 41-8.

277.   Luanpitpong, S., et al., *Mitochondrial superoxide mediates doxorubicin-induced keratinocyte apoptosis through oxidative modification of ERK and Bcl-2 ubiquitination.* Biochem Pharmacol, 2012. **83**(12): p. 1643-54.

278.   Julicher, R.H., et al., *The role of lipid peroxidation in acute doxorubicin-induced cardiotoxicity as studied in rat isolated heart.* J Pharm Pharmacol, 1986. **38**(4): p. 277-82.

279.   Benchekroun, M.N., et al., *Doxorubicin-induced lipid peroxidation and glutathione peroxidase activity in tumor cell lines selected for resistance to doxorubicin.* Eur J Biochem, 1993. **211**(1-2): p. 141-6.

280.   Griffith, O.W. and A. Meister, *Glutathione: interorgan translocation, turnover, and metabolism.* Proc Natl Acad Sci U S A, 1979. **76**(11): p. 5606-10.

281.   Heumuller, S., et al., *Apocynin is not an inhibitor of vascular NADPH oxidases but an antioxidant.* Hypertension, 2008. **51**(2): p. 211-7.

282. Ayala, A., M.F. Munoz, and S. Arguelles, *Lipid peroxidation: production, metabolism, and signaling mechanisms of malondialdehyde and 4-hydroxy-2-nonenal.* Oxid Med Cell Longev, 2014. **2014**: p. 360438.

283. Chaudhary, A.K., et al., *Detection of endogenous malondialdehyde-deoxyguanosine adducts in human liver.* Science, 1994. **265**(5178): p. 1580-2.

284. Wang, Z., et al., *Oxidative Stress and Carbonyl Lesions in Ulcerative Colitis and Associated Colorectal Cancer.* Oxid Med Cell Longev, 2016. **2016**: p. 9875298.

285. Lee, H.J., et al., *Inhibitory effects of dicaffeoylquinic acids from Artemisia dubia on aldo-keto reductase family 1b10.* Journal of the Korean Society for Applied Biological Chemistry, 2010. **53**(6): p. 826-830.

286. Wang, C., et al., *Aldo-keto reductase family 1 member B10 promotes cell survival by regulating lipid synthesis and eliminating carbonyls.* J Biol Chem, 2009. **284**(39): p. 26742-8.

287. Barski, O.A., S.M. Tipparaju, and A. Bhatnagar, *The aldo-keto reductase superfamily and its role in drug metabolism and detoxification.* Drug Metab Rev, 2008. **40**(4): p. 553-624.

288. Baba, S.P., et al., *Reductive metabolism of AGE precursors: a metabolic route for preventing AGE accumulation in cardiovascular tissue.* Diabetes, 2009. **58**(11): p. 2486-97.

289. Takemura, M., et al., *Selective inhibition of the tumor marker aldo-keto reductase family member 1B10 by oleanolic acid.* J Nat Prod, 2011. **74**(5): p. 1201-6.

290. Birlouez-Aragon, I., et al., *The health and technological implications of a better control of neoformed contaminants by the food industry.* Pathol Biol (Paris), 2010. **58**(3): p. 232-8.

291. Medeiros, M.H., *Exocyclic DNA adducts as biomarkers of lipid oxidation and predictors of disease. Challenges in developing sensitive and specific methods for clinical studies.* Chem Res Toxicol, 2009. **22**(3): p. 419-25.

292. Voulgaridou, G.P., et al., *DNA damage induced by endogenous aldehydes: current state of knowledge.* Mutat Res, 2011. **711**(1-2): p. 13-27.

293. Stone, K., A. Uzieblo, and L.J. Marnett, *Studies of the reaction of malondialdehyde with cytosine nucleosides.* Chem Res Toxicol, 1990. **3**(5): p. 467-72.

294. Marnett, L.J., *Lipid peroxidation-DNA damage by malondialdehyde.* Mutat Res, 1999. **424**(1-2): p. 83-95.

295. Yates, S.A., et al., *Quantitative analysis of malondialdehyde-guanine adducts in genomic DNA samples by liquid chromatography/tandem mass spectrometry.* Rapid Commun Mass Spectrom, 2017. **31**(9): p. 762-770.

296. Chaudhary, A.K., et al., *Characterization of an N6-oxopropenyl-2'-deoxyadenosine adduct in malondialdehyde-modified DNA using liquid chromatography/electrospray ionization tandem mass spectrometry.* Carcinogenesis, 1996. **17**(5): p. 1167-70.

297. Hadley, M. and H.H. Draper, *Isolation of a guanine-malondialdehyde adduct from rat and human urine.* Lipids, 1990. **25**(2): p. 82-5.

298. Inoue, Y. and A. Kimura, *Methylglyoxal and regulation of its metabolism in microorganisms.* Adv Microb Physiol, 1995. **37**: p. 177-227.

299. Schumacker, P.T., *Reactive oxygen species in cancer cells: live by the sword, die by the sword.* Cancer Cell, 2006. **10**(3): p. 175-6.

300. Corbett, A.J., et al., *Antigen Recognition by MR1-Reactive T Cells; MAIT Cells, Metabolites, and Remaining Mysteries.* Front Immunol, 2020. **11**: p. 1961.

301. Schweizer, U., S. Bohleber, and N. Fradejas-Villar, The modified base isopentenyladenosine and its derivatives in tRNA. RNA Biol, 2017. **14**(9): p. 1197-1208.

302. Dassano, A., et al., N6-isopentenyladenosine and analogs activate the NRF2-mediated antioxidant response. Redox Biology, 2014. **2**: p. 580-589.

303. Yue, Z., et al., Identification of breast cancer candidate genes using gene co-expression and protein-protein interaction information. Oncotarget, 2016. **7**(24): p. 36092-36100.

304. Yarham, J.W., et al., Defective i6A37 modification of mitochondrial and cytosolic tRNAs results from pathogenic mutations in TRIT1 and its substrate tRNA. PLoS Genet, 2014. **10**(6): p. e1004424.

305. Seistrup, K.H., et al., Bypassing rRNA methylation by RsmA/Dim1during ribosome maturation in the hyperthermophilic archaeon Nanoarchaeum equitans. Nucleic Acids Res, 2017. **45**(4): p. 2007-2015.

306. Grosjean, H., et al., Predicting the minimal translation apparatus: lessons from the reductive evolution of mollicutes. PLoS Genet, 2014. **10**(5): p. e1004363.

307. Ishiwata, S., et al., Comparison of serum and urinary levels of modified nucleoside, 1-methyladenosine, in cancer patients using a monoclonal antibody-based inhibition ELISA. Tohoku J Exp Med, 1995. **176**(1): p. 61-8.

308. Seidel, A., et al., Modified nucleosides: an accurate tumour marker for clinical diagnosis of cancer, early detection and therapy control. Br J Cancer, 2006. **94**(11): p. 1726-33.

309. Glasser, A.L., et al., O-ribosyl-phosphate purine as a constant modified nucleotide located at position 64 in cytoplasmic initiator tRNAs(Met) of yeasts. Nucleic Acids Res, 1991. **19**(19): p. 5199-203.

310. Ratel, D., et al., N6-methyladenine: the other methylated base of DNA. Bioessays, 2006. **28**(3): p. 309-15.

311. Li, X., et al., The DNA modification N6-methyl-2'-deoxyadenosine (m6dA) drives activity-induced gene expression and is required for fear extinction. Nature Neuroscience, 2019. **22**(4): p. 534-544.

312. Hattman, S., et al., Comparative study of DNA methylation in three unicellular eucaryotes. J Bacteriol, 1978. **135**(3): p. 1156-7.

313. Huneeus, V.Q., M.H. Wiley, and M.D. Siperstein, Isopentenyladenine as a mediator of mevalonate-regulated DNA replication. Proc Natl Acad Sci U S A, 1980. **77**(10): p. 5842-6.

314. Laloue, M., C. Terrine, and J. Guern, Cytokinins: Metabolism and Biological Activity of N-(Delta-Isopentenyl)adenosine and N-(Delta-Isopentenyl)adenine in Tobacco Cells and Callus. Plant Physiol, 1977. **59**(3): p. 478-83.

315. Szollosi, M.S., et al., Inhibition of protein kinases by 6-dimethylaminopurine accelerates the transition to interphase in activated mouse oocytes. J Cell Sci, 1993. **104 (Pt 3)**: p. 861-72.

316. Li, Y., Y. Wang, and P. Wu, 5'-Methylthioadenosine and Cancer: old molecules, new understanding. J Cancer, 2019. **10**(4): p. 927-936.

317. Hienzsch, A., et al., Total synthesis of the hypermodified RNA bases wybutosine and hydroxywybutosine and their quantification together with other modified RNA bases in plant materials. Chemistry, 2013. **19**(13): p. 4244-8.

318. Matsuda, T., et al., Effective utilization of N2-ethyl-2'-deoxyguanosine triphosphate during DNA synthesis catalyzed by mammalian replicative DNA polymerases. Biochemistry, 1999. **38**(3): p. 929-35.

319. Vaca, C.E., J.L. Fang, and E.K. Schweda, *Studies of the reaction of acetaldehyde with deoxynucleosides.* Chem Biol Interact, 1995. **98**(1): p. 51-67.

320. Fang, J.L. and C.E. Vaca, *Detection of DNA adducts of acetaldehyde in peripheral white blood cells of alcohol abusers.* Carcinogenesis, 1997. **18**(4): p. 627-32.

321. Avila, M.A., et al., *Methylthioadenosine.* Int J Biochem Cell Biol, 2004. **36**(11): p. 2125-30.

322. Stevens, A.P., et al., *Direct and tumor microenvironment mediated influences of 5'-deoxy-5'-(methylthio)adenosine on tumor progression of malignant melanoma.* J Cell Biochem, 2009. **106**(2): p. 210-9.

323. Toohey, J.I., *Methylthioadenosine nucleoside phosphorylase deficiency in methylthio-dependent cancer cells.* Biochem Biophys Res Commun, 1978. **83**(1): p. 27-35.

324. Harasawa, H., et al., *Chemotherapy targeting methylthioadenosine phosphorylase (MTAP) deficiency in adult T cell leukemia (ATL).* Leukemia, 2002. **16**(9): p. 1799-807.

325. Vasiliou, V., A. Pappa, and D.R. Petersen, *Role of aldehyde dehydrogenases in endogenous and xenobiotic metabolism.* Chem Biol Interact, 2000. **129**(1-2): p. 1-19.

326. Hayes, J.D. and L.I. McLellan, *Glutathione and glutathione-dependent enzymes represent a co-ordinately regulated defence against oxidative stress.* Free Radic Res, 1999. **31**(4): p. 273-300.

327. Zhong, L., et al., *Aldo-keto reductase family 1 B10 protein detoxifies dietary and lipid-derived alpha, beta-unsaturated carbonyls at physiological levels.* Biochem Biophys Res Commun, 2009. **387**(2): p. 245-50.

328. Pavlova, N.N. and C.B. Thompson, *The Emerging Hallmarks of Cancer Metabolism.* Cell Metab, 2016. **23**(1): p. 27-47.

329. Pluskota-Karwatka, D., *Modifications of nucleosides by endogenous mutagens-DNA adducts arising from cellular processes.* Bioorg Chem, 2008. **36**(4): p. 198-213.